ANNUAL TRANSACTIONS OF THE NORDIC RHEOLOGY SOCIETY, VOL. 13, 2005

THESIS ON NATURAL AND EXACT SCIENCES B44

Interactions Between Furcellaran and the Globular Proteins (Bovine Serum Albumin, β-Lactoglobulin)

KATRIN LAOS

TALLINN 2005

Faculty of Chemical and Materials Technology
Department of Food Processing
TALLINN UNIVERSITY OF TECHNOLOGY

Dissertation was accepted for the commencement of the degree of Doctor of Philosophy in Engineering on October 31, 2005

Supervisor: Assoc. Prof. Margus Friedenthal, Department of Food Processing, Tallinn University of Technology, Tallinn, Estonia. Current position: Deputy Director of Agricultural Research Centre, Saku, Estonia

Co-supervisor: Dr. Stephen G. Ring, Division of Food Materials Science, Institute of Food Research, Norwich Research Park, UK

Opponents:

Dr. Sandra E. Hill, Division of Food Sciences, University of Nottingham, Nottingham, England

Prof. Toomas Paalme, Department of Food Processing, Tallinn University of Technology, Tallinn, Estonia

Commencement: January 20, 2006 at Tallinn University of Technology

Declaration: Hereby I declare that this doctoral thesis, my original investigation and achivement, submitted for the doctoral degree at Tallinn University of Technology has not been submitted for any degree or examination

Katrin Laos

ISSN 1406-4723
ISBN 9985-59-590-4

ABSTRACT

The main goal of the present study was to characterize the furcellaran from Estonian *Furcellaria lumbricalis* and to better understand and control the interactions between furcellaran and globular proteins bovine serum albumin (BSA) and β-lactoglobulin (BLG).

The structure of native and alkali modified furcellarans obtained from red algae *Furcellaria lumbricalis* collected in Estonia was determined. The polysaccharide preparation consisted mainly of (1→3) linked β-D-galactopyranose; (1→4) linked 3,6-anhydro-α-D-galactopyranose; and (1→3) linked β-D-galactopyranose 4-sulphate. The alkaline treatment removed the sulphate precursor sequences with formation of 3,6-anhydrogalactose that improved the furcellaran gelling ability.

When furcellaran solution and globular protein solution (BSA, BLG) are mixed following behaviour was observed. On decreasing pH, the furcellaran first formed a soluble complex with the globular proteins at a pH_c, which showed a maximum in its dependence on ionic strength. On further decrease in pH, the onset of a more substantial aggregation, as indicated by a marked increase in turbidity occurred in the vicinity of the isoelectric point of the protein. Between these pH's the globular protein/furcellaran complex had a characteristic average size which was larger than the isolated furcellaran chain in solution. Complexation occurred when the protein carried an average net charge of the same sign as the furcellaran.

In mixed gelling systems, physically cross-linked networked gels were obtained. Proteins strongly influenced the shear modulus. At low pH the phase-separation occurred with the change in loss tangent.

The experiments with concentrated furcellaran systems suggest that furcellaran can be used as film-forming agent. The furcellaran based films exhibited good mechanical barrier properties. The addition of BSA makes films more pliable, however the film properties decline as the tensile strength and elongation at break of composite films decrease and water vapour permeability increases.

The formation of multilayer films of poly-L-lysine (PLL) and furcellaran was investigated surface plasmon resonance (SPR), quartz crystal microbalance with dissipation monitoring (QCM-D) and Fourier transform infrared spectroscopy with attenuated total reflection (FTIR-ATR). The progressive form of the growth of mass of polymer deposited for the multilayer was consistent with the ability of the PLL to diffuse within the furcellaran layer. Using the same experimental approaches the pH-dependent adsorption of the globular proteins bovine serum albumin (BSA) and β-lactoglobulin (BLG) to the PLL/furcellaran multilayers was also examined. Substantial adsorption was observed even at pH's where the net charge on the protein was of the same sign as that of the furcellaran.

LIST OF PUBLICATIONS

The present dissertation is based on the following papers, which are referred to in the text by their Roman numerals I-VI:

I Parker, R., Noel, T.R., Brownsey, G.J., **Laos, K.**, Ring, S.G. 2005. The Non-Equilibrium Phase and Glass Transition Behavior of β-Lactoglobulin. –Biophysical Journal, vol 89, no. 2, pp. 1227-1236

II **Laos, K.**, Ring, S.G. 2005. Characterisation of furcellaran samples from Estonian *Furcellaria lumbricalis*. – Journal of Applied Phycology, vol 17, 461-464

III **Laos, K.**, Brownsey, G.J., Friedenthal, M., Ring, S.G. 2005. Rheological properties of gels formed with furcellaran and globular proteins bovine serum albumin and β–lactoglobulin. – Annual Transactions of the Nordic Rheology Society, vol 13, 269-275

IV **Laos, K**., Mironova, M., Friedenthal, M. 2005 Development of furcellaran and furcellaran-bovine serum albumin films to improve food quality and safety. – Innovations in Traditional Foods (eds. Fito, P. and Toldra, F.), Elsevier, London, pp.1343-1346.

V **Laos, K.,** Brownsey, G.J., Ring, S.G. 2005 Interactions between furcellaran and the globular proteins bovine serum albumin and β-lactoglobulin. – Carbohydrate Polymers. Accepted

VI **Laos, K**., Parker, R., Moffat, J., Wellner, N., Ring, S.G. The adsorption of globular proteins, bovine serum albumin and β-lactoglobulin, on poly-L-lysine – furcellaran multilayers. – Manuscript.

In the appendix of this thesis, copies of the papers I-VI have been included. Papers I-IV are reproduced with permission from the publishers.

THE AUTHOR'S CONTRIBUTION TO PUBLICATIONS

Paper I:

The author performed the experimental work and interpreted the data concerned photon correlation spectroscopy and is the co-author of the paper.

Paper II:

The author performed all the experimental work and interpreted the results. She wrote the paper and is the corresponding author. The author also presented the results at the 12th Gums and Stabilisers for the Food Industry Conference, 24-27 June 2003, Wrexham, UK

Paper III:

The author performed all the experimental work and interpreted the results. She wrote the paper and is the corresponding author. The author also presented the results at the 14th Nordic Rheology Conference, 1-3 June 2005, Tampere, Finland

Paper IV:

The author supervised the experimental study, participated together with BSc. student, and interpreted the obtained data. She wrote the paper and is the corresponding author. The author also presented the results at the EFFoST Conference INTRADFOOD: Innovations in Traditional Foods 25-28 October 2005, Valencia, Spain.

Paper V:

Author performed all the experimental work, interpreted the results and is the co-author of the paper. The author presented the results at the satellite to the XVIII International Seaweed Symposium - Marine Biopolymers: Structure, Functionality and Applications, 27-29 June 2004, Trondheim, Norway

Paper VI:

The author performed all the experimental work, interpreted the results and is the co-author of the paper.

TABLE OF CONTENTS

ABBREVIATIONS

^{13}C- NMR	carbon nuclear magnetic resonance spectroscopy
BLG	β-lactoglobulin
BSA	bovine serum albumin
E	elongation at break
FTIR-ATR	Fourier transform infrared spectroscopy with attenuated total reflection
GC-MS	gas chromatograph with a mass-selective detector
PCS	photon correlation spectroscopy
PEC	polyelectrolyte complexes
pH_c	complexation pH
pH_i	initial pH
pH_ϕ	phase separation pH
pK_a	solution phase acidity
PLL	poly-L-lysine
QCM-D	quartz crystal microbalance with dissipation monitoring
SPR	surface plasmon resonance
TS	tensile strength
UV/VIS	ultraviolet irradiation/visible light
WVP	water vapour permeability
σ	charge density

INTRODUCTION

Furcellaran is an anionic sulphated polysaccharide extracted from the red alga *Furcellaria lumbricalis*. Estonia is a large potential source of this marine alga. In Kattegat (Denmark) it is declining and no longer present in Puck Bay (Poland). The current abundance of these seaweeds in Estonia is the greatest in Europe and probably in the world (Truus et al., 1997). Furcellaran is a type of carrageenan that can be used as stabilizing, thickening and gelling agent in the food, agricultural, cosmetics and pharmaceutical industries (Guiseley et al., 1980; Hidalgo and Hansen, 1969; Huffman and Shah, 1995, Moirano, 1977; Piculell, 1995; Thomas, 1992; Tziboula and Horne, 1997). In dairy products, it may be used at levels of 0,005-3 % to confer the functional properties (Thomas, 1992). If some polysaccharides provide stability by modifying the rheological properties of the continuous aqueous phase, the carrageenans interact directly with the milk proteins (Drohan et al., 1997). Physical stability, an important factor in the quality and self life of various dairy products including puddings, ice cream, yogurt etc., depends mainly on the presence of stabilizers such as polysaccharides (Hidalgo and Hansen, 1969; Moirano, 1977). The control or manipulation of the protein-polysaccharide interactions is a key factor in the development of novel food and pharmaceutical products. The overall function-structure relationship of a food containing protein and polysaccharide depends on both the individual biopolymers and also on the strength and interaction of the mixed biopolymers (Gazaka et al., 1999). The study of the interaction of milk proteins and polysaccharides may not only enhance the application of the polysaccharides in dairy products, but also may improve their functional properties. Several variables including pH, ionic strength, temperature, and variations in biopolymer structure can determine the type of the polysaccharide-protein interactions that will occur. Thus, understanding of furcellaran/globular protein interactions aids in controlling undesired phase instabilities. In contrast to avoiding instabilities, phase instabilities can also purposely utilised to create anisotropic structures.

Furcellaran is a polyeletrolyte that carries sulphate groups and it is negatively charged over a large range of pH. This makes it an interesting material for multilayers. Charge reversal of alternate polyanion and polycation permits the build-up of oppositely charged polyelectrolytes and also the films to absorb a variety of compounds such as particles, crystals, inorganic complexes, enzymes or proteins. This offers almost infinite possible film architecture and is an important area of research in various fields, such as microcapsules (Dahne et al., 2001; Vinogradova, 2004), tissue engineering (Zhu et al., 2004), protection for biomaterials (Etienne et al., 2004; Boulmedais et al., 2004), etc.

In this thesis, furcellaran/globular protein (BSA and BLG) interactions in solutions, gel systems and concentrated systems are characterised. Also the furcellaran/poly-L-lysine multilayers have been made and the adsorption of bovine serum albumin and β-lactoglobulin onto it was studied.

LITERATURE REVIEW

1.1 Furcellaran

Furcellaran is an anionic sulphated polysaccharide extracted from the red alga *Furcellaria lumbricalis*. It is currently considered to be a copolymer of β- and κ-carrageenan and usually represented structurally as a repeating unit of alternating 3-linked β-D-galactopyranose and 4-linked α-D-galactopyranose residues, with part of the latter existing as a 3,6-anhydro derivate (Figure 1) (Hugerth and Sundelöf, 2001). Hydroxyl groups in the polysaccharide chain may be substituted (sulphated, methylated, etc.) and other monomer residues such as xylose and glucose may be found (Van de Velde et al., 2002).

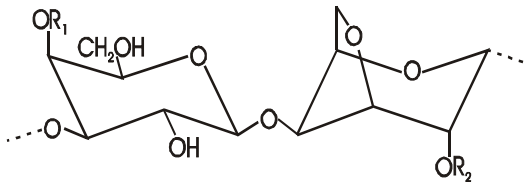

Figure 1.1 Primary structure formulae of the repeating disaccharide unit of β-(R_1=R_2=H) and κ-(R_1=OSO_3^-, R_2=H) carrageenan (Hugerth and Sundelöf, 2001)

Furcellaran is a polyelectrolyte that carries sulphate groups and it is negatively charged over a wide range of pH. The charge density is usually one sulphate per three or four monomer units (Glicksman, 1983).

At high temperatures furcellaran are believed to behave as stiff coiled polyelectrolytes. Clearly the degree of expansion of the coil in solution is dependent on the level of sulphation of the polysaccharide and the ionic strength of the medium. Under appropriate conditions aqueous preparations (sols) of furcellaran can be induced to form thermoreversible gels. Gelation can be induced by the presence of either monovalent or divalent cations (Morris, 1998).

1.2 Serum albumin

Serum albumin is a globular protein much studied as the form of bovine serum albumin (BSA). The molecular weight is 69 267, it contains 101 carboxylate groups (41 aspartic acid residues, 59 glutamic acid residues, plus 1 for the terminal group). It is a very soluble and stable molecule in aqueous solution and comprises 60% of total blood plasma protein.

The published X-ray crystal structure of serum albumin indicates a heart-shaped molecule which can be approximated to an equilateral triangular prism

with sides of 8 nm and a depth of 3 nm (Figure 1.2). Under conditions of neutral pH BSA has an axial ratio of approximately 2.66. The conformation of BSA shows pH dependence, with the native form being found between pH's 4 and 8 (Carter and Ho, 1994).

Figure 1.2 Ribbon diagram of serum albumin (Carter and Ho, 1994)

The single peptide chain forms a series of 9 helical loops. These loops form hydrophobic pockets which bind and transport large, nonpolar molecules such as fatty acids (eg. oleate, stearate, linoleate and palmitate). The bound fatty acids thermally stabilize the protein. Of the 35 cysteine residues in the BSA molecule, 34 form 17 disulfide bonds per monomer. These bridges maintain the loops in the structure. The free sulfhydryl group located at cysteine 34 is protected from oxidation by steric factors. The thermal transition point of denaturation for BSA is 338 K (65ºC). Most BSA molecules lose their bound fatty acids with heating to about 333K at pH 7, and this results in denaturation (dimerization, aggregation and precipitation) (Rouhana, et al., 1997).

1.3 β-Lactoglobulin

β-Lactoglobulin (BLG) is the major protein constituent of whey protein from milk. The BLG monomer has a molecular weight of ~18 000 corresponding to a chain of some 162 amino acid residues. It occurs in two common genetic variant forms A and B differing in amino acid content at two disulphide bridges and a free cysteine residue. The exact function of BLG in milk is unknown, but a crystal structure for the bovine form shows that it has a similar fold to human plasma retinol-binding protein, so it may be involved in transport processes (Clark, 1998).

The structure revealed by X-ray diffraction (Figure 1.3) is made up of a short segment of α-helix (15%) and eight strands of antiparallel β-sheet (50%), forming a so-called "beta-barrel" (Clark, 1998).

The crystal structure in Figure 1.3 emphasises the monomeric form, but normally BLG occurs in solution as a dimer and in the pH range 4.4 to 4.7 it can

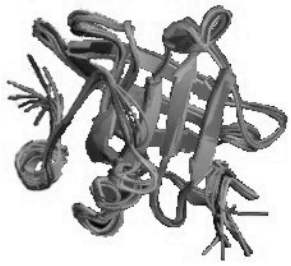

Figure 1.3 Representation of the three-dimensional structure of the β-lactoglobulin monomer (Kuwata et al., 1999)

polymerise to higher aggregate forms such as an octamer (tetrameric form of the dimer). The dimer is not universally stable, however, and enters into a monomer-dimer equilibrium whose position is affected by lowering pH (dissociation), changing ionic strength, or raising temperature (Clark, 1998).

1.4. Polysaccharide/protein interactions

Foods contain a complex mixture of proteins and polysaccharides, both of which are multifunctional and fulfil several, similar structural functions simultaneously. For instance, they can simultaneously act as thickening, emulsifying, foaming, gelling, and water binding agents. Mixtures of biopolymers are often unstable, which leads to a separation of the mixture into two phases, as illustrated in Figure 1.4 (Tolstoguzov, 1991).

A diluted non-interactive biopolymer mixture of polysaccharides and proteins may be co-soluble. Two phase separation phenomena can be observed, depending on the affinity between the different biopolymers and the solvent (Doublier et al., 2000). If the biopolymers are incompatible, *i.e.* they repel each other, thermodynamic phase separation occurs, also called segregation or depletion interaction. After phase separation, the mixture exhibits two phases: one rich in polysaccharide and the other one rich in protein. On the other hand, if polysaccharides and proteins show net attraction, usually through electrostatic interactions (when they have oppositely charged groups), complex coacervation or associative phase separation occurs, giving rise to the formation of polysaccharide/protein complexes. The mixture separates into two phases: the lower phase containing the polysaccharide/protein complex and the upper phase containing mainly the solvent (Dickinson, 1988).

In the presence of gelation, the rate and extent of phase separation may be greatly reduced, although the local heterogeneity induced by the material instability will still make an impact on the microstructure of the mixed biopolymer system (Morris, 1991). Depending on the strength and nature of the protein-polysaccharide interactions, macromolecular gels containing the two mixed biopolymers may form interpenetrating (homogeneous), associative or

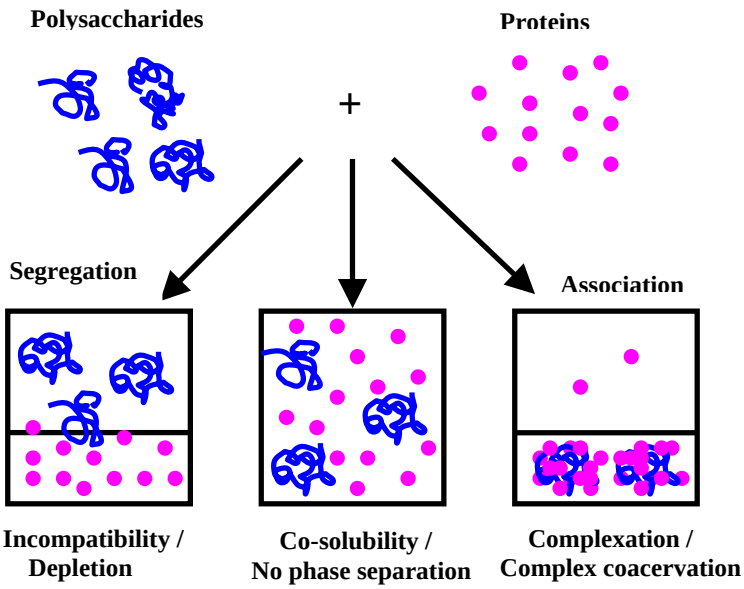

Figure 1.4 Main trends in the behaviour of polysaccharide/protein mixtures (Tolstoguzov, 1991)

phase-separated (heterogeneous) networks. When phase separation takes place, a competition between the phase separation and gelation process generally takes place, resulting in an increase in the complexity of the system (Ould Eleya et al., 2000).

What actually happens in any particular system is dependent on the concentrations of the two biopolymers and the detailed nature of the intermolecular interactions.

1.4.1 Co-solubility

Co-solubility is the least typical situation in view of the polymeric nature of proteins and polysaccharides and presence of various functional groups in their macromolecules (Tolstoguzov, 1991). If contact between different biopolymers is similar to contact between like biopolymer species, spontaneous mixing occurs. The system remains homogeneous, also at high polymer concentrations. With increasing polymer molecular weight, however, the balancing between not too repulsive and not too attractive polymer interactions becomes difficult, as even slightly repulsive or attractive interaction potentials per polymer segment add up to considerable values per molecule. This means that high molecular weight

polymers tend either to complex coacervation or incompatibility, but not to miscibility (Syrbe et al., 1998).

In case of gelation, interpenetrating networks form. The two components gel separately and form independent networks. Both networks are continuous throughout the sample but any interaction between them is only topological (Morris, 1986).

1.4.2 Thermodynamic incompatibility

The incompatibility of certain polymers in aqueous solution was first noted by Beijerinck in 1896. In this case two phases were formed when agar was mixed with soluble starch or gelatine. Since then, many two phase aqueous systems have been found (Chaplin, 2005). In ternary systems containing proteins and polysaccharides in aqueous medium the thermodynamic incompatibility is a general phenomenon. It generally arises in conditions when the protein is in the presence of a neutral polysaccharide or of an anionic polysaccharide bearing a charge of the same sign as the protein (close to neutrality); obviously, the main parameters involved in the mechanism are pH and ionic strength (Tolztoguzov, 2000; 2002; Schmitt et al., 1998).

The thermodynamic incompatibility appears when there is a net repulsion between the biopolymers. Clearly, solvent/biopolymer(s) interactions are favoured to the detriment of biopolymer(s)/biopolymer(s) and solvent – solvent interactions, so that the system finally demixes into two phases, each being enriched with one of the two biopolymers. These two phases are in thermodynamic equilibrium (Schmitt et al., 1998). The phase diagram for a typical protein/polysaccharide system exhibiting thermodynamic incompatibility is shown in Figure 1.5. The bold curve is usually called the binodal (or cloud point) line. When the overall composition of the system with respect to the two biopolymers lies below the binodal line, the system remains as a single homogeneous phase when viewed on the macroscopic scale. (On the molecular scale, of course, the two biopolymer solute species may be far from evenly distributed). For compositions corresponding to the points above binodal line, the system is materially unstable with respect to thermodynamic phase separation into two coexisting liquid phases – one rich in protein and the other rich in polysaccharide (Dickinson and McClements, 1995).

Figure 1.5 shows that on mixing aqueous solutions of a protein and a polysaccharide, the mixture may either be stable as a single phase (A-B_1) or break down spontaneously into two phases (A-B). For instance, by mixing solutions A and B in the volume proportion BC/AC, a mixture of composition C is obtained. This mixed solution C breaks down into two liquid phases D and E. Points D and E are binodal points. The binodal branches do not coincide with the biopolymer concentration axes. They are located fairly close to the axes. This means that

biopolymers have limited co-solubility in the common solvent, water, and that each biopolymer is mainly concentrated in one of the phases (Tolstoguzov, 1997).

The binodal branches are intersected at the critical point F, where the two coexisting phases are of the same composition and volume. At the critical point the composition of the phases are equal to that of the initial system. The compositional difference between the coexisting phases usually increases with distance from the critical point F. Point G is the phase separation threshold for a given biopolymer pair, i.e., the minimal total concentration of biopolymers required for phase separation to occur (Tolstoguzov, 1997).

The line ED is the tie-line. The tie-line connects the binodal points corresponding to the compositions of the co-existing phases. A point on the tie-line (e.g., C) corresponds to the composition of systems breaking down into phases, each with the same composition as those of D and E. The length ratio of

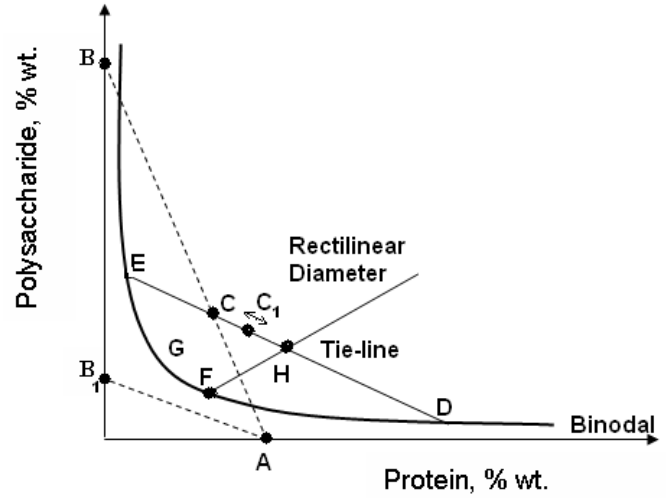

Figure 1.5 Schematic picture of a typical phase diagram of a protein-polysaccharide-water system showing the positions of binoidal curve (DFGE), critical point (F), phase separation threshold G, tie line (ED), and rectilinear diameter (FH) (Tolstoguzov, 1997)

the tie-line segments EC/CD represents the volume ratio of phases D and E. The rectilinear diameter (F-H) is the line connecting the critical point and the midpoint of the tie- line. The mixed solution corresponding to the midpoint of a tie-line breaks down into two phases of the same volume. A phase inversion phenomenon can take place in a water-in-water emulsion when its composition goes from one side of the rectilinear diameter F-H to the other side (Tolstoguzov, 1997).

1.4.2.1 Incompatibility in gelling systems

Even without phase separation, the existence of a net repulsive protein-polysaccharide interaction can influence the kinetics of gelation of one or both of the biopolymer components, as well as the microstructure and rheology of the resulting gel (Dickinson and McClements, 1995). For instance, a low level of dextran (0.2 wt%, 6.5 x 10^4 dalton) at 6^oC can greatly accelerate the rate of formation of the cross-links responsible for gelatin gelation. That is, on adding increasing amounts of dextran at a constant gelatin concentration (10 wt%), it is found that the initial effects is to increase the shear modulus of the gel as measured after a fixed gelation period, as would be expected from an enhancement in the extent of triple helix formation. However, beyond a concentration of ca 0,35 wt% dextran, any further addition of polysaccharide leads to a lowering of the modulus owing to the onset of phase separation (Dickinson and McClements, 1995).

The morphology of a two-phase gel depends on the relative proportions of the macromolecular components. When a mixed gel is formed from two incompatible copolymers A and B, there is a particular concentration ratio [A]/[B] called the "phase inversion point" where the system changes from two matrix gel A containing inclusions of gel B to a matrix of gel B containing inclusions of gel A (Brownsey and Morris, 1988).

There are some important additional complications with mixed biopolymer gels that do not arise with simple polymer composites. One problem is that the compositions of coexisting phases tend to change somewhat during gelation; this is due to solvent becoming redistributed between the phases under the influence of the polymeric conformational changes accompanying gelation. Another problem is associated with the differing rates of biopolymer gelation for the two components: the network may be almost fully formed from one of the gelling biopolymers before gelation of the second component is properly started. The process of gelation itself necessarily inhibits compositional change by greatly reducing the macromolecular diffusion coefficients. This means that the properties of a mixed gel may reflect the polymer concentrations in the two phases at the time of gelation, rather than the final "equilibrium" concentrations (Dickinson and McClements, 1995).

1.4.3 Complex coacervation

Complex coacervation occurs when the interactions between the two biopolymers are favoured. This occurs when both polymers carry an opposite charge, for instance at a pH slightly lower than the isoelectric point of the protein, while the polysaccharide still carries a negative charge. Complexation takes place, which can yield either the formation of soluble complexes or an aggregative phase

separation. In an associative phase separation, the two coexisting phases have the following composition: a rich solvent phase with very small amounts of biopolymer(s) and a rich biopolymer(s) phase forming the so-called coacervate. A schematic picture of the complex coacervation mechanism is given in Figure 1.6. The coacervation can take place in very dilute solution (Syrbe et al., 1998).

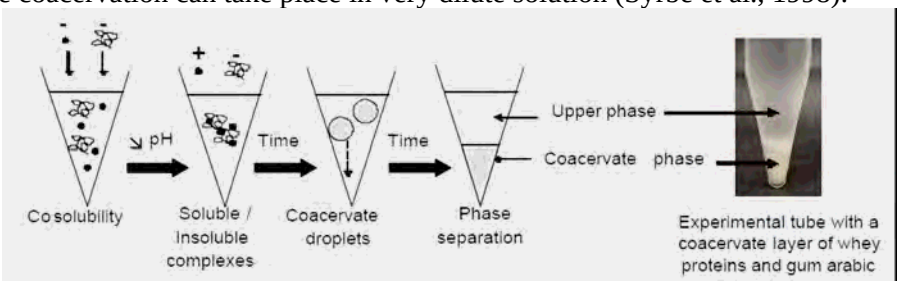

Figure 1.6 Schematic representation of the phase separation by complex coacervation (Weinbreck, 2004)

The coacervation phenomenon can sometimes be defined as simple when it involves only one biopolymer. If the biopolymer is mixed with an incompatible or poor solvent, phase separation can also occur (Schmitt et al., 1998).

1.4.3.1 Theoretical description of complex coacervation

The theory of polyelectrolyte coacervation was first addressed by Voorn and Overbeek (1957). According to it complex coacervation reflects a competition between the favorable electrical free energy, due to the attraction of oppositely charged particles, and the unfavorable entropy of mixing, which would tend to disperse the particles. Short-range electrostatic interactions are neglected, and the possibility of complexation between particles with the same charge sign is excluded. On the basis of work, with gelatins of different isoionic points, Veis and Aranyi (1960) suggested a modification to the Voorn-Overbeek theory, central to which is the formation of soluble complexes prior to coacervation. Phase separation is a result of the aggregation of these nearly neutral polyions.

The Tainaka theory (1979, 1980) is the most recent model developed for complex coacervation. According to Tainaka, the driving forces for phase separation are the electrostatic and the attractive force between the aggregates, which become stronger when the molar mass and the charge density of the polymers increase. Charge density and molar mass of the polymers should fall within a critical range for coacervation to occur. If the charge density or molar mass of the polymer becomes higher than the critical range, then a concentrated gel or a precipitate, induced by the long-range attractive forces among the aggregates, will be formed. On the other hand, for charge densities or molar mass below the range, short range repulsive forces will stabilize the dilute solution and coacervation will not occur. The Tainaka theory is more general than all the

previous theories and is applicable to both high and low charge density systems. It provides an adequate explanation of the complex coacervation process for a large number of systems (Weinbreck, 2004).

1.4.3.2 Relevance of the attractive interactions

Attractive interactions between proteins and polysaccharides are means of improving the functional properties of each biopolymer. These properties can be modulated by controlling the conditions of formation of the complexes, that is, pH, ionic strength, biopolymer concentration, biopolymer ratio, heat, and mechanical treatments. These original functional properties have been recognized for a century, and a number of industrial applications have been developed. Protein-polysaccharide complexes are used in food industry, biotechnologies, medicine, pharmacy, or cosmetic. Three important applications of complexes seem to retain higher interest than the others, namely, purification of macromolecules, microencapsulation and new materials, as ingredients (food formulation) or as biomaterials (food protection and packaging, multilayers) (Schmitt et al., 1998).

Purification of macromolecules

The extraction or purification of macromolecules through chromatographic or membrane filtration techniques is generally difficult and expensive. This is often due to the lack of selectivity and efficiency of the methods, but also to the utilization of solvents in the down process and the plugging of filtration membranes (presence of impurities), which require high amounts of energy. In contrast, the use of attractive interactions in the purification of biopolymers is a simpler and cheaper method (the cost of the method being practically only dependent of the biopolymer price). A negatively charged polymer can be added to a protein medium, and after pH adjustment, precipitation of the protein/polymer complexes occurs and the proteins are reclaimed through centrifugation and filtration. This method have been developed on a lab scale, but not yet used on an industrial scale. However, various studies have shown the good selectivity and efficiency of this method by controlling the environmental conditions (*e.g.* pH, nature of the polymer, salt) (Hidalgo and Hansen, 1971; Serov et al., 1985; Strege et al.,1990; Wang et al., 1996).

Microencapsulation

One of the most important industrial applications of complex coacervation is microencapsulation. Application of this technique is widespread in several industrial fields, including the manufacture of foods, cosmetics, pesticides, and

especially pharmaceuticals (Gennadios et al., 1994). Microencapsulation formation result from the ability to form a solid film around emulsion droplets containing the product to be encapsulated (microcapsules) and also the possibility of entrapping solvent molecules into the coacervate (see for example: Burgess, 1994; Daniels and Mittermaier, 1995; Luzzi, 1970). When coacervate droplets are formed, they usually coalesce and sediment as a separate (coacervate) phase. If an insoluble material (such as a drug particle or an oil droplet containing flavours) is present in the mixture, the coacervates will deposit at the surface of this material and, if sufficient stirring is applied to prevent sedimentation of the coacervate droplets, the compound to be encapsulated will be homogeneously coated by a layer of coacervate. A prerequisite is that the coacervate phase wets the particles or oil droplets.

Microencapsulation is a means of protecting sensitive materials (volatiles, enzymes, dyes, drugs, etc.) from the environment but also of controlling and targeting the release (Luzzi, 1970).

Food ingredients and biomaterials

Since proteins and polysaccharides are of biological origin, they can be used in products that are directly in contact with the living organism with more limited allergic risks than products with synthetic polymers (Schmitt et al., 1998). Also these macromolecules are entirely biodegradable, which limits environmental hazards. Thus, the use of protein/polysaccharide complexes in the food and cosmetics industries is not surprising. The textural properties of the coacervates allowed their use as new food ingredients, *e.g.* fat substitutes and meat analogues. An example of microparticulation treatment for the manufacture of fat replacer is given in the patent application proposed by Chen et al. (1989) using milk protein/xanthan gum complexes. Use of microprecipitated complexes to make fat substitutes has been patented by Bakker et al. (1994). Here the gelatin/galacturonic acid coacervates with a spherical shape of 11 μm diameter and a melting point of about 31.5°C was used, so that the mouthfeel was supposed to mimic that of fat. The texture of minced or fibre meat can be obtained with utilization of protein/polysaccharide complexes. Tolstoguzov et al. (1974b) used mainly caseins with addition of alginates, pectates, and low-ester pectins to prepare foodstuffs that resembled minced meat. As the protein/polysaccharide complexes exhibit many functional properties (e.g., hydration, interface stabilization, aggregation, gelation) they are able to provide new food texturization and stabilization methods.

Protein/polysaccharide complexes can be used in the manufacture of biomaterials, which can be separated into two classes, namely, biopackagings or edible films, and grafts, bioprothesis, sutures, wound dressings used in medicine. The main reasons for the use of protein/polysaccharide complexes in food packaging and protection are the biodegradability and the safety of these

macromolecules (Schmitt et al., 1998). The formation of a complex between soy isolate/sodium alginate/propylene glycol was found to have beneficial effects on the solubility and emulsifying properties of the polymers, resulting in better film properties (Shih, 1994). Another study reported the formation of edible films based on a blend of sodium caseinate and wheat or corn starch in water (Arvanitoyannis et al., 1996). Most of the films with less than 15 wt % of water displayed good strength and gas barrier properties. Some recent research found that chitosan/alginate polyelectrolyte complexes (PEC) films could be prepared by casting and drying suspensions of chitosan/alginate coacervates (Yan et al., 2001). The PEC films exhibited good *in vitro* biocompatibility with mouse and human fibroblasts, suggesting that they can be further explored for biomedical applications.

In the past 20 years, protein/polysaccharide complexes have received increased attention as biomaterials in medicine, *e.g.* for wound dressings, sutures, blood substitutes, articular prostheses, artificial grafts, or vessels (Easton and Gorham, 1986; Ellis and Yannas, 1996; O'Brien et al., 2004; Prouchayret et al., 1992; Taravel and Domard, 1995, 1996; Zaleskas et al., 2001).

Multilayers

The alternated physisorption of oppositely charged polyions at a solid/liquid interface, introduced by Decher in 1992, constitutes a versatile and powerful assembling technique for supramolecular architectures. This deposition process appears very versatile and allows the construction of films ranging in thickness from nanometers to microns. Since their discovery, many different polyelectrolyte multilayers have been reported. Combinations of polyelectrolytes with other materials, including proteins (Lvov et al., 1993, 1995, 1998; Decher et al., 1994), clay minerals (Kleinfeld and Ferguson, 1994; Lvov et al., 1996), viruses (Lvov et al., 1994), dendrimers (Watanabe and Regan, 1994) gold colloid (Feldheim et al., 1996) silica (Ariga et al., 1997; Lvov et al., 1997a) and other inorganics (Kotov et al., 1995) have mushroomed. This is an evidence for the flexibility and promise of the technique. Applications have been quick to surface. In addition to the preparation of conducting layers the following have been demonstrated: multilayers containing bound, active enzymes (Onda et al., 1996), light-emitting thin films (Ferreira et al., 1993; Fou et al., 1995; Onoda and Yoshino, 1995), permselective gas membranes (Stroeve et al., 1996; Lehr et al., 1996) noncentrosymmetric films for nonlinear optics (Laschewsky et al. 1996; Lvov et al., 1997b), selective area patterning (Hammond and Whitesides, 1995), electrochromic films (Stepp and Schlenoff, 1997), electrocatalysis (Laurent and Schlenoff, 1997) and sensors (Sun et al., 1996) with potential applications in fields as different as electrooptical devices, biomaterial coatings or drug delivery.

MATERIALS AND METHODS

2.1 Materials

For the study on the furcellaran/protein interactions, which is described in this thesis, a model system was chosen which consists of furcellaran and two globular proteins, bovine serum albumin and β-lactoglobulin.

In this thesis three furcellaran samples were analyzed, namely, native Estonian furcellaran (*Papers II, IV, V*) alkali treated Estonian furcellaran (*Papers II, IV*) and commercial furcellaran (*Papers II, III, V, VI*).

The native and alkali treated furcellaran samples were made as following. Fronds of *Furcellaria lumbricalis* were collected in Kassari Bay (the Baltic Sea, Estonia), cleaned of epiphytes and washed with tap water. For alkaline treatment 150 ml of aqueous KOH solution (2% w/w) was added to 30 g of the dry alga and stored for 7 days at room temperature. The alga was washed thoroughly with tap water until the wash water was neutral. The galactans were extracted according to Amimi et al. (2001). The crude furcellaran preparation (3g) was dissolved in 2 L milliQ water at ~100^{o}C. The solution was passed through diatomaceous earth (Sigma-Aldrich Co, Ltd., UK) and dialyzed. The Na^{+} furcellaran was obtained by elution through an ion-exchange (Amberlite IR-120) column in the Na^{+} form at 4°C. The eluant was freeze-dried.

The commercial furcellaran was a gift from FMC BioPolymer.

Bovine serum albumin and β-lactoglobulin were chosen mainly because of their good experimental accessibility. In order to build-up the furcellaran multilayers, poly-L-lysine hydrobromide with a mean degree of polymerisation of 70 was used (*Paper VI*). The BSA, BLG and PLL preparations were obtained from Sigma-Aldrich Co, Ltd., UK, and used without further purification.

2.2 Analyses used for furcellaran characterisation

Papers II and V

During the last decade, increasingly sophisticated techniques have been applied to the analysis of red algal galactans and have enabled the discovery and characterization of unusual or novel substitution patterns (Falshaw et al., 1996; 2003; Chiovitti et al., 1997a, 1997b; Errea and Matulewicz et al., 2003). These techniques include chemical methods, such as reductive hydrolysis (Stevenson and Furneaux, 1991; Usov and Klochkova, 1992), which permits the quantitative recovery and analysis of the acid-labile anhydrogalactose; reductive partial hydrolysis (Usov and Klochkova, 1992; Falshaw and Furneaux, 1995) and two-dimensional nuclear magnetic resonance (NMR) spectroscopy (Falshaw et al., 1996, 2003; Chivovitti, et al., 1997a).

The analyses used for this study for furcellaran characterisation is summarised in Table 2.1. The characteristics of furcellarans samples are presented in *Paper II*.

Table 2.1 List of analyses and analytical methods used for furcellaran characterisation

Analysis	Analytical instrument/Method	Reference	Paper
Monosaccharide composition	GC-MS	Stevenson, Furneaux, 1991; Harris et al., 1988	II, V
Sulphate	Colorimetry	Silvestri et al., 1982	II, V
Structure	^{13}C- NMR	Truus et al., 1997	II, V
Intrinsic viscosity	Ubbelholde viscometer	II, V	II, V

Typical chromatogram of furcellaran obtained by GC-MS used for qualitative and quantitative analyses of monosaccharides (*Papers II, V*) is presented in Figure. 2.1. The ^{13}C- NMR spectrum of furcellaran is shown in *Papers II* and *V*.

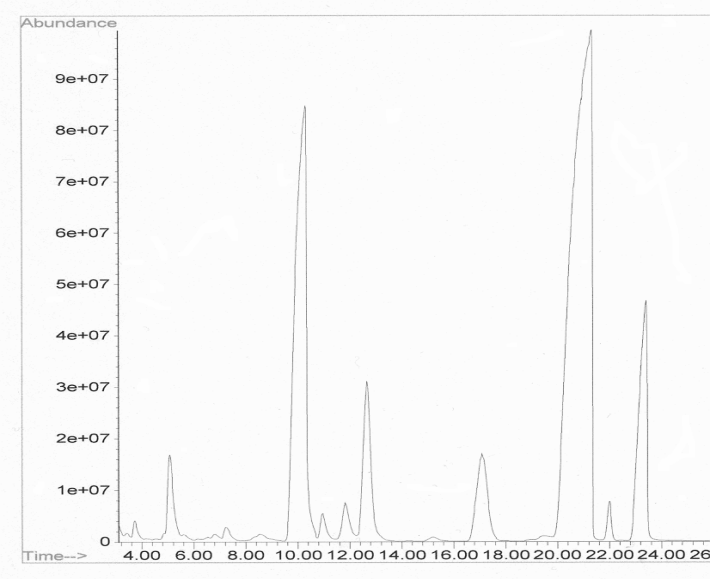

Figure 2.1. Typical GC-MS chromatogram of furcellarans

2.3 Furcellaran/globular protein (BSA, BLG) solutions

Paper V

2.3.1 Turbidimetric titration

Turbidimetric titration method have been extensively used to study polyelectrolyte-protein complexes (see for example Seyrek et al., 2003; Mattison et al., 1995; Park et al.,1992 Hattori et al., 2001). The increase of turbidity of solution referees to the formation of the complexes.

Solutions of 3.0 g L^{-1} of protein and 0.6 g L^{-1} of furcellaran were prepared in 0.03M NaCl. The initial pH was adjusted to 10.00 for BSA and 9.0 for BLG. The intensity of light scattered by, or the turbidity due to, the dispersed particles of the solution is measured as a function of pH at 600 nm (Perkin-Elmer Lambda 15 UV/VIS Spectrophotometer, Beaconsfield, Bucks) and reported as 100-%T.

2.3.2 Potentiometric titration

It is to be expected that polyelectrolyte binding must alter the local electrostatic environment of ionizable amino acid residues and thus shift their p*K*a's, making them more acidic. In the present work, we focused on the way in which the pH titration curves of BSA and BLG respond to the presence of furcellaran as a function of pH.

pH titrations were carried out with a Jenway pH meter equipped with a combination electrode, under N_2, at room temperature. A microburette was used to add 0.1 M HCl to 15 ml of a 3 g L^{-1} protein solution in 0.03M NaCl with or without 0.6 g L^{-1} furcellaran. Prior to titration the pH was adjusted to 9, pH values were recorded when the change in pH with time was < 0.01 pH units per minute.

2.3.3 Photon correlation spectroscopy

Papers I and V

Photon Correlation Spectroscopy (PCS) is a dynamic light scattering technique used to investigate dynamical properties of materials. The basic idea is to send in laser light with well defined properties (wavelength, polarization etc.) into a sample and investigate the properties of light scattered by the sample (Svanberg and Bergman, 1998).

This technique was used to characterise the dilute solution behaviour of the BLG preparation (*Paper I)* and the interaction between furcellaran and the globular proteins, BSA and BLG (*Paper V*), through the determination of an effective particle size from measurements of a translational diffusion coefficient

D_t (*Paper V, eq. 1*). The hydrodynamic radius of the particle, R_h, was calculated using the *eq. 3, Paper V*.

The apparatus employed was an ALV/SP-86 spectrogoniometer (ALV, Langen, Germany) equipped with a Coherent Radiation Innova 100-10 vis Argon Ion laser operating at 0.5 W and wavelength of 514 nm. Furcellaran (0.6 g L^{-1}) and protein solution (3g L^{-1}), at pH 9, were filtered through a 0.2 μm Millipore filter. The biopolymer solutions were weighed into a washed cuvette, mixed, and the pH of the mixture adjusted through the addition of dilute HCl. After the experiment the pH was measured.

The scattered light intensity was monitored using an ALV/PM-15 ODSIII detection system at a fixed scattering angle of 90°. After amplification and discrimination, signals were directed to an ALV/5000E digital multiple-tau correlator and time-intensity correlation functions recorded, typically for 600 seconds duration. Size distribution functions were computed using the appropriate Windows-based ALV software which incorporated regularised inverse Laplace transform and ALV-CONTIN packages. Additional analysis was undertaken using Origin V6 (Microcal) proprietory software.

2.4 Furcellaran/globular protein (BSA, BLG) gel systems

Paper III

2.4.1 Preparation of gels

For characterisation of gelation behaviour of furcellarans (*Papers II and III*) the samples were dissolved in deionised-water and dialyzed against 1M KCl solution at 4°C overnight.

In case of furcellaran protein systems (*Paper III*) mixed gels were prepared as following. Protein and furcellaran samples were dissolved separately in deionised-water at room temperature and then mixed. The solutions were dialyzed against 50 mM KCl solution at 4°C overnight to obtain gels. In case of analysing the effect of pH to the gels, the 0,01M acetate or phosphate buffer was used instead of water.

2.4.2 Rheometry

The stiffness of the gels at 25°C was determined as the shear modulus at 200 Hz calculated from the measured velocity of a shear-wave passing through the gel using a Rank pulse shearometer. In experiments on elastic gels (such as gelatin and carrageenan) which behaved as Hookean solids, it was found that the shear

modulus measured in this way was comparable to that measured using small static deformations (Ring and Stainsby, 1985).

Dynamic oscillatory rheology was used to monitor more detailed gel characteristics. The rheological properties of the gels were analysed by dynamic oscillatory controlled strain measurements using the Advanced Rheometric Expansion System (ARES-LS2). The viscoelastic properties of the gels were analysed by recording the storage modulus (*G'*), loss modulus (*G''*), and loss tangent (tanδ) during strain and frequency sweeps at 25˚C. A parallel plate measuring geometry was used with gel diameter 4mm. For frequency sweep measurements the strain value 0.1% was chosen.

2.5 Furcellaran/bovine serum albumin concentrated systems

Paper IV

2.5.1 Preparation of films

For preparation of furcellaran and furcellaran/BSA films, the aqueous solutions of furcellaran or furcellaran/protein mixture were prepared and 5g of the film-forming solution was poured onto polystyrene Petri-dishes (30 x 10 mm^2). The film-forming solutions were allowed to dry at ambient conditions for about 48 h and dried films were manually peeled off from the plates. Film thickness was measured using a micrometer (Model 102, MK-75, Kalibr, Moskva, Russia) at a 0.01-mm accuracy.

2.5.2 Water vapour permeability

Gravimetric techniques are commonly used to determine water vapour permeability (WVP) of edible films. This test has been standardized by ASTM E96-92. Two versions of this technique, the desiccant method and the water method are available. In this work, the water method was used.

The films were firmly fixed onto opening of the cells containing distilled water and placed in desiccators at 0% RH using anhydrous calcium phosphate at 25^{o}C. The cups were weighed at intervals of 1h over a 6h period and then the acquired weight was used to calculate the WVP. There were three repetitions per experiment to give the standard deviation.

2.5.3 Mechanical properties

The tensile testing provides an indication of the strength and elasticity of the film, which can be reflected by tensile strength (TS) and elongation (E) at break.

Tensile strength and percentage of elongation at break were determined using a Texture Analyzer (TA.XT2i Stable Micro Systems, UK), operated according to ASTM method D 882–22. Three rectangular strips (width 10 mm; length 5 mm) were cut from each film to measure mechanical properties. Initial grip separation and cross-head speed were set at 10 mm and 1 mm s^{-1}, respectively. The TS was calculated by dividing maximum force at break by thickness, and E was calculated by the difference in distance between grips holding the film specimen before and after the break. There were three repetitions per experiment to give the standard deviation.

2.6 Poly-L-lysine – furcellaran multilayers and the adsorption of bovine serum albumin and β-lactoglobulin onto it

Paper VI

2.6.1 Surface plasmon resonance

Measurements were carried out using a Biacore X instrument. The sensing element was a thin film of gold (~50 nm), deposited on a glass substrate mounted in a sensor chip cartridge (Biacore AB, Uppsala, Sweden). The instrument monitors changes in refractive index adjacent to the surface of the gold film by measuring the intensity of polarised light reflected from the reverse side of the glass-gold interface. The mass of adsorbed polymer per unit area (c_{spr}) was calculated using *eq. 2, Paper VI*.

Multilayers were built up by the layer-by-layer technique at a flow rate of 25 μL min^{-1}. A buffer baseline was established, then a PLL base layer was laid down by injecting 50 μL of PLL solution, followed by ~75 μL of buffer, 50 μL of furcellaran solution, and a buffer rinse as before. The sequence was repeated to form the multilayer. The gold surface was regenerated by flowing 0.1 M NaOH through the measurement cell. All measurements were made at 20 °C.

2.6.2 FTIR-ATR spectroscopy

FTIR has been extensively used to probe polyelectrolyte adsorption at surfaces (Sukhishvili et al., 1999; Sukhishvili and Granick, 1999). Infrared spectra were collected on the 860 Nicolet FTIR spectrometer fitted with a micro CIRCLE liquid ATR cell (Spectra-Tech, Warrington, UK). The ATR crystal was a cylindrical ZnSe prism, with 11 internal reflections, mounted in a thermostatted steel jacket set at a temperature of 20 °C. Biopolymer solutions were prepared as described above using D_2O instead of H_2O. 1 mL of biopolymer solution was injected and left for 16 min. After each deposition step the cell was rinsed with

2 mL of deuterated buffer. Spectra were accumulated by co-adding 1024 scans at a resolution of 2 cm^{-1} and subtracted from a background of the buffer alone.

2.6.3 Quartz Crystal Microbalance

The Quartz Crystal Microbalance (QCM) is an extremely sensitive mass sensor, capable of measuring mass changes in the nanogram range.

Measurements were carried out using a D300 quartz crystal microbalance with dissipation monitoring (QCM-D) from Q-Sense AB (Västra Frölunda, Sweden) with a QAFC 302 axial flow measurement chamber.

The formation of multilayers was investigated at 20 °C. Starting with the system primed with buffer solution, a base layer is formed by first flowing ~2.0 mL of PLL solution into a thermostatic coil in the measurement head to flush out the previous solution and allow the solution to reach thermal equilibrium. After 5 min, ~0.5 mL of this solution was allowed to flow into the measurement cell to replace the existing solution, driven by the head of liquid in the sample reservoir which flows into the thermostatic coil. The same procedure was repeated with buffer, followed by solution, buffer solution, and so on. Between each experiment the crystal chip was cleaned by sonication in 99% ethanol solution for 5 min followed by sonication in 2% Hellmanex solution for 5 min. The chips were rinsed in distilled water and then dried with N_2.

PRESENT INVESTIGATION

3.1 Objectives

Objectives of the current study were

- to extract and characterize the furcellaran from Estonian *Furcellaria lumbricalis* and to compare it with commercial Danish furcellaran
- to study the interactions between furcellaran and globular protein (bovine serum albumin and β-lactoglobulin) in solutions, gel systems and concentrated systems
- to build-up furcellaran-Poly(L)lysine multilayers and to study the protein (bovine serum albumin, β-lactoglobulin) onto it

3.2 Results and discussion

3.2.1 Characterisation of furcellaran samples from Estonian *Furcellaria lumbricalis*

The aim of this work was to extract and characterize the furcellaran from Estonian *Furcellaria lumbricalis* and to compare it with commercial Danish furcellaran.

Two different extracting conditions were used: without any treatment to get native furcellaran and alkaline pre-treatment. The alkali treatment is used to form 3,6-anhydro-α-D-galactose units from α-D-galactose 6-sulphate residues (Figure 3.1). It is important and well-known reaction of carrageenans and is used commercially to enhance gelation behaviour.

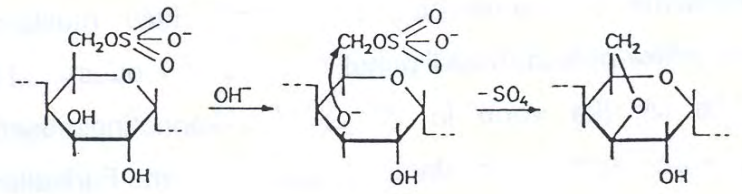

Figure 3.1. The formation of 3,6-anhydro-D-galactose unit by alkali treatment

3.2.1.1 Furcellaran compositions

Constituent sugar analysis showed that all furcellaran samples were predominantly galactans, with galactose and 3,6-anhydrogalactose the dominant sugars (*Paper II, Table1*). The reminder comprised 6-*O*-methylgalactose, xylose, glucose and mannose. Native preparation had a sulphate content approximately

18%, which decreased to approximately 16.5% after alkali modification. The sulphate content of the alkali treated preparation was comparable to that of commercial furcellaran. These results indicate that there is an average approximately one charge for every three monomer residues. Alkali treatment also resulted in a decrease in proportion of galactose and glucose residues (5% and 0,9%, respectively) and increase of 3,6-anhydrogalactose and 6-*O*-methylgalactose (6% and 0.6%, respectively). The changes in sulphate content and constituent sugars associated with alkali treatment demonstrated the presence of precursor residues in native preparation. The commercial furcellaran has more 3,6-anhydrogalactose and less galactose, xylose and mannose content compared with Estonian furcellaran.

The intrinsic viscosity results indicate that the polysaccharides have a relatively expanded conformation in 0.1M NaCl. The high intrinsic viscosity for alkali modified furcellaran of 1304 ml g^{-1}, is almost 2.5 x that of the native furcellaran.

3.2.1.2 Furcellaran structure

The ^{13}C-NMR spectrum of furcellaran is shown in *Papers II and V, Figure 1*.This spectrum was performed at 85^{o}C in order to decrease the line widths by reduce the viscosity of the samples. The assignments of this spectrum (*Papers II and V, Table 2*) were done by comparison with those of basic agar and carrageenan structures (Van de Velde, et al., 2002). The main signals are due to (1→3) linked β-D-galactopyranose; (1→4) linked 3,6-anhydro-α-D-galactopyranose; and (1→3) linked β-D-galactopyranose 4-sulphate. The different furcellarans had similar spectra; the observed differences in intensity were in agreement with the results obtained by GC/MS. The native furcellaran had more intense peaks corresponding to (1→3) linked β-D-galactopyranose residues and alkali treated and commercial furcellarans had more intense peaks corresponding to (1→4) linked 3,6-anhydro-α-D-galactopyranose.

3.2.2 Interactions between furcellaran and globular proteins bovine serum albumin and β-lactoglobulin

The aim of the study was to examine the interactions between furcellaran and globular protein (bovine serum albumin and β-lactoglobulin) in solutions, gels and concentrated systems.

3.2.2.1 Interactions in solution

Turbidimetric titrations, potentiometric titrations and photon correlation spectroscopy experiments were performed with mixtures of furcellaran and globular proteins bovine serum albumin and β-lactoglobulin at various pH and ionic strengths to obtain qualitative information about the interaction of furcellaran and globular proteins.

Behaviour of the system as a function of pH, ionic strength and furcellaran concentration

The turbidimetric titration curves for a commercial, alkali treated and native furcellaran solution containing either BSA or BLG are shown in Figure 3.2, 3.3 and in *Paper V Figure* 2, respectively. Under acidification, the mixtures of furcellaran/globular protein showed an increase of turbidity. The turbidity curves increased in two steps. These two pH transitions were designated as pH_c and pH_ϕ. The first increase appeared at pH_c of 7.5 for both BSA and BLG, and the second at pH_ϕ of 5.0 and 5.3 for BSA and BLG respectively, below which macroscopic phase separation took place. In previous research on polyelectrolyte/protein complexes (Hattori et al., 2001; Li, et al., 1996) it was shown that when the pH is independent of pH there is no complexation between polyelectrolyte and protein. Both polymers are negatively charged, which prevents their complexation. At pH_c, the turbidity of the mixture increased, showing that some attraction between polymers took place with the formation of a soluble polyelectrolyte/protein complex. The more marked change in turbidity at pH_ϕ is associated with precipitation and complex coacervation of the polyelectrolyte with the protein. As the isoionic point of the isolated proteins is ~ 5.3 for defatted BSA (Tanford et al., 1955) and ~ 5.1 for BLG (Cannan et al., 1942) this change in behaviour is occurring in the region of the isoelectric point. The more substantial aggregation and turbidity increase at lower pH's is occurring when the protein is expected to have a net positive charge.

The interaction between the globular protein and the furcellaran as a function of pH was also probed by potentiometric titration. The addition of polyanion decreases the acidity of titratable groups on the protein. For the furcellaran/BSA mixture there is a gradual divergence in the titration curve at a pH in the region of ~7.5-8.0 (*Paper V, Figure 6a*). For BLG there is a more marked divergence at pH ~7.5 (*Paper V, Figure 6b)*. For both proteins there is another change in the titration behaviour in the region of pH 5.0 – 6.0. In previous research (Wen and Dubin, 1997), the transition at the higher pH was associated with complex formation at pH_c. It was proposed that the binding of charged groups of the polyelectrolyte to proteins results in changes in local environment of the charged

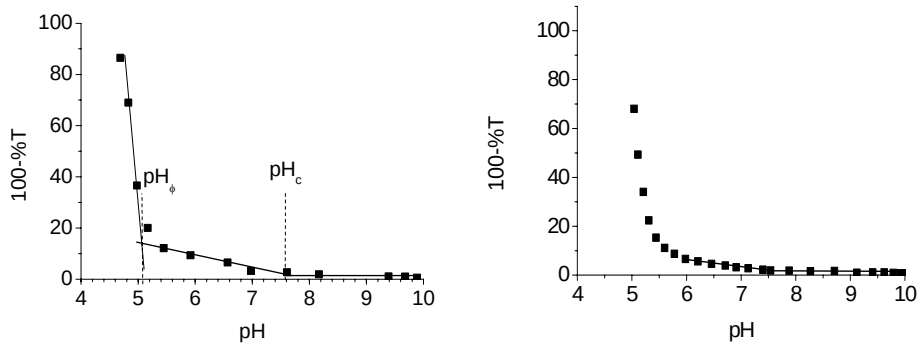

Figure 3.2 Turbidimetric titration of commercial furcellaran (0,6 g L^{-1}) BSA (3 g L^{-1}) mixture (A) and commercial furcellaran (0,6 g L^{-1}) BLG (3 g L^{-1}) mixture (B)

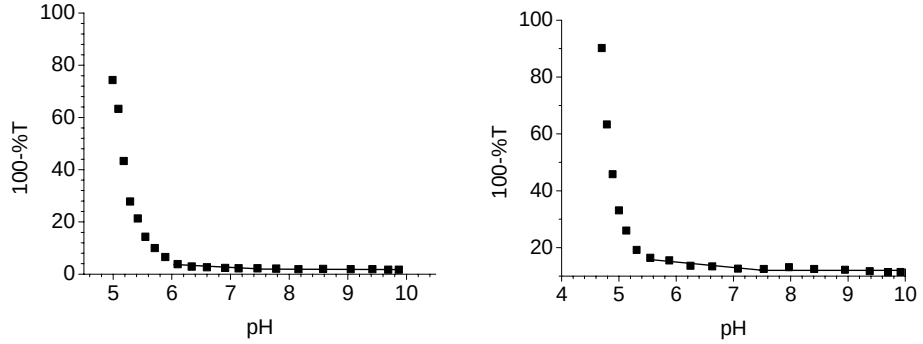

Figure 3.3 Turbidimetric titration of alkali treated Estonian furcellaran (0,6 g L^{-1}) BSA (3 g L^{-1}) mixture (A) and alkali treated Estonian furcellaran (0,6 g L^{-1}) BLG (3 g L^{-1}) mixture (B)

residues on the protein and in the pK_a of the titrable groups of the protein (Mattison et al., 1995).

The values of pH_c obtained by turbidimetric and potentiometric titration differ somewhat, perhaps as a result of their different physicochemical origins.

Next, to check whether the complexes were reversible, the turbidimetric titration upon pH was carried out. At pH > 6 the turbidity is stable over minutes (Figure 3.4 a, b) and the turbidity increase can be reversed by raising the pH (Figure 3.5 a, b). If the pH is lowered to pH 4, and then raised again, then for both BSA and BLG the turbidity increase is substantially reversible (>95%) indicating that the more substantial aggregation observed at pH's below the isoelectric point also involves a limited kinetic arrest.

The pH transitions are salt dependent, which is a well-known phenomenon. The microions screen the charges of the polymers and thus reduce the range of

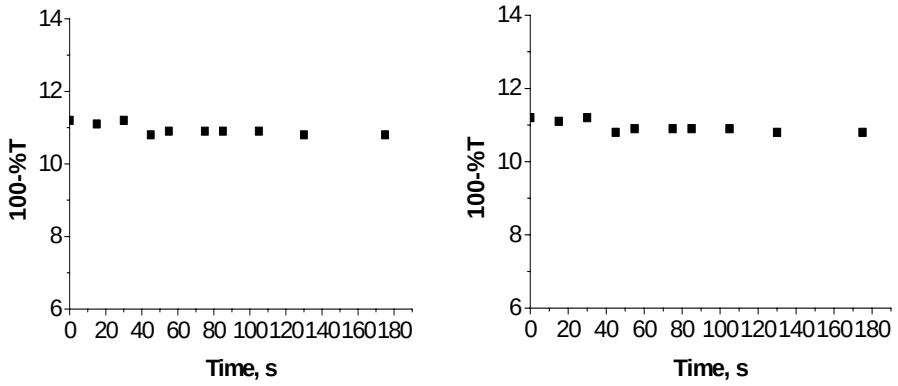

Figure 3.4. Dependence of time on the turbidity of (A) BSA-furcellaran and (B) BLG-furcellaran complex in pH 6.08

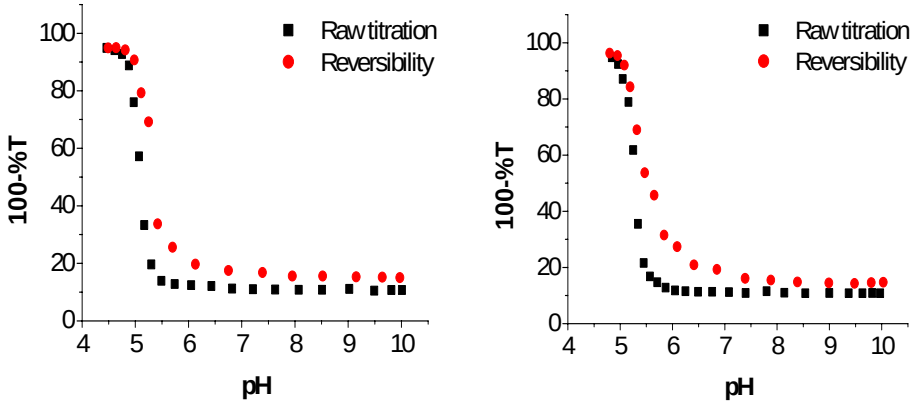

Figure 3.5 Reversibility of (A) BSA-furcellaran and (B) BLG-furcellaran mixture

their associative interaction (Schmitt et al., 1998). The ionic strength study of furcellaran and globular protein solutions showed that the values of pH_c depend on ionic strength (*Paper IV, Figure 3*). In dilute salt solutions in the range 0.01 to 0.075M, the pH_c transition is shifted to higher pH's as the ionic strength increases and then decreases on further increase in ionic strength for both BLG and BSA. This ionic strength dependence is a generally observed feature for the complexation of polyelectrolytes and proteins (Seyrek et al., 2003). Over the range of ionic strength examined the net charge on the protein at pH_c ranges from ~-9 to ~-15 (Tanford et al., 1955; Cannan et al., 1942). At each ionic strength, the charge on the proteins, BSA and BLG, at pH_c is comparable.

The dependence of furcellaran concentration on turbidity at different initial pH's for both BSA and BLG shows that at pH_i 7.0, the addition of polymer results a very small gradual increase in turbidity, but no phase separation (*Paper V, Figure 4 a,b*). It can be say that only soluble complexes form and their concentration increases with furcellaran concentration. For the lower pH_i's the addition of polymer results in a rapid turbidity increase. At pH_i 4 the turbidity increased rapidly with furcellaran concentration, goes through the maximum and then decreases again. All furcellarans behaved the same similar way.

The maximum in turbidity as a function of furcellaran concentration, which is observed for BSA, occurs in the region of charge balance. For BLG there is a broad plateau in the expected region of charge balance. For the interaction of synthetic polyelectrolytes with globular proteins, similar behaviour is observed (Wen and Dubin, 1997).

Behaviour at the molecular level

Photon correlation spectroscopy was used to get more insights into the complexation at the molecular level of furcellaran and the globular proteins, BSA and BLG. The translational diffusion coefficient D_t for BSA, BLG and furcellaran alone was first measured.

For a 0.6% w/w solution of BSA in 30 mM sodium chloride at pH 5.4 and 20°C, the measured diffusion coefficient was 5.7×10^{-11} m^2s^{-1}. The measured value of D_t is in good agreement with published research (Gaigalas et al., 1992; Meechai et al., 1999), with a calculated hydrodynamic radius of 4.2 nm.

The measured value of D_t for a 0.6% w/w BLG solution in 30 mM NaCl at pH 7.9 was 7.5×10^{-11} m^2s^{-1}, also in agreement with previous measurements carried out under similar conditions (Beretta et al., 2000; Phillies et al., 1976), with a calculated hydrodynamic radius of 3.2 nm. As the pH was reduced the presence of a slower diffusive process in the autocorrelation function was observed, which was attributed to a limited aggregation, in agreement with published research (Takata et al., 2000). At pH's of 5.5 and 4.2, a more substantial aggregation was noted, related to the phase separation/precipitation of BLG from aqueous solution.

The D_t of furcellaran in 30 mM NaCl solution (0.6% w/w) at pH 7.4 was 5.2×10^{-12} m^2s^{-1}, similar to (6.9×10^{-12} m^2s^{-1}) a κ-carrageenan preparation in 0.1M NaCl, with a average molecular weight of 421 kDa (Meunier et al., 2001).

Photon correlation spectroscopy of mixtures of furcellaran and BSA or BLG, at pH's above pH_c showed the presence of two diffusive processes corresponding to the translational diffusion of the furcellaran macromolecule and the globular protein. As the pH was lowered below pH_c there was a marked reduction in the slower process. The faster process had diffusion coefficients comparable to that of the globular protein in solution. Above the pH_c determined by turbidimetric titration, the hydrodynamic radius of the polymers in the mixture is comparable to

that of the pure polymer in solution under the same conditions. Below pH_c there is a marked stepped increase in the hydrodynamic radius of the furcellaran component. Although the total intensity of the scattered light continues to increase with decreasing pH, at pH's between pH_c and the pH_ϕ, the hydrodynamic radius of the furcellaran component does not show a strong pH dependence. Above pH_c the furcellaran in solution can be approximated to an equivalent sphere with an R_h, ~32 nm. In the region below pH_c, where it is proposed that the furcellaran forms a complex with the globular protein, this size had increased to ~135 nm for the furcellaran/BLG mixture, and ~115 nm for the furcellaran/BSA mixture.

Various models could be considered for the structure of the complex. If the globular protein could bind to more than one furcellaran chain it is possible that it could act as a crosslink. This crosslinking process would lead to the formation of large aggregates. The relatively well defined size of the BLG and BSA furcellaran complexes over a range of pH's argues against this proposal. An alternative view is that the globular proteins 'decorate' the furcellaran chain. Polysaccharides in general are fairly stiff molecules with a relatively long persistence length, it is therefore unlikely that the furcellaran chain can completely wrap around the globular protein but rather that part of the globular protein surface can interact with the polysaccharide chain and that the polysaccharide chain becomes decorated with globular protein. This interaction then results in an effective increase in size of the equivalent sphere which represents the behaviour of the complex in solution. The related increase in size could result from a more expanded/extended conformation, or a denser, less free-draining, conformation of the complex compared to the furcellaran chain in solution. The maintainence of particle size below pH_c while the intensity of scattered light is increasing suggests competition between different processes. For polyelectrolyte/protein complexation both an increase (Ball et al., 2002; Grymonpre et al., 2001) and a decrease (Weinbreck et al., 2003) in particle size of the complex relative to that of the polyelectrolyte have been observed. The origins of these differences in behaviour are not clear.

3.2.2.2 Interactions in gel systems

Gelling behaviour of furcellaran

The dependence of shear modulus *G'* on the furcellaran concentration is shown in *Paper II*, Figure 2 and *Paper III, Figure 3*. The results showed that shear modulus increased with increasing concentration of furcellaran for all three furcellaran preparations, showing most stiff gels of commercial furcellaran. The native Estonian furcellaran showed the lowest gel stiffness that was improved with alkali

treatment. There is positive correlation between 3,6-anhydrogalactose content and gel stiffness, with the alkali treatment increasing gel stiffness.

In Figure 3.6 is shown the shear modulus of furcellaran gels obtained by dialysing 1.5% w/w solution of the Na^+ form of furcellaran solution against different KCl concentrations. For the furcellarans examined, gel stiffness increased with KCl concentration, and was more marked in the concentration range 0 to 0.4 M KCl.

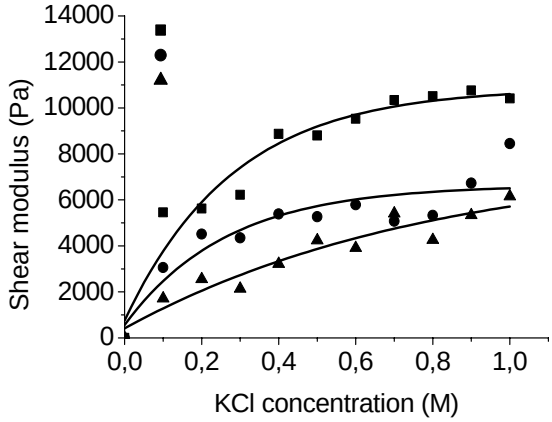

Figure 3.6. Dependence of furcellarans gels shear modulus on KCl concentration

Dynamic oscillatory rheology was used to monitor more detailed gel characteristics. The furcellaran and mixed gels in the studied pH range, showed a frequency dependence of *G'* but no *G'-G''* crossover and can be categorised as a typical physically cross-linked network gel.

Gelling behaviour of furcellaran/globular protein (BSA, BLG) mixtures

For the shear modulus in mixed furcellaran/protein gels, complex behaviour was observed (*Paper III*, *Figure 7*). Considering the work of Oakenfull et al. (1999) with gels made with κ-carrageenan and sodium caseinate, the behaviour between furcellaran and protein can be explained as follows: when small amounts of protein are added, the the *G'* increases. When more protein is added, some of the furcellaran is bound to the protein. Bound furcellaran is no longer available to contribute to the furcellaran network. Thus *G'* decreases. As the concentration of protein increases protein aggregates with bound furcellaran become sufficiently abundant to form a continuous network, *G'* then increases. All furcellarans behaved in the same general way.

The structure of the mixed furcellaran/protein gels was pH dependent. At pH 7 the gels were translucent but became turbid with decreasing pH (*Paper III*, *Figure 8*).

This change indicates a phase separation between furcellaran and the protein. The furcellaran/BSA mixed gel at pH=3.4 shows a coarse, phase separated structure (*Paper III, Figure 9*).

The study of loss tangent showed linear increase in case of pure furcellaran gels. But for mixed systems there was decrease in loss tangent between pH 3.4 and 4 where the associated phase separation occurs.

3.2.2.3 Interactions in concentrated systems – films

The objective of this study was to examine filmogenic properties of native and alkali modified Estonian furcellaran. Also the effect of globular protein BSA to furcellaran film properties was studied.

Furcellaran films

Furcellaran films were all transparent and stiff. Increasing the furcellaran concentration, the colour of the films changed from light brown to brown and the surface of the film changed from smooth to coarse. The native furcellaran films were slightly thicker than the alkali modified furcellaran films. The thickness was increasing with the furcellaran concentration (*Paper IV, Table 1*).

High tensile strengths are generally necessary for edible films in order to withstand the normal stress encountered during their application, subsequent shipping and food handling. However, flexibility of edible films, *i.e*. elongation at break should be adjusted according to the intended application of edible films (Tanaka et al., 2001). The native furcellaran films were stronger than alkali modified furcellaran films, since the tensile strength of a film is the amount of force necessary to pull the material apart (*Paper IV, Table 1*). The increase of furcellaran concentration increases the tensile strength and the elongation at break of the films. Furcellaran based films exhibited high mechanical barrier properties and are comparable with polyethylene films (TS=13–28MPa) (Park, 1996). Compared with κ-carrageenan films (TS=30MPa and E=5.0%) (Park et al., 2001), the furcellaran based films showed lower tensile strength but higher elongation at break.

The water vapour permeability of the furcellaran films increased with increasing furcellaran concentration in the film (*Paper V, Table 1)*. The reason for the increase in the permeability value may be due of the coarse surface of the film as there could be some bubbles or pinholes in it. Compared with κ-carrageenan films (0.19 ng m^{-1} s^{-1} Pa^{-1}) (Park et al., 2001), the WVP of furcellaran films was ten times smaller.

Furcellaran/BSA films

When mixing furcellaran and BSA, the films dried slower than pure furcellaran films, resulting transparent and more pliable films. The thickness of the mixed films was increasing with BSA concentration (*Paper IV, Table 2*).

The addition of BSA to furcellaran films decreases the tensile strength and elongation at break (*Paper IV, Table 2*). The decrease is more favourable with increasing the BSA content. The WVP of the films increases with the addition of BSA to furcellaran films as the protein has hydrophilic properties and is more favourable with increasing the BSA content.

3.2.2.4 Interactions in concentrated systems - multilayers

The aim of the study is to build-up furcellaran-Poly(L)lysine multilayers and to study the protein (bovine serum albumin, β-lactoglobulin) adsorption onto it.

Multilayer fabrication

Multilayer fabrication was monitored by SPR, FTIR-AR and QCM-D. Furcellaran/PLL multilayers were prepared by layer-by-layer deposition at pH 5.6. Under these conditions both polyelectrolytes are essentially fully charged. For SPR technique, PLL was initially deposited on a gold surface followed by attachment of furcellaran. Through the sequential deposition of PLL and furcellaran a 10 layer multilayer was fabricated. The build up of the multilayer was followed by surface plasmon resonance. The mass deposited shows a relatively smooth progressive increase with each new layer, with approximately equal amounts of PLL and furcellaran being laid down (*Paper VI, Figure 1*). The progressive increase in response with increasing layer number is characteristic of polyelectolyte multilayers in which one, lower molecular size component, has the ability to diffuse to the growing multilayer surface resulting in an increased capture of the next layer of oppositely charged polymer. Furcellaran carries less charge per unit mass than poly-L-lysine, because of its higher average molecular mass per repeating unit, and through one residue in every ~2.8 being charged. A consequence of the approximately equal mass deposition of furcellaran and PLL, assuming that both species are fully charged, is that the multilayer carries an excess of positive charge.

FTIR-ATR was used to obtain information on the chemical characteristics of the deposited species. Comparing the PLL and furcellaran spectras at concentration of 0.3 and 0.8 % w/w at pD 5.6 (*Paper VI, Figure 2*), it can be seen that the PLL spectrum has strong absorbances at 1643 cm^{-1} and 1460 cm^{-1}. The latter is the amide II' band which includes contributions from CN stretching and other backbone modes, and the absorbance at 1643 cm^{-1} the amide I band, the

precise location of which is conformation dependent, and for poly-L-lysine in a random coil conformation (Jackson et al., 1989) occurs in the range 1643-1648 cm^{-1}. The furcellaran spectrum is similar to reported spectra of κ-carrageenan and includes features which have been assigned to 3,6-anhydro-D-galactose (932 cm^{-1}) and glycosidic linkages (1075 cm^{-1}) (Pereira et al., 2003). The spectra of assembled PLL/furcellaran multilayer films in the region 800-1800 cm^{-1} is shown in *Paper VI, Figure 3*. The bands at 1456 and 1643 cm^{-1} are characteristic of the presence of PLL in the multilayer. The subsequent addition of furcellaran causes little change in the peak absorbance of these bands but does lead to an increase in absorbance of the bands associated with furcellaran at 932 and 1075 cm^{-1}. The alternating, stepwise addition is shown by examining how the absorbance of bands characteristic of furcellaran (1075 cm^{-1}) and PLL (1643 cm^{-1}) increases with increasing number of layers (*Paper VI, Figure 4*).

The assembly of the multilayer film was also monitored by QCM-D starting with a PLL layer (*Paper VI, Figure 5a*). It shows the frequency shift for the deposition of the first 5 layers starting with the deposition of PLL on the sensor surface. The decrease in Δf observed for the first PLL and furcellaran layers is associated with an increase in adsorbed hydrated mass. Subsequent addition of PLL to the furcellaran layer leads to little significant change in Δf (*Paper VI, Figure 5a,b*). The trends observed for layer deposition using QCM-D are qualitatively different from those observed by SPR and FTIR-ATR, with the latter techniques probing the mass of polymer deposited and the QCM-D probing hydrated mass. The large response during the contact of the film with the polyanion solution and the very small response during contact with polycation solution, suggests that the smaller molecular size polycationic PLL is diffusing within the furcellaran layer, and that the observed QCM-D response is a balance between the small increase in mass associated with the deposition of PLL, and its effect on deswelling the multilayer arising as a result of the replacement of monovalent cationic counterions with a polyvalent counterion (PLL). The QCM-D experiment also contains information on the viscous dissipation of the multilayer (*Paper VI, Figure 5c*) indicating that PLL crosslinks the furcellaran layer, and interpreting this change using the fit to the Voigt viscoelastic model (*Paper VI*, eq. 5,6), a reduction in hydrated mass and shrinkage of the adsorbed layer. This phenomen has been previously been observed in the assembly of high DE pectin/PLL multilayers (Krzeminski et al., 2005). The hydrated mass from the QCM-D modelling, combined with polymer mass from the SPR, yields a solids concentration of 7.0±1.0% w/w for the adsorbed layer, indicating that under these conditions of preparation a relatively hydrated, porous multilayer was formed.

Globular protein binding to the multilayer

Six layer PLL/furcellaran multilayers were prepared with furcellaran as the topmost layer. The binding of the globular proteins BSA and BLG to the multilayer was examined as a function of pH. *Figure 6 a, b* in *Paper VI* shows the FTIR spectra of multilayers before and after the binding of BSA and BLG at pH 5.0. There is a substantial FTIR spectral change on binding, with a particularly marked increase in the absorbance of the amide I and amide II' bands. As the isoionic point of the isolated proteins is ~5.3 for defatted BSA (Tanford et al., 1955) and ~5.1 for BLG (Cannan et al., 1942) at pH 5.0, it is expected that the proteins will carry a small net positive charge. Solution studies on the interaction of globular proteins (BSA and BLG) with furcellaran shows that globular protein/furcellaran complexes may be formed at pHs where the protein carries a net charge of the same sign as the polyelectrolyte, with a more substantial aggregation or coacervation occurring below the isoelectric point when the protein acquires a net positive charge (*Paper V*). In the region where both polymers carry a net charge of the same sign it is considered that the polyelectrolyte interacts with oppositely charged patches on the protein surface (Hallberg and Dubin, 1998; Seyrek et al., 2003). The adsorption of BSA and BLG to the PLL/furcellaran multilayer was pH-dependent (*Paper VI, Figure 7*). Over the pH range 6.5 to 8 there is relatively little adsorption. As the pH is reduced to 5.0 there is a progressive increase in the amount adsorbed, and the observed behaviour is comparable to the generic complexation behaviour of polyelectrolytes and proteins which is observed in aqueous solution, and more particularly the observed complexation of furcellaran and globular proteins (*Paper V*). The pH-dependent adsorption was reversible. For both BSA and BLG the amount adsorbed at pH 5.0, calculated from the resonance response, is ~ 650 ng cm^{-2}, substantially more than the amount of PLL that would be deposited on the furcellaran layer (*Paper VI, Figure 1*), and partially reflecting differences in mass/charge ratio. Over the pH range 6.5 to 5 the PLL/furcellaran multilayer shows a limited change in hydration leading to a frequency response in the QCMD experiment of < -50 Hz. The sign of the frequency response indicates that deposition of the globular proteins leads to an increase in hydrated mass, and the effect of partially neutralizing the charge on the furcellaran with a polyampholyte (leading to deswelling, and mass loss) is more than compensated for by the mass of protein deposited. This is in contrast to the behaviour observed on PLL deposition and reflects differences in mass/charge ratio for the different species. The observed pH-dependent response (*Paper VI, Figure 7*), is similar to the observed pH-dependent complexation of the globular proteins BSA and BLG with furcellaran (*Paper V*).

Studies on the binding of globular proteins to polyelectrolyte multilayers show that the observed behaviour may be rather complex (Gergely et al., 2004; Ladam

et al., 2000; Salloum and Schlenoff, 2004). There is general agreement that electrostatic interactions dominate the observed behaviour. In a recent study it was found that the amount of protein adsorbed showed characteristically different behaviour depending on the charge on the terminating layer. It was proposed that the protein was drawn into the whole multilayer when the terminating layer was of opposite charge, whereas a more limited adsorption occurred when the terminating layer was of like charge (Salloum and Schlenoff, 2004). In the present study, the amounts of protein adsorbed are comparable to a limited adsorption. From the molecular sizes and weights of the proteins it is possible to calculate the adsorbed amount for monolayer coverage. Assuming that both BLG and BSA can be represented as an equivalent sphere in solution, with hydrodynamic radii of 2.93 (Baldini et al., 1999), and 3.7 nm (Carter and Ho, 1994), and that surface coverage is 60% of the available area, then monolayer adsorption for both BLG and BSA would give an adsorbed amount of ~ 130 ng cm^{-2}. For a furcellaran terminated multilayer at pH 5, the amount adsorbed is equivalent to the deposition of ~ 5 protein layers. As pH is increased towards neutrality the amount adsorbed decreases, in a similar way to that observed for the binding of human serum albumin to a polyglutamic acid terminated layer. For polyanion/protein complexes, decreases in the ability of the polyanion to complex protein are also observed in this pH range (Hallberg and Dubin, 1998). It is proposed that in the current study, that the furcellaran terminated layer is relatively permeable to the globular proteins and allows their complexation.

CONCLUSIONS

Based on the current study, following conclusions can be made.

Comparing the Estonian furcellaran with the commercially available furcellaran, there is no difference in structure but there is some difference in monosaccharide composition: the Estonian furcellaran has less 3,6-anhydrogalactose and more galactose, xylose and mannose content compared with commercial furcellaran. Remarkable difference occurred in rheological properties of furcellarans. The Estonian furcellaran has higher intrinsic viscosity and smaller shear modulus than commercial furcellaran.

Furcellaran can form soluble complexes with the globular proteins, bovine serum albumin and β-lactoglobulin. The complexation occurs at a pH where the protein carries a net negative charge. With increasing ionic strength, as the charge on the polymers becomes screened, the attractive interaction between the negatively charged furcellaran and positively charged patches on the protein becomes more favoured. Further increase in ionic strength then reduces the strength of this interaction. The observed ionic strength dependence is consistent with observation and indicates that the release of counterions associated with the protein on complexation, is an important driving force for complex formation. The onset of complex coacervation/precipitation occurs in the region of the isoelectric point of the protein and becomes increasingly favoured as the protein acquires a net positive charge, opposite in sign to that of the furcellaran.

Furcellaran and globular proteins can form physically cross-linked network gels. The initial addition of protein to furcellaran solution increased shear modulus, further increase in BSA content leads to a decrease in gel shear modulus. The structure of the mixed furcellaran/protein gels was pH dependent. At low pH the associated phase separation occurred and loss tangent changed.

Furcellaran can be used as film-forming agent. The furcellaran based films exhibited good mechanical barrier properties. The addition of BSA makes films more pliable, however the film properties decline as the tensile strength and elongation at break of composite films decrease and water vapour permeability increases.

Furcellaran can be used to fabricate multilayer structures with PLL by a layer-by-layer technique. These structures can bind the globular proteins, BSA and BLG, the pH dependence of the binding is comparable to the observed complexation behaviour of furcellaran with globular proteins in aqueous solution, with complexation occurring at pH’s where both biopolymers carry an average net charge of the same sign.

REFERENCES

Amimi, A., Mouradi, A., Givernaud, T., Chiadmi, N., Lahaye, M. 2001. Structural analysis of *Gigartina pistillata* carrageenans (Gigartinaceae, Rhodophyta). *Carbohydrate Research* 333: 271-279.

Antosiewicz, J., McCammon, J. A. and Gilson, M. K. 1996. The determinants of pKas in proteins. *Biochemistry* 35: 7819-7833.

Ariga, K., Lvov, Y., Onda, M., Ichinose, I. and Kunitake, T. 1997. Alternately assembled ultrathin films of silicananoparticles and linear polycations. *Chemistry Letters:* 125-126.

Arvanitoyannis, I., Psomiadov, E. and Nakayama, A. 1996. Edible films made from sodium caseinate, starches, sugar or glycerol. I. *Carbohydrate Polymers* 31: 179-192.

Asakura S. and Oosawa, F. 1954. On interaction between two bodies immersed in a solution of macromolecules. *Journal of Chemical Physics* 22: 1255-1256.

ASTM D882-22. 1992. Test Methods for Tensile Properties of Thin Plastic Sheeting. In: *Annual Book of ASTM Standards.* ASTM, Philadelphia, USA, p.182-187.

ASTM E96-92. 1992. Water Vapour Transmission of Materials. In: *Annual Book of ASTM Standards.* ASTM, Philadelphia, USA, p.702-709.

Bakker, M. A. E., Koning, M. M. G. and Visser, J. 1994. Fatty ingredients, WO Patent Application 94/14334, Unilever.

Baldini, G., Beretta, S., Chirico, G., Franz, H., Maccioni, E., Mariani, P. and Spinozzi, F. 1999. Salt-induced association of beta-lactoglobulin by light and X- ray scattering. *Macromolecules* 32: 6128-6138.

Ball, V., Winterhalter, M., Schwinte, P., Lavalle, P., Voegel, J. C. and Schaaf, P. 2002. Complexation mechanism of bovine serum albumin and poly(allylamine hydrochloride). *Journal of Physical Chemistry B* 106: 2357-2364

Beretta, S., Chirico, G. and Baldini, G. 2000. Short-range interactions of globular proteins at high ionic strengths. *Macromolecules* 33 : 8663-8670.

Boulmedais, F., Frisch, B., Etienne, O., Lavalle, P., Picart, C., Ogier, J., Voegel, J.C., Schaaf, P. and Egles, C. 2004. Polyelectrolyte multilayer films with pegylated polypeptides as a new type of anti-microbial protection for biomaterials. *Biomaterials* 25(11):2003-2011.

Brownsey, G. J. and Morris, V. J. 1988. Food Structure – Its Creation and Evaluation (eds. J.M.V. Blanshard and J.R. Mitchell), Butterworths, London, p.7

Burgess, D. J. 1994. Complex coacervation: microcapsule formation. In: *Macromolecular complexes in chemistry and biology*. (Eds. Dubin, Bock, Davis, Schulz, Thies). Springer Verlag: Berlin, Ch. 17, p. 285-300.

Burgess, D. J. and Carless, J. E. 1985. Manufacture of gelatin/gelatin coacervate microcapsules. *International Journal of Pharmaceutics* 27: 61-70.

Cannan, R. K., Palmer, A. H. and Kibrick, A. C. 1942. The hydogen ion dissociation curve of β-lactoglobulin. *Journal of Biological Chemistry* 142: 803-822.

Carter, D. C. and Ho, J. X. 1994. Structure of serum albumin. *Advances In Protein Chemistry* 45: 153-203.

Chaplin, M. 2005. Aqueous biphasic systems. Water structure and behaviour. (http://www.lsbu.ac.uk/water/index.html)

Chen, W.-S., Henry, G. A., Gaud, S. M., Miller, M. S., Kaiser, J. M., Balmadeca, E. A., Morgan, R. G., Baer, C. C., Borwankar, R. P., Hellgeth, L. C., Strandholm, J. J., Hasenheuttl, G. L., Kerwin, P. J., Chen, C. C., Kratochvil, J. F. and Lloyd, W. L. 1989. Microfragmented ionic polysaccharide/protein complex dispersions. European Patent Application, 0,340,035,A2, Kraft General Foods Inc.

Chiovitti, A., Bacic, A., Craik, D. J., Munro, S. L. A., Kraft, G. T. and Liao, M.-L. 1997a. Cell-wall polysaccharides from Australian red algae of the family Solieriaceae (Gigartinales, Rhodophyta): novel, highly pyruvated carrageenans from the genus *Callophycus*. *Carbohydrate Research* 299: 229– 243.

Chiovitti, A., Bacic, A., Craik, D. J., Munro, S. L. A., Kraft, G. T. and Liao, M.-L. 1997b. Carrageenans with complex substitution patterns from red algae of the genus *Erythroclonium*. *Carbohydrate Research* 305: 243–253.

Clark, A. H. 1998. Gelation of globular proteins. In: Functional properties of Food Macromolecules (Eds. S. E. Hill, J. Mitchell and D. Ledward), Aspen Publishers Inc., Maryland, pp. 77-142

Dahne, L., Leporatti, S., Donath E. and Mohwald, M. 2001. Fabrication of micro reaction cages with tailored properties. *Journal of the American Chemical Society* 123: 5431-5436

Daniels, R. and Mittermaier, E. M. 1995. Influence of pH adjustment on microcapsules obtained from complex coacervation of gelatin and acacia. *Journal of Microencapsulation* 12(6): 591-599.

De Kruif C. G. and Tuinier R. 2001. Polysaccharide protein interactions. *Food Hydrocolloids* 15: 555-563.

Decher, G., Hong, J. D. and Schmitt, J. 1992. Buildup of Ultrathin Multilayer Films by a Self-Assembly Process: III. Consecutively Alternating Adsorption of Anionic and Cationic Polyelectrolytes on Charged Surfaces. *Thin Solid Films 210/211:* 831-835.

Decher, G., Lehr, B., Lowack, K., Lvov, Y. and Schmitt, J. 1994. New nanocomposite films for biosensors: layer-by-layer adsorbed film of polyelectrolytes, proteins or DNA. *Biosensensors & Bioelectronics* 9: 677-684.

Dickinson, E. 1988. The role of hydrocolloids in stabilising particulate dispersions and emulsions. In: *Gums and stabilisers for the food industry* (eds G.O. Phillips, D.J. Wedlock and P.A. Williams), IRL Press, Oxford, vol. 4, p. 249-263

Dickinson, E. and McClements, D.J. 1995. Protein-Polysaccharide Interactions. In: *Advances in Food Colloids* (Eds. E. Dickinson and D.J. McClements), Chapman and Hall, UK p.81-101

Doublier, J.-L., Garnier, C., Renard, D. and Sanchez, C. 2000. Protein-Polysaccharide Interactions. *Current Opinion in Colloid & Interface Science* 5: 202-214.

Drohan, D.D., Tziboula, A., McNulty, D. and Horne, D.S. 1997. Milk protein-carrageenan interactions. *Food Hydrocolloids* 11: 101-107.

Easton, I. A. and Gorham, S. D. 1986. Protein/polysaccharide complexes. US Patent Application 4,614,794, Johnson and Johnson.

Edelman, M. W., 2003. Segregative phase separation in aqueous mixtures of polydisperse biopolymers. *PhD thesis, Wageningen University, The Netherlands*

Ellis, D. L. and Yannas, I. V. 1996. Recent advances in tissue synthesis *in vivo* by use of collagenglycosaminoglycan copolymers. *Biomaterials* 17(3): 291-299.

Errea, M.I. and Matulewicz, M.C. 2003. Unusual structures in the polysaccharides from the red seaweed *Pterocladiella capillacea* (Gelidiaceae, Gelidiales). *Carbohydrate Research* 338: 943–953.

Etienne, O., Picart, C., Taddei, C., Haikel, Y., Dimarcq, J. L., Schaaf, P., Voegel, J. C., Ogier, J. A. and Egles, C. 2004. Multilayer Polyelectrolyte Films Functionalized by Insertion of Defensin: a New Approach to Protection of Implants from Bacterial Colonization. *Antimicrobial Agents and Chemotherapy* 48(10): 3662-3669

Falshaw, R. and Furneaux, R. H. 1995. The structural analysis of disaccharides from red algal galactans by methylation and reductive partial-hydrolysis. *Carbohydrate Research* 269: 183–189.

Falshaw, R., Furneaux, R. H. and Wong, H. 2003. Analysis of pyruvylated β-carrageenan by 2D NMR spectroscopy and reductive partial hydrolysis. *Carbohydrate Research* 338: 1403–1414.

Falshaw, R., Furneaux, R. H., Wong, H., Liao, M.-L., Bacic, A. and Chandrkrachang, S. 1996. Structural analysis of carrageenans from Burmese and Thai samples of *Catenella nipae* Zanardini. *Carbohydrate Research* 285: 81–98.

Feldheim, D. L., Grabar, K. C., Natan, M. J. and Mallouk, T. C. 1996. Electron Transfer in Self-Assembled inorganic Polyelectrolyte/Metal Nanoparticle Heterostructures. *Journal of American Chemical Society* 118: 7640-7641.

Ferreira, M., Rubner, M. F. and Hsieh, B. R. 1993. Luminescence Behaviour of Self-Assembled Multilayer Heterostructure of Poly(Phenylene Vinylene). In: *Materials Research Society Symposium Proceedings*. 328: 119.

Fou, A. C., Onitsuka, O., Ferreira, M., Rubner, M. F. and Hsieh, B. R. 1995. Interlayer Interaction In Self-Assembled Poly(P-Phenylene Vinylene) Multilayer Hetrostructures: Implications For Light Emitting And Photorectifying Diodes. In: *Materials Research Society Symposium Proceedings* 369: 575.

Gaigalas, A. K., Hubbard, J. B., McCurley, M. and Woo, S. 1992. Diffusion of bovine serum albumin in aqueous solutions. *Journal of Physical Chemistry* 96: 2355-2359.

Galazka, V.B., Smith, D., Ledward, D.A., and Dickinson, E. 1999. Complexes of bovine serum albumin with sulphated polysaccharides: effects of pH, ionic strength and high pressure treatment. *Food Chemistry* 64: 303-310.

Gennadios, A., McHugh, T. H., Weller C. L. and Krochta J. M. 1994. Edible films and coatings based on proteins. In *Edible Films and Coatings to Improve Food Quality*. (Eds. J.M. Krochta, E. Baldwin and M.O. Nisperos-Carriedo), Technomic Publishing Co., Lancaster, PA. pp. 201-278

Gergely, C., Bahi, S., Szalontai, B., Flores, H., Schaaf, P., Voegel, J. C. and Cuisinier, F. J. G. 2004. Human serum albumin self-assembly on weak polyelectrolyte multilayer films structurally modified by pH changes. *Langmuir* 20: 5575-5582.

Glicksman, M. 1983. Red seaweed extracts (agar, carrageenan, furcellaran). In: *Food Hydrocolloids* (Ed. M. Glicksman), CRC Press, New York, pp 73-113.

Grymonpre, K. R., Staggemeier, B. A., Dubin, P. L. and Mattison, K. W. 2001. Identification by integrated computer modeling and light scattering studies of an electrostatic serum albumin-hyaluronic acid binding site. *Biomacromolecules* 2: 422-429.

Guiseley, K.B., Stanley, N.F. and Whitehouse, P.A. 1980. Carrageenan. In: *Handbook of water-soluble gums and resins* (Ed. R.L.Davidson), McGraw-Hill Inc., New York, Ch. 5., pp.1-30.

Hallberg, R. K. and Dubin, P. L. 1998. Effect of pH on the binding of beta-lactoglobulin to sodium polystyrenesulfonate. *Journal of Physical Chemistry B* 102: 8629-8633.

Hammond, P. T. and Whitesides, G. M. 1995. Formation of Polymer Microstructures by Selective Deposition of Polyion Multilayers Using Patterned Self-Assembled Monolayers as a Template. *Macromolecules* 28: 7569-7571.

Harris, P.J., Blakeney, A.B., Henry, R.J., Stone, B.A. 1998. Gas chromatographic determination of the monosaccharide composition of plant cell wall preparations. *Journal of the Association of Official Analytical Chemists* 71: 272-275

Hattori, T., Kimura, K., Seyrek, E. and Dubin, P.L. 2001. Binding of Bovine Serum Albumin to Heparin Determined by Turbidimetric Titration and Frontal Analysis Continuous Capillary Electrophoresis. *Analytical Biochemistry* 295: 158–167

Hidalgo J. and Hansen, P. M. T. 1971. Selective precipitation of whey proteins with carboxymethylcellulose. *Journal of Dairy Science* 54(9): 1270-1274.

Hidalgo, J. and Hansen, P.M.T. 1969. Interactions between food stabilizers and β-lactoglobulin. *Journal of Agricultural and Food Chemistry* 17: 1089-1092.

Huffman, F.G. and Shah, Z.C. 1995. Carrageenans. Uses in food and other ingredients. *Nutrition Today* 30: 246-253.

Hugerth, A. and Sundelöf, L.-O. 2001. The effect of polyelectrolyte counterion specificity, charge density, and conformation on polyelectrolyte-amphiphile interaction: the carrageenan/furcellaran – amitriptyline system. *Biopolymers* 58:186-159

Jackson M., Haris, P. I., and Chapman, D. 1989. Conformational Transitions in Poly(L-lysine) - Studies Using Fourier-Transform Infrared-Spectroscopy. *Biochimica et Biophysica Acta* 998: 75-79.

Jung, L. S., Campbell, C. T., Chinowsky, T. M., Mar, M. N., and Yee, S. S. 1998. Quantitative interpretation of the response of surface plasmon resonance sensors to adsorbed films. *Langmuir* 14: 5636-5648.

Kleinfeld, E. R. and Ferguson, G. S. 1994. Stepwise formation of multilayered nanostructural films from macromolecular precursors. *Science* 265: 370-373.

Kotov, N. A., Dekany, I. and Fendler, J. H. 1995. Layer-by-Layer Self-Assembly of Polyelectrolyte-Semiconductor Nanoparticle Composite Films. *Journal of Physical Chemistry* 99: 13 065-13069.

Kuwata, K., Hoshino, M., Forge, V., Era, S., Batt, C. A. and Goto, Y. 1999. Solution structure and dynamics of bovine beta-lactoglobulin A. *Protein Science* 8: 2541-2545.

Ladam, G., Gergely, C., Senger, B., Decher, G., Voegel, J. C., Schaaf, P. and Cuisinier, F. J. G. 2000. Protein interactions with polyelectrolyte multilayers: Interactions between human serum albumin and polystyrene sulfonate/polyallylamine multilayers. *Biomacromolecules* 1: 674-687.

Laschewsky, A., Mayer, B., Wischerhoff, E., Arys, X., Bertrand, P., Delcorte, A. and Jonas, A. 1996. A new route to thin polymeric, non-centrosymmetric coatings. *Thin Solid Films* 284/5: 334-337.

Laurent, D. and Schlenoff, J. B. 1997. Multilayer assemblies of redox polyelectrolytes. *Langmuir* 13: 1552-1557.

Lehr, B., Seufert, M., Wenz, G. and Decher, G. 1996. Fabrication of poly(p-phenylene vinylene) (PPV) nano-heterocomposite films via layer-by-layer adsorption. *Supramolecular Science* 2: 199-207.

Li, Y. J., Mattison, K. W., Dubin, P. L., Havel, H. A. and Edwards, S. L. 1996. Light scattering studies of the binding of bovine serum albumin to a cationic polyelectrolyte. *Biopolymers* 38: 527-533.

Luzzi, L. A. 1970. Microencapsulation. *Journal of Pharmaceutical Science* 59(10): 1367-1376.

Lvov, Y., Ariga, K., Ichinose, I. and Kunitake, T. 1995. Assembly of multicomponent protein films by means of electrostatic layer-by-layer adsorption. *Journal of American Chemical Society* 117: 6117-6122.

Lvov, Y., Ariga, K., Ichinose, I. and Kunitake, T. 1996. Formation of ultrathin multilayers and hydrated gel from montmorillonite clay and linear polycations. *Langmuir* 12, 3038-3044.

Lvov, Y., Ariga, K., Ichinose, I. and Kunitake, T. 1997. Alternate assembly of ordered multilayers of SiO2 and other nanoparticles and polyions. *Langmuir* 13: 6195-6203.

Lvov, Y., Decher, G. and Sukhorukov, G. 1993. Assembly of thin films by means of successive deposition of alternate layers of DNA and poly(allylamine). *Macromolecules* 26: 5396-5399.

Lvov, Y., Haas, H., Decher, G., Möhwald, H., Mikhailov, A., and Vainshtein, B. 1994. Successive deposition of alternate layers of polyelectrolytes and charged virus. *Langmuir* 10, 4232-4236.

Lvov, Y., Lu, Z., Schenkman, J. B. and Rusling, J. F. 1998. Direct electrochemistry of myoglobin and cytochrome P450cam in alternate layer-by-layer films with DNA and other polyions. *Journal of American Chemical Society* 120: 4073-4080.

Lvov, Y., Yamada, S. and Kunitake, T. 1997b. Nonlinear optical effects in layer-by-layer alternate films of polycations and an azobenzene-containing polyanion. *Thin Solid Films* 300: 107-112.

Mattison, K.W., Brittain, I.J. and Dubin, P.L. 1995. Protein-Polyelectrolyte Phase Boundaries. *Biotechnology Progress* 17: 632-637

Meechai, N., Jamieson, A. M. and Blackwell, J. 1999. Translational Diffusion Coefficients of Bovine Serum Albumin in Aqueous Solution at High Ionic Strength *Journal of Colloid and Interface Science* 218: 167-175.

Meunier, V., Nicolai, T. and Durand, D. 2001. Structure of aggregating kappa-carrageenan fractions studied by light scattering. *International Journal of Biological Macromolecules* 28: 157-165.

Moirano, A.L. 1977. Sulfated seaweed polysaccharides. In: *Food colloids* (Ed. H.D. Graham), The AVI Publishing Company, Inc., Westport, Ch. 8, pp.347-381.

Morris, V. J. 1986. Multicomponent gels. In *Gums and stabilisers for the food industr*y 3 (eds. G.O. Philips, D.J. Wedlock, P.A. Williams), Elsevier, London, pp. 87-99

Morris, V. J. 1998. Gelation of polysaccharides. In: Functional properties of Food Macromolecules (Eds. S. E. Hill, J. Mitchell and D. Ledward), Aspen Publishers Inc., Maryland, pp. 143-226

Morris, V.J. 1991. Food Polymers, Gels and Colloids (ed. E.Dickinson), Royal Society of Chemistry, Cambridge, p. 310.

Nakajima, A. and Sato, H. 1972. Phase relationships of an equivalent mixture of sulfated polyninyl alcohol and aminoacetalyzed polyvinyl alcohol in microsalt aqueous solution. *Biopolymers* 10: 1345-1355.

O'Brien, F. J., Harley, B. A., Yannas, I. V. and Gibson, L. 2004. Influence of freezing rate on pore structure in freeze-dried collagen-GAG scaffolds. *Biomaterials* 25(6): 1077-1086.

Oakenfull, D., Miyoshi, E., Nishinari, K. and Scott, A. 1999. Rheological and thermal properties of milk gels formed with κ-carrageenan. I. Sodium caseinate. *Food Hydrocolloids* 13: 525-533

Onda, M., Lvov, Y., Ariga, K. and Kunitake, T. 1996. Sequential reactions by glucose oxidase/peroxidase molecular films assembled by layer-by-layer alternate adsorption. *Biotechnology & Bioengineering* 51: 163-166.

Onoda, M. and Yoshino, K. 1995. Heterostructure electroluminescent diodes prepared from self-assembled multilayers of poly(p-phenylene vinylene) and sulfonated polyaniline. *Japanese Journal of Applied Physics* 34: 260-263.

Ould Eleya, M.M. and Turgeon, S.L. 2000. Rheology of κ–carrageenan and β-lactoglobulin mixed gels. *Food Hydrocolloids* 14: 29-40

Park, H. J. 1996. Physical propertie os carrageenan films. *Food Science and Industry* 29: 47–53

Park, J.M., Muhoberac, B.B., Dubin, P.L. and Xia, J. 1992. Effects of Protein Charge Heterogeneity in Protein-Polyelectrolyte Complexation. *Macromolecules* 25: 290-295

Park, S. Y., Lee, B. I., Jung, S. T. and Park, H. J. 2001. Biopolymer composite films based on κ-carrageenan and chitosan. *Material Research Bulletin* 36: 511-519.

Pereira, L., Sousa, A., Coelho, H., Amado, A. M. and Ribeiro-Claro, P. J. A. 2003. Use of FTIR, FT-Raman and (13)C-NMR spectroscopy for identification of some seaweed phycocolloids. *Biomolecular Engineering* 20: 223-228.

Phillies, G. D. J., Benedek, G. and Mazer, N. A. 1976. Diffusion in Protein Solutions at High Concentrations: A Study by Quasielastic Light Scattering Spectroscopy *Journal of Chemical Physics* 65: 1883-1892.

Picart, C. Lavalle, P., Hubert, P., Cuisinier, F. J. G., Decher, G., Schaaf, P. and Voegel, J.-C. 2001. Buildup Mechanism for Poly(L-lysine)/Hyaluronic Acid Films onto a Solid Surface. *Langmuir* 17: 7414-7424

Piculell, L. 1995. Gelling carrageenans. In: *Food polysaccharides and their applications* (Ed. A.M.Stephen), Marcel Dekker Inc., New York, Ch.8, pp. 205-244.

Prouchayret, F., Fasan, G., Grandgeorge, M., Vigneron, C., Menu, P., Dellacherie, E. A. 1992. Potential blood substitute from carboxylic dextran and oxyhemoglobin. I. Preparation, purification and characterization. Biomaterials Artificial Cells and Immobilization Biotechnology 20(2-4): 319-322.

Ring, S.G. and Stainsby, G. 1985. A simple method for determining the shear modulus of food dispersions and gels. *Journal of Science of Food and Agriculture* 36: 607-613

Rouhana, R., Budge, S. M., MacDonald, S. M., Roscoe, S. G. 1997. Electrochemical studies of the interfacial behaviour of α-lactoglobulin and bovine serum albumin. *Food Research International* 30: 13-20.

Salloum, D. S. and Schlenoff, J. B. 2004. Protein adsorption modalities on polyelectrolyte multilayers. *Biomacromolecules* 5: 1089-1096.

Sauerbrey, G. 1959. Verwendung von Schwingquarzen zur Wagung dunner Schichten und zur Mikrowagung. *Zeitschrift Fur Physik* 155: 206-222.

Schmitt, C., Sanchez, C., Desobry-Banon, S. and Hardy, J. 1998. Structure and technofunctional properties of protein-polysaccharide Complexes: a review. *Critical Reviews in Food Science and Nutrition 38*(8): 689-753.

Serov, A. Antonov, V., Yu. A and Tolstoguzov, V. B. 1985. Isolation of lactic whey proteins in the form of complexes with apple pectin. *Nahrung* 1: 19-30.

Seyrek, E., Dubin, P.L., Tribet, C. and Gamble, E.A. 2004. Ionic Strength Dependence of Protein-Polyelectrolyte Interactions. *Biomacromolecules* 4: 273-282

Shih, F. F. 1994. Interaction of soy isolate with polysaccharide and its effect on film properties. *Journal of the American Oil Chemists' Society* 71(11): 1281-1285.

Silvestri, L.J., Hurst, R.E., Simpson, L., Settine, J.M. 1982. Analysis of sulfate in complex carbohydrates. *Analytical Biochemistry* 123: 303-309.

Stepp, J. and Schlenoff, J. B. 1997. Electrochromism and electrocatalysis in viologenpolyelectrolyte multilayers. *Journal of Tthe Electrochemical Society* 144: 155-157.

Stevenson, T. T. and Furneaux, R. H. 1991. Chemical methods for the analysis of sulphated galactans from red algae. *Carbohydrate Research* 210: 277–298.

Strege, M. A., Dubin, P. L., West, J. S. and Flinta, C. D. 1990. Protein separation via polyelectrolyte complexation. In *Protein purification: from molecular mechanisms to large scale process*. (eds. M. Ladisch, R. C. Wilson, C. C. Painton, S. E. Builder), American Chemical Society Symposium Series 427, Ch. 5: 66-79.

Stroeve, P., Vasquez, V., Coelho, M. A. N. and Rabolt, J. F. 1996. Gas transfer in supported films made by molecular self-assembly of ionic polymers. *Thin Solid Films* 284: 708-712

Sukhishvili, S. A. and Granick, S. 1999. Adsorption of human serum albumin: Dependence on molecular architecture of the oppositely charged surface. *Journal of Chemical Physics* 110: 10153-10161.

Sukhishvili, S. A., Dhinojwala, A., and Granick, S. 1999. How polyelectrolyte adsorption depends on history: A combined Fourier transform infrared spectroscopy in attenuated total reflection and surface forces study. *Langmuir* 15: 8474-8482.

Sun, Y., Zhang, X., Sun, C., Wang, B. and Shen, J. 1996. Fabrication of ultrathin film containing bi-enzyme of glucose oxidase and gluoamylase based on electrostatric interaction and its potential application as a maltose sensor. *Macromolecular Chemistry and Physics* 197: 147-153.

Svanberg, C. and Bergman, R. 1998. Photon Correlation Spectroscopy. Chalmers University of Technology. p.7

Syrbe, A. Bauer, W.J. and Klostermeyer, H. 1998. Polymer Science Concepts in Dairy Systems – An Overview of Milk Protein and Food Hydrocolloid Interaction. *International Dairy Journal* 8: 179-193

Takata, S., Norisuye, T., Tanaka, N. and Shibayama, M. 2000. Heat-Induced Gelation of β-Lactoglobulin. 1. Time-Resolved Dynamic Light Scattering. *Macromolecules* 33: 5470-5475.

Tanaka, M., Ishizaki, S., Suzuki, T. and Takai, R. 2001. Water vapor permeability of edible films prepared from fish water soluble proteins as affected by lipid type. *Journal of Tokyo University of Fisheries* 87: 31-37

Tanford, C., Swanson, S. A. and Shore, W. S. 1955. Hydrogen Ion Equilibria of Bovine Serum Albumin. *Journal of American Chemical Society* 77: 6414-6421.

Taravel M. N. and Domard, A. 1995. Collagen and its interaction with chitosan, II influence of the physicochemical characteristics of collagen. *Biomaterials* 16(11): 865-871.

Thomas, W.R. 1992. Carrageenan. In: *Thickening and gelling agents for food* (Ed. A.Imeson), Blackie Academic & Professional,Cambridge, pp. 24-39.

Tolstoguzov, V. B. 1991. Functional properties of food proteins and role of protein–polysaccharide interaction. *Food Hydrocolloids* 4(6): 429-468.

Tolstoguzov, V. B., Izjumov, D. B., Grinberg, V. Y., Marusova, A. N. and Chekhovskaya, V. T. 1974. Method of making protein-containing foodstuffs resembling minced meat. US Patent Application 3,829,587.

Tolstoguzov, V.B. 1997. Protein-polysaccharide interactions. In *Food proteins and their applications*, (eds. S. Damodaran and A. Paraf), Marcel Dekker, Inc., New York, pp 171-198.

Tolstoguzov, V.B. 2002. Thermodynamic aspects of biopolymer functionality in biological systems, foods, and beverages. *Critical Reviews in Biotechnology* 22(2): 89-174.

Tolztogusov, 2000. Compositions and phase diagrams for aqueous systems based on proteins and polysaccharides. *International Review of Cytology* 192: 3-31.

Truus, K., Vaher, M., Usov, A. I., Pehk, T. and Kollist, A. 1997. Gelling galactans from the algal community of Furcellaria lumbricalis and Coccotylus truncatus (the Baltic Sea, Estonia): a structure-property study. *International Journal of Biological Macromolecules* 21: 89-96

Turgeon, S. L., Beaulieu, M., Schmitt, C. and Sanchez, C. 2003. Protein – polysaccharide interactions: phase-ordeing kinetics, thermodynamic and structural aspects. *Current opinion in colloid and interface science* 8(4-5): 401-414.

Tziboula, A., and Horne, D.S. 1997. Influence of milk proteins on the gel transition temperature and the mechanical properties of weak b-carrageenan gels. In *Gums and stabilizers for the food industry 9* (Ed. P.A. Williams and G.O. Phillips), The Royal Society of Chemistry, Cambridge, pp. 201-211.

Usov, A. I. and Klochkova, N. G. 1992. Polysaccharides of algae. 45. Polysaccharide composition of red seaweeds from Kamchatka coastal waters (Northwestern Pacific) studied by reductive hydrolysis of biomass. *Botanica Marine* 35: 371–378.

Van de Velde, F., Knutsen, S. H., Usov, A. I., Rollema, H. S. and Cerezo, A. S. 2002. ^{1}H and ^{13}C high resolution NMR spectroscopy of carrageenans: applications in research and industry. *Trends in Food Science and Technology* 13: 73-92

Van der Schoot, 1998. Protein-induced collapse of polymer chains. *Macromolecules* 31: 4635-4638.

Vinogradova, O.I. 2004. Mechanical properties of polyelectrolyte multilayer microcapsules. *Journal of Physics: Condensed Matter* 16: 1105-1134

Voinova, M. V., Rodahl, M., Jonson, M. and Kasemo, B. 1999. Viscoelastic acoustic response of layered polymer films at fluid-solid interfaces: Continuum mechanics approach. *Physica Scripta* 59: 391-396.

Vrij, A. 1976. Polymers at interfaces and the interactions in colloidal dispersions. *Pure and Applied Chemistry* 48: 471-483.

Wang, S., van Dijk, J. A. P. P., Odijk, T. and Smit, J. A. M. 2001. Depletion-induced demixing in aqueous protein-polysaccharide solutions. *Biomacromolecules* 2: 1080-1088.

Wang, Y.-F., Gao, J. Y. and Dubin, P. L. 1996. Protein separation via polyelectrolyte coacervation: selectivity and efficiency. *Biotechnology Progress* 12: 356-362.

Watanabe, S. and Regan, S. L. 1994. Dendrimers as Building Blocks for Multilayer Construction. *Journal of American Chemical Society* 116: 8855-8856.

Weinbreck, F. 2004. Whey protein / polysaccharide coacervates: structure and dynamics. Thesis Utrecht University, The Netherlands

Weinbreck, F., de Vries, R., Schrooyen, P. and de Kruif, C. G. 2003. Complex coacervation of whey proteins and gum arabic. *Biomacromolecules* 4 : 293-303.

Wen, Y. P. and Dubin, P. L. 1997. Potentiometric studies of the interaction of bovine serum albumin and poly(dimethyldiallylamonium chloride). *Macromolecules* 30: 7856-7861.

Williams, C.A. 1998. Application of photon correlation spectroscopy to a macromolecular system. Physics Department, The College of Wooster, Wooster, Ohio

Yan, X.-L., Khor, E. and Lim, L.-Y. 2001. Chitosan – alginate films prepared with chitosan at different molecular weights. *Journal of Biomedical Materials Research* 58(4): 358-365.

Zaleskas, J. M., Kinner, B., Freyman, T. M., Yannas, I. V., Gibson, L. J. and Spector, M. 2001. Growth factor regulation of smooth muscle actin expression: contraction of human articular chondrocytes and meniscal cells in a collagen-GAG matrix. *Experimental Cell Research* 270(1): 21-31.

Zhu, H., Ji, J. and Shen, J. 2004. Electrostatic Self-assembly on 3-Dimensional Tissue Engineering Scaffold. *Biomacromolecules* 5(5): 1933-1939

ACKNOWLEDGEMENTS

In four and half exciting years working on polyelectrolyte interactions at Department of Food Processing in Tallinn University of Technology and at Institute of Food Research in Norwich, I learned a lot in the field of science and I owe it to a lot of people. This work couldn't be achieved without the help and support of a great amount of people to whom I wish to express my sincere gratitude:

I am deeply grateful to Dr. Stephen G. Ring, for accepting me in his group and to introducing me into the field of polyelectrolytes. His expertise and his guidance were fundamental to the completion of this work.

I am very thankful to Assoc. Prof. Margus Friedenthal, for giving me the opportunity to perform my research, his support, his encouragement and his help.

I wish to thank Head of the Department of Food Processing, Prof. Raivo Vokk for providing the facilities and position for my work in the department.

Prof. Toomas Paalme is thanked for making this department scientifically stimulating.

I am grateful to Dean of the Faculty of Chemical and Materials Technology of Tallinn University of Technology, Prof. Andres Öpik for giving the opportunity to perform my eleven-and-half-years study (1994-2006) from the first-year of Diploma studys till the end of my PhD studies at the Program of Bio- and Food Technology.

I am thankful to AS EstAgar, especially to Tiit Sarapuu, for introducing me the technology of furcellaran and for providing me with *Furcellaria* seaweed.

My sincere thanks to all my colleagues of the Department of Food Processing at Tallinn University of Technology and at Institute of Food Research, for helping me out when I had questions and doubts, but essentially for the good time I had during my PhD. Special thanks are extended to Tim Noel for his assistance with DSC and help during my stay in England, to Geoff Brownsey for fruitful cooperation in rheometry and photon correlation spectroscopy, to Roger Parker and Alistair Macdougall for helping me with the numerous things in the lab, to Mike Whitcombe for the NMR experiments, to Jonathan Moffat for introducing me SPR, FTIR-ATR and QCM-D experiments, to Tiina Veskus for her advices in home-lab, to Tiina and Kairit from TUT, Mounira, Maria, Giusy, Alessandra, Valeria, Denisa, Simone, Kerstin, Kasia, Christian, Alina and the other foreign guests who spent some time at IFR, for all kinds of help and for creating a pleasant atmosphere. I am grateful to the BSc. student Marina Mironova for experimental assistance.

My warmest thank to my relatives and friends who always supported me even if they didn't (and probably still don't) understand what I was doing during these last four-and-half years! I would especially like to thank my parents for their understanding and support. My greatest graditude is to my fiance Teo Pent for being by my side during these years, for the interest he has always shown in my PhD, his help and above all, for his love.

The financial support of BBSCR (core strategic grant), European Commission (Marie Curie fellowship); Estonian Science Foundation (grant 5189), Ministry of Education and Research of Estonia and Archimedes Foundation (Kristjan Jaak Fellowships), as well as, Fond of Development at Tallinn University of Technology (Eesti Energia AS scholarship) are gratefully acknowledged.

KOKKUVÕTE

Toiduained koosnevad paljude toidukoostisosade keerukast kogust, mille seas mängivad toidusüsteemide struktureerimisel ja stabiliseerimisel põhirolli valgud ja polüsahhariidid läbi oma geelistuvate, paksendavate ja pindstabiliseerivate omaduste. Tootmise käigus mõjutavad iga individuaalse komponendi omadused, nagu ka koostoime erinevate komponentide vahel, toiduaine lõppstruktuuri, tekstuuri ja stabiilsust.

Palju on uuritud seerumalbumiini ja β-laktoglobuliini struktuuri ja omadusi ning nende koostoimeid teiste toidukoostiskomponentidega, et mõista kuidas vastavad valgud mõjutavad toiduainete funktsionaalsust ning kuidas toota uusi funktsionaalseid toiduaineid. Viimane põhjus viibki furtsellaraani ja veise seerum albumiini ning β-laktoglobuliini koostoimete uurimisele. Põhjalik arusaam valk-polüsahhariid interaktsioonidest ja nende kontrollimisest võimaldab luua vajaliku struktuuri ja tekstuuriga tooteid.

Käesoleva doktoritöö eesmärk oli kirjeldada Eestist pärinevast punavetikaliigist *Furcellaria lumbricalis*'est saadavat polüsahhariidi furtsellaraani ning mõista ja kontrollida furtsellaraani ja globulaarsete piimavalkude (veise seerum albumiini ja beeta-laktoglobuliini) vahelisi koostoimeid.

Eestist korjatud punavetikast *Furcellaria lubricalisest* eraldati furtsellaraan vesiekstraktsioonil (looduslik furtsellaraan) ning viidi läbi leelistöötlus (modifitseeritud furtsellaraan) ning mõõdeti nende struktuur. Polüsahhariid koosnes põhiliselt (1→3) seotud β-D-galaktoosist; (1→4) seotud 3,6-anhüdro-α-D-galaktoosist ja (1→3) seotud β-D-galaktoos 4-sulfaadist. Leelistöötlus eemaldas sulfaatrühmad galaktoostsükli 6. asendist, moodustades 3,6-anhüdrogalaktoosi, mis tõstis furtsellaraani geelitugevust.

Furtsellaraani ja globulaarsete valkude segamisel moodustas furtsellaraan valkudega lahustuva kompleksi pH 7,5 juures, mille maksimum sõltus ioontugevusest. Edasisel pH alanemisel toimus valgu isoelektrilise täpi läheduses märkimisväärne agregatsioon. Nende kahe pH vahemikus oli valgu/furtsellaraani kompleks suurem kui furtsellaraani ahela suurus lahuses. Kompleks moodustus kui valk oli negatiivselt laetud, nagu ka furtsellaraan.

Segude geelistumisel saadi füüsikaliselt ristühendatud võrgustikuga geelid. Valgud mõjutasid tugevasti furtsellaraani geeli elastsusmoodulit. Madala pH juures toimus faaside eraldumine, mille tõttu muutus kaonurga tangens.

Kontsentreeritud furtsellaraani süsteemidega tehtud katsed näitasid, et furtsellaraani saab edukalt kasutada kilemoodustajana. Furtsellaraanil põhinevad kiled omasid häid takistusomadusi. Veise seerum albumiini lisand muutis kiled paindlikumaks, kuid komposiitkilede omadused halvenesid, sest kilede tõmbejõud ja elastsus vähenesid ning veeauru läbilaskvus suurenes.

Uuriti ka mitmekihiliste kilede moodustumist furtsellaraanist ja polü(L)lüsiinist (PLL). Polümeeri ladestumisel toimus järkjärguline polümeeri massi kasv ning polü(L)lüsiin difundeerus furtsellaraani kihti. Uuriti ka globulaarsete valkude adsorbeerumist PLL/furtsellaraani mitmekihiliste kiledele. Leiti, et märkimisväärne adsorptsioon toimub pH juures, kus valgu laetus oli negatiivne, nagu furtsellaraanilgi.

APPENDIX 1

ARTICLE I

Parker, R., Noel, T.R., Brownsey, G.J., Laos, K., and Ring, S.G. 2005. The Non-Equilibrium Phase and Glass Transition Behavior of β-Lactoglobulin – ***Biophysical Journal, Vol. 89, no 2, 1227-1236***

The Nonequilibrium Phase and Glass Transition Behavior of β-Lactoglobulin

Roger Parker,* Timothy R. Noel,* Geoffrey J. Brownsey,* Katrin Laos,† and Stephen G. Ring*
*Institute of Food Research, Norwich Research Park, Norwich NR4 7UA, United Kingdom; and †Department of Food Processing, Tallinn Technical University, Tallinn 19086, Estonia

ABSTRACT Concentrated solutions of bovine β-lactoglobulin were studied using osmotic stress and rheological techniques. At pH 6.0 and 8.0, the osmotic pressure was largely independent of NaCl concentration and could be described by a hard sphere equation of state. At pH 5.1, close to the isoelectric point, the osmotic pressure was lower at the lower NaCl concentrations (0 mM, 100 mM) and was fitted by an adhesive hard sphere model. Liquid-liquid phase separation was observed at pH 5.1 at ionic strengths of 13 mM and below. Comparison of the liquid-liquid and literature solid-liquid coexistence curves showed these solutions to be supersaturated and the phase separation to be nonequilibrium in nature. In steady shear, the zero shear viscosity of concentrated solutions at pH 5.1 was observed at shear rates above 50 s^{-1}. With increasing concentration, the solution viscosity showed a progressive increase, a behavior interpreted as the approach to a colloidlike glass transition at ~60% w/w. In oscillatory shear experiments, the storage modulus crossed the loss modulus at concentrations of 54% w/w, an indication of the approaching glass transition. Comparison of the viscous behavior with predictions from the Krieger-Dougherty equation indicates the hydrodynamic size of the protein decreases with increasing concentration, resulting in a slower approach to the glass transition than a hard sphere system.

INTRODUCTION

Recent advances in the theory of concentrated particulate dispersions have lead to the prediction of nonequilibrium states such as repulsive and attractive glasses (1), transient gels, and also to equilibrium cluster phases (2). The occurrence of such states depends upon the range and strength of the attractive and repulsive forces acting between the particles. Experimentally these states have been principally observed in colloidal systems although it has been shown that there are strong analogies between the behavior of colloidal and concentrated globular protein solutions (2). In model colloidal systems the particles are generally spherical although they may have a limited polydispersity, and the system prepared so as to have well-defined interparticle forces. On the other hand, globular proteins are generally nonspherical and there remain uncertainties in the prediction of interparticle forces. Part of this uncertainty arises as a result of the polyampholyte characteristics of the protein. Although the protein globule may carry a zero net charge, its surface charge distribution is heterogeneous and the net charge reflects the balance between positive and negative charges. This results in an orientation-dependent interparticle force and the possibility of dipolar interactions. In the experimental situation, although the protein particle is expected to be monodisperse, in practice a limited aggregation is often observed.

For colloidal systems with a dominant repulsive interaction, the viscosity of a suspension progressively increases with increasing volume fraction, ϕ, of particles (3,4). At high volume fractions there is a sufficient slowing of particle dynamics such that liquidlike configurations cannot be explored over practical timescales (5,6). For small applied stresses, the material has the solidlike characteristics of a glass with the particles forming jammed structures that are stress bearing. For a random packing of noninteracting monodisperse hard spheres, these structures may form at volume fractions in the vicinity of 0.6 with a random close packing limit, ϕ_c, of $\approx$0.644 (7,8). These structures result from repulsive excluded volume interactions. As short-ranged attractive interactions between particles are introduced (9), the attraction first ''melts'' the glass and then leads to the formation of a qualitatively different glassy state. With increasing attraction, three dimensional particle networks, with solidlike characteristics (colloidal gels), form at significantly lower particle volume fractions (10). Recent research has emphasized the similarities between jammed structures which form with increasing volume fraction of particles and those, more open structures which form as a result of an increasing attractive interaction between particles (9). A further aspect of nonequilibrium behavior exhibited by solutions of proteins with short-ranged attractive interactions is metastable liquid-liquid separation (11,12). The metastability is with respect to solid-liquid coexistence, that is, the solutions are supersaturated. In contrast to the glasses and networks, these are relatively low viscosity liquid states.

Earlier research (13) examined the colloidal glass transition behavior of a globular protein (bovine serum albumin) where there was a net repulsion between the protein globules. This article examines the rheological behavior of concentrated aqueous solutions of the globular protein β-lactoglobulin (BLG) as the colloidal glass transition is

Submitted April 8, 2005, and accepted for publication May 25, 2005.

Address reprint requests to Dr. Steve Ring, Institute of Food Research, Norwich Research Park, Colney Lane, Norwich NR4 7UA, UK. Tel.: 44-0-1603-255031; Fax: 44-0-1603-507723; E-mail: steve.ring@bbsrc.ac.uk.

0006-3495/05/08/1227/10 $2.00

doi: 10.1529/biophysj.105.064246

approached. The strength of the interparticle attraction is controlled through varying pH and ionic strength and the interparticle interaction probed through the determination of the osmotic pressure as a function of composition.

MATERIALS AND METHODS

Materials

BLG was obtained from Sigma-Aldrich (Poole, UK) (L0130) and is a mixture of genetic variants A and B. A polyethylene glycol fraction (PEG 20—average molecular mass of 20 kDa) and silicone oil (200/500 cs) were obtained from VWR (Poole, UK). Spectro/Por dialysis tubing, molecular mass cutoff 8 kDa, was a regenerated cellulose obtained from Spectrum Laboratories, NBS Biologicals (Huntingdon, UK). All other chemicals were Analar grade.

Mass spectrometry

The BLG preparation was examined by liquid chromatography-mass spectroscopy using reverse phase chromatography with on-line electrospray-ionization mass spectrometry (MicroMass, Cary, NC) as described previously (14). The preparation contained approximately equal amounts of BLG A (mass 18365) and BLG B (mass 18278). Small amounts (~10% w/w) of lactosylated BLG (masses 18690, 18603) were also present in the preparation.

Photon correlation spectroscopy

The apparatus employed was an ALV/SP-86 spectrogoniometer (ALV, Langen, Germany) equipped with a Coherent (Ely, UK) Radiation Innova 100-10 vis Argon Ion laser operating at 0.5 W and a wavelength of 514 nm. BLG (6 g/L) was dissolved in 0.03 M NaCl and adjusted to the required pH with dilute NaOH. The aqueous solutions were filtered through a 0.22 μm Millipore (Billerica, MA) filter into a quartz cuvette and maintained at 25°C. The scattered light intensity was monitored using an ALV/PM-15 ODSIII detection system at a fixed scattering angle of 90°. After amplification and discrimination, signals were directed to an ALV/5000E Multiple Tau Digital Correlator and time-intensity correlation functions recorded, typically for 600 s duration. Size distribution functions were computed using the appropriate Windows-based ALV software, which incorporated regularized inverse Laplace transform and ALV-CONTIN packages. Additional analysis was undertaken using Origin V6 (Microcal, Studio City, CA) proprietary software.

Osmotic stress technique

The dependence of the osmotic pressure of BLG solutions on protein concentration, pH, and added NaCl concentration was determined using an osmotic stress technique. Two ml of a buffered BLG solution was dialyzed against buffered PEG solutions of known osmotic pressure (15,16) at 20°C for 24 h. After dialysis the dialysis tube was removed from the PEG solution and the BLG concentration determined by spectrophotometry. Under certain conditions either limited aggregation, as evidenced by turbidity, or the formation of two distinct liquid phases was observed. The amount of aggregated material, or the composition of the coexisting phases, was measured by centrifuging the samples for 5 min at 4000 g, removal of the upper phase, and determination of protein content of the aggregates or the concentration in each coexisting phase using spectrophotometry.

Modeling of osmotic pressure

The adhesive hard sphere (AHS) model is capable of describing the phase diagram and osmotic pressure of globular proteins taking account of excluded volume and short-ranged attractive contributions to the interparticle potential. Approximate analytic solutions are available for the pressure, Π (17–19)

$$\frac{\Pi}{\rho k_B T} = \frac{1+\phi+\phi^2}{(1-\phi)^3} - \phi\lambda\left(\frac{18(2+\phi)-\phi\lambda^2}{36(1-\phi)^3}\right) \quad (1)$$

and

$$\lambda = 6\left[\left(1-\tau+\frac{\tau}{\phi}\right) - \left[\left(1-\tau+\frac{\tau}{\phi}\right)^2 - \frac{1}{6}\left(1+\frac{2}{\phi}\right)\right]^{\frac{1}{2}}\right] \quad (2)$$

where ϕ is the hard sphere volume fraction of the protein solution, ρ the protein number density, k_B Boltzmann's constant, and T absolute temperature. The dimensionless parameter τ is a measure of the strength of the attraction or the adhesiveness (stickiness) of the potential which is represented as an infinitely narrow deep well at the particle surface. An infinite value of τ corresponds to negligible attraction, i.e., hard sphere behavior, and a value tending to zero to infinite adhesiveness. In practice the hard sphere osmotic pressure characteristic is realized for $\tau > 100$, and only the first term on the right hand side of Eq. 1 need be retained. For $\tau \leq 0.113$ the AHS model predicts liquid-liquid phase separation (20) which is metastable with respect to solid-liquid coexistence (21).

Rheological measurements

The rheology of BLG solutions at 20°C was determined using a Rheometrics (Ithaca, NY) ARES-LS2 rheometer with parallel plate geometry. The lower platen consisted of a Peltier temperature control surface. The upper platen was of ceramic (diameter, 25 mm or 50 mm). The minimum torque limit was 2×10^{-6} Nm. The BLG solutions were prepared using the osmotic stress technique. The sample was transferred directly from the dialysis bag onto the lower platen, and upper platen lowered until the sample filled the gap (typical gap was 0.3 mm). The visible sample surface was then coated in silicone oil (200/500 cs) to prevent water loss. The normal force was constantly monitored, while manually adjusting the gap, and not allowed to exceed 0.2 N. The normal force had relaxed to <0.05 N before testing commenced. Dynamic tests were performed over the frequency range 0.02–30 Hz and constant shear rate measurements (clockwise and counterclockwise) from 0.005 to 500 s^{-1}. The viscoelastic behavior was measured as a function of applied strain, γ, at a fixed oscillatory frequency of 1 Hz to determine the region of linear viscoelasticity. The frequency-dependent response was then examined at a γ within this region.

RESULTS AND DISCUSSION

Photon correlation spectroscopy

Photon correlation spectroscopy was used to characterize the dilute solution behavior of the BLG preparation through the determination of a translational diffusion coefficient, D_t. For a particle in solution subject to Brownian motion, the translational diffusion coefficient is related to the measured intensity correlation function $g^{(2)}(\tau)$ by the expression (22)

$$g^{(2)}(\tau) = 1 + \exp(-2D_t K^2 \tau), \quad (3)$$

where K, the scattering vector, is given by

$$K = \frac{4\pi n}{\lambda}\sin\frac{\theta}{2}, \quad (4)$$

where n is the refractive index of the solution, θ, the scattering angle, and λ the wavelength of light.

The conformation and association behavior of BLG are pH dependent (23,24). The monomeric unit has a molecular mass of 18.3 kDa. At pH ≥3.5 there is significant protein dimerization. This monomer-dimer equilibrium is dependent on ionic strength and protein concentration. At lower pHs an increase in ionic strength screens the electrostatic repulsion of positive charges on the monomer and stabilizes the dimer (25,26). At pH 4.6, the dimers may further aggregate to form an octamer, a structure observed predominantly at subambient temperatures (27,28). At pH 7.5 the protein conformation undergoes a reversible transition which leads to a swelling of the monomeric unit (29,30). At higher pHs there is the potential for a time-dependent irreversible aggregation.

The effective hydrodynamic radius, R_h, of BLG was obtained from the Stokes-Einstein relation

$$D_t = k_B T/6\pi\eta R_h, \quad (5)$$

where η is the solvent viscosity. Fig. 1 shows a compilation of experimental values of the hydrodynamic radius, R_h, as a function of pH for BLG in aqueous solution obtained from this and previous studies (25,31–34). Only broad comparisons can be made as the studies were carried out at different ionic strengths and different protein concentrations. At low pHs (2.0–3.0) the calculated value of R_h, obtained by extrapolation of the diffusion coefficients to zero concentration, is ~2.2 ± 0.1 nm, reflecting the hydrodynamic size of the monomeric unit and its associated electrolyte cloud (25,31). At pHs in the vicinity of neutrality (pH 6.0–8.0) the calculated values of R_h range from 2.6 to 4.9 nm. This range of values in part reflects the equilibrium between monomer and dimer. If the dimer is modeled as two touching spheres (31), the ratio of the R_h of dimer and monomer is ~1.33 giving an estimated R_h of the dimer of 2.93 nm.

In this study at pH 7.9, the measured value of D_t for a 0.6% w/w BLG solution in 30 mM NaCl was 7.5×10^{-11} m^2s^{-1}, in agreement with previous measurements carried out under similar conditions and concentration (33). As the pH was reduced below 7.9, or increased above 10, the presence of a second slower diffusive process in the autocorrelation function was observed, which was attributed to a very limited aggregation/association of BLG (34). At pHs in the vicinity of the isoelectric point (pH 5.1), the calculated R_h of both the protein in solution and its aggregate increased in size and was correlated to the phase separation/precipitation of BLG from aqueous solution at these concentrations and ionic strength (34).

Osmotic stress and nonequilibrium phase diagram

In Figs. 2–4, the osmotic pressure determined using the osmotic stress technique is plotted as the dimensionless compressibility factor, $\Pi/\rho k_B T$, as a function of protein mass fraction for pH 8.0, 6.0, and 5.1 (10 mM buffer) and NaCl concentrations of 0 mM, 100 mM, and 1 M. To calculate the protein number density, the dimer molecular mass of 36.6 kDa and a protein specific volume of 0.75 ml g^{-1} (35) were assumed. At pH 8.0 the osmotic pressure is independent of ionic strength and increases monotonically with protein mass fraction. At this pH (and pH 6.0) the osmotically stressed solutions were single phase with no visible turbidity. Also plotted in Fig. 2 is the osmotic pressure calculated using an approximate hard sphere equation of state (only the first term on the right hand side of Eq. 1 is used) assuming the apparent specific volume of the protein phase to be 1.12 ml g^{-1}. The

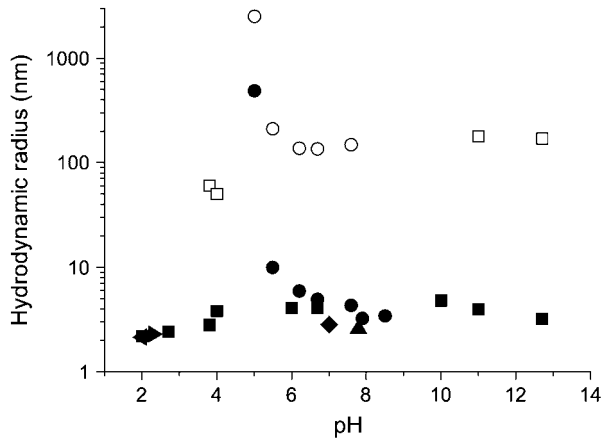

FIGURE 1 Hydrodynamic radius of BLG as a function of pH. This study (●, ○); Takata et al. (34) (■, □); Aymard et al. (25) (◀); Baldini et al. (31) (▶); Beretta et al. (32) (▲); Le Bon et al. (33) (♦). Open symbols represent second slower diffusive process, where reported, attributed to aggregated/associated BLG (34).

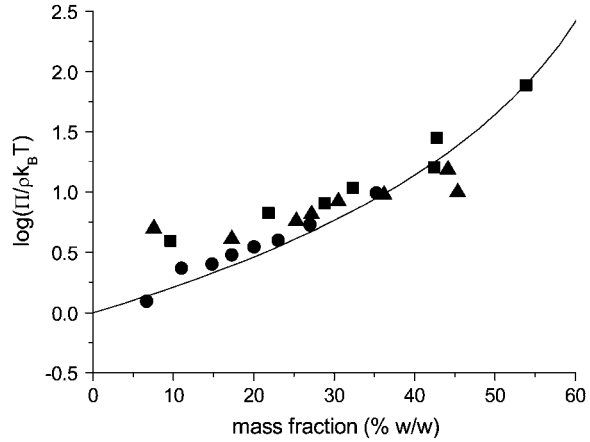

FIGURE 2 Dimensionless osmotic compressibility of BLG at pH 8.0 (10 mM buffer) as a function of mass fraction and NaCl concentration: 0 mM (■); 100 mM (●); 1 M (▲). Solid line is the equation of state for hard spheres calculated assuming an apparent protein specific volume of 1.12 ml g^{-1}.

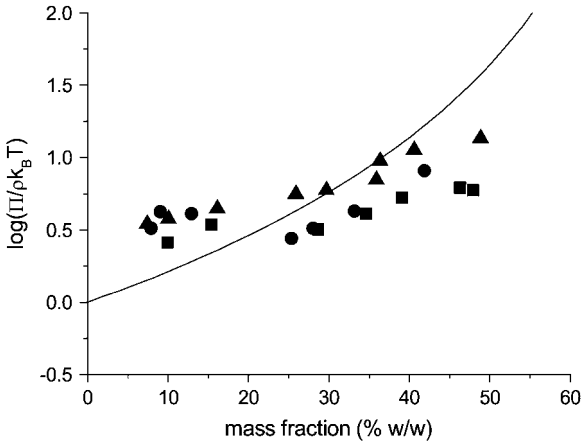

FIGURE 3 Dimensionless osmotic compressibility of BLG at pH 6.0 (10 mM buffer) as a function of mass fraction and NaCl concentration: 0 mM (■); 100 mM (●); 1 M (▲). Solid line is the equation of state for hard spheres calculated assuming an apparent protein specific volume of 1.12 ml g^{-1}.

ability of this model to fit the data indicates that the protein-protein interactions under these conditions are predominantly repulsive. At this pH the protein has a net negative charge, the dimer carrying a charge of $-17e$ (36), where e is the protonic charge; and so the apparent specific volume would be expected to have a contribution from net repulsive electric double layer interactions in addition to the excluded volume of the hydrated protein itself. The insensitivity of the osmotic pressure to salt concentration indicates that the Donnan effect is apparently making little contribution to the overall osmotic pressure (37,38). Qualitatively similar osmotic behavior is observed at pH 6.0 (Fig. 3). At this pH, the osmotic pressure is weakly dependent upon salt concentration, increasing at high salt concentrations. The theoretical equation of state does not describe the experimental results as well as at pHs 8.0 (hard spheres, Fig. 2) or 5.1 (AHS, Fig. 4). The discrepancy at the lower concentrations (mass fraction ~7–16% w/w) could be decreased if the assumed molecular weight (MW) were reduced from the dimer MW to the monomer MW. However, the photo correlation spectroscopy results at pH 6.0 do not support this explanation (Fig. 1).

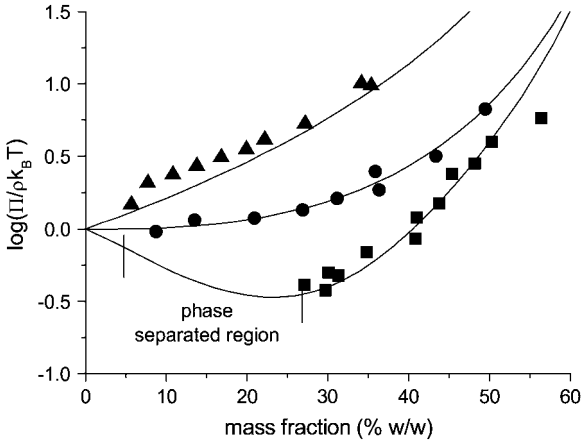

FIGURE 4 Dimensionless osmotic compressibility of BLG at pH 5.1 (10 mM buffer) as a function of mass fraction and NaCl concentration: 0 mM (■); 100 mM (●); 1 M (▲). Solid lines are the equation of state for AHSs calculated assuming apparent protein specific volume of 1.12 ml g^{-1} and stickiness parameters of 0.11 (NaCl concentration, 0 mM); 0.24 (100 mM); and 1000 (1 M). With a stickiness parameter of 1000 the 1M NaCl line is essentially that for hard spheres.

At pH 5.1, close to the isoelectric point, the osmotic pressure was significantly lower at lower ionic strengths (Fig. 4), the compressibility factor being ≤ 1 for mass fractions up to ~40% w/w. Whereas at 100 mM NaCl a limited aggregation occurred (this amounted to <15% of the protein), for the 10 mM buffer without added NaCl a liquid-liquid phase separation was observed for mass fractions below 27% w/w. Fig. 5 shows the coexisting phases for a solution which contained 15% w/w BLG overall. Mass spectrometry showed that there was no significant fractionation of BLG A and BLG B in either the aggregation or the phase separation. No extensive crystallization was observed under the conditions and timescales of our experiments. At this pH the ability of the AHS model to describe the osmotic behavior was examined, holding the apparent protein specific volume constant at 1.12 ml g^{-1} and varying the stickiness parameter. At the highest salt concentration (1 M) the magnitude of the stickiness parameter ($\tau \sim 1000$) was indicative of a system with negligible stickiness, that is, the interactions could be modeled simply using an excluded volume hard sphere model. At the two lower ionic strengths, the osmotic data could be modeled with stickiness parameters, τ, of 0.24 (100 mM NaCl) and 0.11 (10 mM buffer alone). As the ionic strength is lowered there are increasingly strong short-ranged attractive interparticle interactions. The observation of liquid-liquid phase separation in the solution with no added NaCl and a stickiness parameter of 0.11 is the predicted behavior for a system of AHSs under these conditions (18,20).

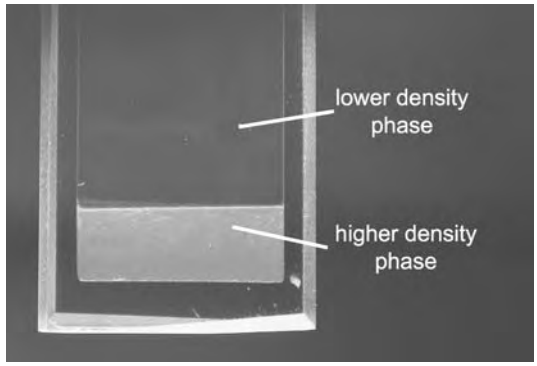

FIGURE 5 15% w/w BLG solution in 10 mM pH 5.1 acetate buffer showing phase separation.

The dependence of the phase behavior on ionic strength at pH 5.1 was examined more extensively, resulting in the nonequilibrium phase diagram shown in Fig. 6. At 20°C the solution has a critical point at ionic strengths of ~13 mM and becomes increasingly subcritical as the ionic strength is lowered. In addition to the homogeneous liquid phases, the conditions under which limited aggregation occurred are also noted. Aggregation occurs at the protein concentrations at which phase separation occurs (<30% w/w) but at higher ionic strengths 20 mM $< I <$ 200 mM. At higher ionic strengths (≥400 mM) and protein concentrations (≥30% w/w), only transparent single phase solutions are found.

The observed phase behavior is consistent with literature measurements of both the second virial coefficient (39,40) and the solid-liquid coexistence line (41). The second virial coefficient is negative in this pH region, indicative of there being short-ranged attractive forces. Piazza and Iacopini's light scattering study using BLG A (39) showed a minimum in the second virial coefficient at pH 4.2, which was found to be related to a transient clustering rather than phase separation. However, at pH 5.0 the virial coefficient remained negative as also found by Schaink and Smit (40) using membrane osmometry (mixed BLG A and B) at pH 5.2. The ionic strength dependence of the solid-liquid coexistence line for BLG at pH 5.1 as measured by Grönwall (41) is plotted in Fig. 6. This shows that liquid-liquid separation occurs in a region of the phase diagram which is metastable with respect to solid-liquid phase separation. This is a common behavior of protein phase diagrams and of particles with short-ranged attractive interparticle forces, e.g., AHSs (11,12). What is more unusual is the salting-in behavior which affects both the solid-liquid and the liquid-liquid coexistence lines. At pH 5.1 BLG is close to its isoelectric point and so, in terms of electrostatic interactions, those depending upon the charge heterogeneity rather than the net charge will tend to dominate. Early measurements (42) showed BLG has a dipole moment of a sufficient magnitude to generate significant attractive dipole-dipole interactions which are predicted to be screened by increasing ionic strength at the concentrations relevant to this study (40,43).

Results of osmotic squeezing at pH 3.6 were affected by an aggregation process which led to poor reproducibility particularly at low NaCl concentration. The overall effect of pH on the osmotic compressibility at 1 M NaCl is shown in Fig. 7. Whereas the results at pH 5.1, close to the isoelectric point, and pH 6.0 and 8.0, when the protein carries a net negative charge, can be described by hard sphere behavior those at pH 3.6 when the protein has a high net positive charge (dimer > +36e) are lower, indicating the presence of attractive forces and aggregation processes under these conditions.

Rheology

We have previously proposed that the rheology of globular protein solutions may be usefully compared to the rheology of colloidal suspensions (13). The rheology of polymer latex and microgel suspensions has been the subject of extensive investigation (4,44–47), with the viscosity showing a characteristic dependence on particle volume fraction. When the viscous behavior is examined as a function of shear rate, suspensions of intermediate volume fraction (0.2–0.5) show two Newtonian plateaus separated by a shear thinning region (48). For hard sphere suspensions the low shear viscosity, η_0, includes contributions from hydrodynamic forces associated with minimally perturbed equilibrium structures, whereas for the high shear viscosity, η_∞, the structure is substantially perturbed. For noninteracting particles, the shear stress, σ, at which the viscosity is intermediate between η_0 and η_∞, is of the order of

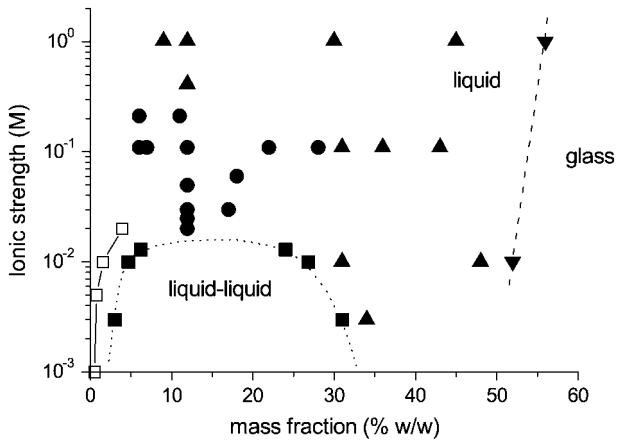

FIGURE 6 Nonequilibrium phase diagram of BLG at pH 5.1 as a function of ionic strength showing liquid phase (▲); liquid phase + limited aggregation (●); liquid-liquid coexistence (■ and *short dashed line*); liquid-glass transition (▼ and *long dashed line*); solid-liquid coexistence (Grönwall (41)) (□ and *solid line*). Lines are only an aid to the eye.

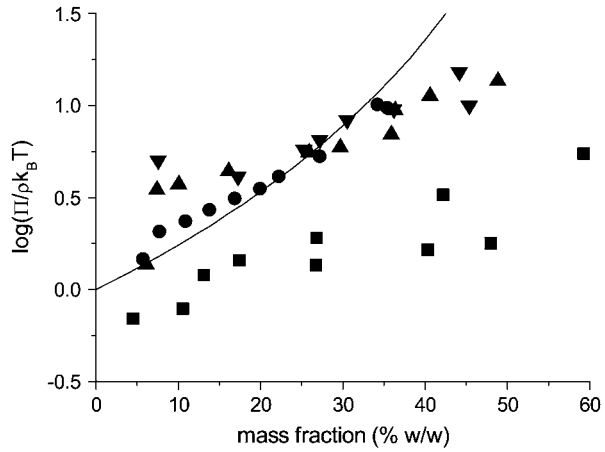

FIGURE 7 Effect of pH on the dimensionless osmotic compressibility of BLG as a function of mass fraction at a NaCl concentration on 1 M. pH: 3.6 (■); 5.1 (●); 6.0 (▲); 8.0 (▼). Solid line is hard sphere equation of state calculated assuming an apparent protein specific volume of 1.12 ml g^{-1}.

$$\sigma \approx k_B T/a^3, \quad (6)$$

where a is the particle radius (4,48). For a particle the size of the BLG dimer, the calculated value of σ is ~50 kPa. Shear stresses in excess of this are required to overcome diffusion driven equilibria. Given the comparatively low viscosity of the system, this relates to a shear rate in excess of 10^3 s^{-1}.

Fig. 8 shows a plot of shear viscosity versus shear rate for BLG solutions in the concentration range 23–52% w/w at pH 5.1 in 10.0 mM acetate buffer containing 1 M NaCl at 20°C. At the lower concentrations, Newtonian behavior was observed at shear rates, $\dot{\gamma}$, in the range 10–100 s^{-1}. As the associated shear stress was $\ll$50 kPa, we ascribe this behavior to being equivalent to the η_0 of hard sphere colloidal suspensions. Below the short Newtonian plateau, the viscosity increases with decreasing shear rate. These observations are consistent with reports of the solidlike behavior of relatively dilute globular protein solutions (0.1–10% w/w) with strong shear thinning behavior being observed with increasing shear rate (49–51) and the storage modulus, G', being larger than the loss modulus (49–53), G''. One proposed explanation for this behavior is that at low concentrations, a lattice type structure is formed. An alternative explanation is that in this concentration range, the presence of an interfacial layer of protein has a marked influence on the observed rheology. The interfacial layer can form both at an air/water (54–57) and an immiscible liquid/water interface (58,59). In a study (60) of the interfacial rheology of BLG, it was found that the protein formed a gellike elastic layer at the interface. The addition of the surfactant Tween 20 to the subphase abolished the shear elasticity as a consequence of the disruption of the adsorbed layer (60).

From the Newtonian region, η_0 of the protein solution was obtained and the relative viscosity, $\eta_{r,0} = \eta_0/\eta_s$, calculated where η_s is the solvent viscosity assumed to be 1.0 mPas. Fig. 9 shows the dependence of $\eta_{r,0}$ on BLG concentration at pH 5.1 in 10 mM acetate buffer and in this buffer containing 100 mM and 1.0 M NaCl. $\eta_{r,0}$ increases with increasing mass fraction of protein. At a fixed mass fraction, the solution viscosity of BLG in 100 mM and 1.0 M NaCl at pH 5.1 is similar but is higher at the lower ionic strength.

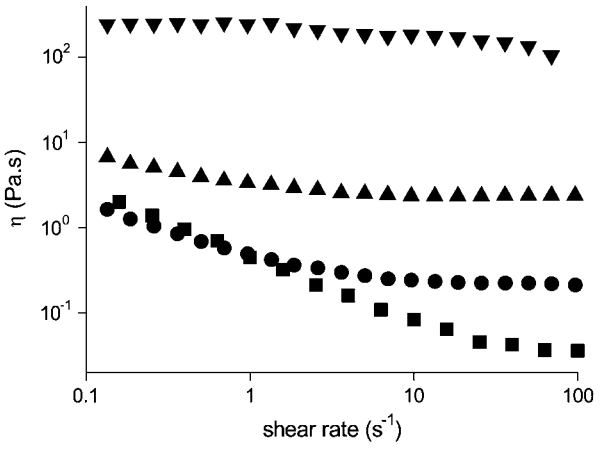

FIGURE 8 Shear-rate dependence of the viscosity of BLG solutions in 10 mM pH 5.1 acetate buffer containing 1 M NaCl for mass fractions: 23.0% w/w (■); 27.0% w/w (●); 45% w/w (▲); 52% w/w (▼).

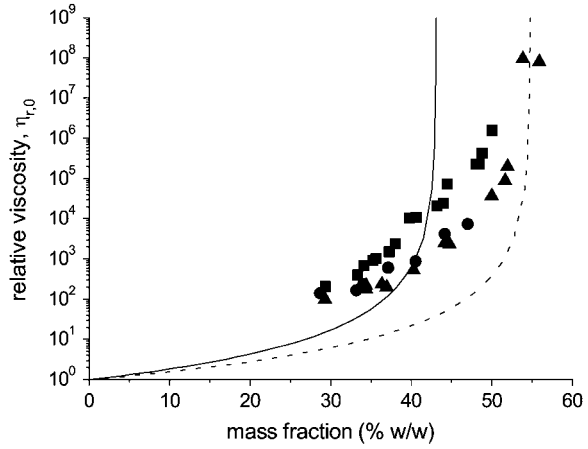

FIGURE 9 Effect of mass fraction and NaCl concentration on the relative zero shear viscosity of BLG solutions at pH 5.1. NaCl concentration: 0 mM (■); 100 mM (●); 1.0 M (▲). Equation 6 also plotted with $\nu = 3.6$ and $\phi_{max} = 0.71$ and apparent protein specific volume 1.47 ml g^{-1} (*solid line*) and 1.12 ml g^{-1} (*dashed line*).

For suspensions of spherical particles the dependence of relative viscosity, η_r, on volume fraction, ϕ, is given to a first approximation by Berli and Quemada (61)

$$\eta_r = (1 - \phi/\phi_{max})^{-2}, \quad (7)$$

where ϕ_{max} is the maximum packing fraction, which is 0.63 ± 0.02 at low shear and 0.70 ± 0.02 at high shear (4). In experimental studies on essentially monodisperse hard sphere suspensions, the value of ϕ_{max}, required to fit the dependence of η_r on ϕ (based on measurements of η_0 and various forms of Eq. 7), ranged from 0.58 to 0.64. The observed variability is in part dependent on polydispersity and its effect on packing and in part dependent on uncertainties in the volume fraction (62). By rescaling the volume fraction, it was possible to obtain a master curve of published data. For particles which have a diffuse outer layer, ϕ may be replaced by an effective volume fraction (61), ϕ_{eff}, which may be calculated from a hydrodynamic size determined from measurements of the viscosity of dilute suspensions. Particle deformability may also influence the observed viscous behavior with the increase in η_r with ϕ being less pronounced at the higher volume fractions (45). Deformability has a major effect on the relative high shear viscosity, $\eta_{r,\infty}$, and a much weaker effect for the relative zero shear viscosity, $\eta_{r,0}$. Weak attractive interactions between particles are expected to primarily affect $\eta_{r,0}$.

Solutions of globular proteins are particulate suspensions. Ideally, the suspensions are monodisperse although in practice there is often a limited amount of aggregated material present. An important additional factor which should be considered is their shape. Although globular proteins may be

approximated to spherical particles, they are usually asymmetric. An alternative expression to Eq. 7 which allows for the effects of particle asymmetry through a parameter, v, is given by

$$\eta_r = (1 - \phi/\phi_{max})^{-v\phi_{max}}. \quad (8)$$

This is the Krieger-Dougherty equation, where v for hard spheres is expected to be 2.5 (3,63). Particle asymmetry also has an impact on the maximum packing fraction (64). For example, it has recently been shown that the simulated packing of ellipsoidal particles showed a dependence on aspect ratio and can approach a packing, ϕ_{max}, of ~0.74. The ''bare'' BLG dimer may be approximated to a prolate ellipsoid with a length of 6.9 nm and a width of 3.6 nm (24). For prolate ellipsoids of this aspect ratio, the maximum packing fraction is ~0.71 (64). The value of v estimated from measurements of the reduced viscosity of dilute solutions of BLG as a function of concentration or from the known dimensions of the dimer is in the range 3.6–4.5 (35). Based on the R_h of the monomer of 2.2 nm, a specific volume of 1.47 ml g^{-1} was used to convert protein mass to volume. A specific volume of protein of 0.75 ml g^{-1} was then used to obtain the mass of water in the hydrodynamic domain of the protein, and from this the volume fraction of protein at known mass fractions was estimated. The predicted dependence of η_r on mass fraction for particles with a v of 3.6 and a ϕ_{max} of ~0.71 is plotted in Fig. 9. At the higher ionic strengths, and at mass fractions in the vicinity of 30% w/w (ϕ ~0.5), there is some correspondence between the measured and expected values of $\eta_{r,0}$. With increasing mass fraction, the expected increase in $\eta_{r,0}$ with ϕ is less than expected. The origin of this difference arises from the estimation of ϕ from mass fraction. Using a specific volume of 1.47 ml g^{-1}, obtained from the R_h of the BLG monomer in dilute solution, leads to values of ϕ for the more concentrated solutions which are above the expected ϕ_{max} or, using the reverse of the above conversion, a mass fraction of 43.1% w/w. Although this value of specific volume is required to approximate the viscous behavior at intermediate protein concentrations, the specific volume used for approximating the concentration-dependent osmotic pressure (1.12 ml g^{-1}) gives better agreement at higher protein concentrations (Fig. 9).

It is well accepted that water in the vicinity of the protein globule contributes toward its hydrodynamic behavior, particularly in dilute solution (65,66). Bead-modeling methodologies are available which allow the calculation of hydrodynamic quantities from the detailed atomic-level structure (65). For a range of proteins, a typical value of the thickness of the hydration layer is ~0.15 nm. For small globular proteins, such as BLG, the volume of this layer is comparable to the volume of the dry protein. The viscous behavior of globular protein solutions will therefore be strongly influenced by the characteristics of this hydration layer. Information on the dynamics of protein hydration may be obtained from ^{17}O magnetic relaxation dispersion measurements, which indicate that water molecules at protein surfaces are highly mobile (66,67). A recent dynamic hydration model has established a link between protein hydrodynamics and hydration dynamics, more particularly the effect of hydration dynamics on rotational and translational diffusion (66). The observed concentration-dependent behavior suggests that the influence of this hydration layer on viscosity decreases with increasing concentration.

For the BLG solutions containing 1 M NaCl at pH 5.1, the osmotic pressure data indicate that the dominant interaction between the protein particles is repulsive. In the solutions containing 100 mM NaCl and 10 mM acetate buffer alone, this interaction becomes increasingly attractive at short range. For colloidal systems, the initial effects of attraction, particularly at high volume fractions, is a reduction in viscosity as the initial clustering of particles increases the free volume available for structural rearrangement (1). With increasing attraction there is the potential to form particle networks or gels (68–70). In the case here, the effect of the weak attraction between the BLG particles is an increase in $\eta_{r,0}$ at a fixed ϕ.

At high BLG concentrations, the marked increase in $\eta_{r,0}$ with increasing ϕ and the consequent slowing of structural rearrangement indicates the onset of solidlike behavior. The viscoelastic behavior of BLG solutions in 1.0 M NaCl at pH 5.1 in the concentration range 45–54% w/w was determined by oscillatory rheometry. At small strains, $\gamma < 0.01$, both G′ and G″ were independent of γ. The frequency dependence of G′(ω) and G″(ω) is shown in Fig. 10 for 45%, 52%, and 54% w/w BLG solutions. For the concentrations 45% and 52% w/w, G″ > G′ over the frequency range examined of 0.02–30 Hz, a viscous liquid-like response. For the 54% w/w solution, G′ crosses G″ at ~2 Hz, a transition to an elastic solidlike response. This crossover indicates the approach of

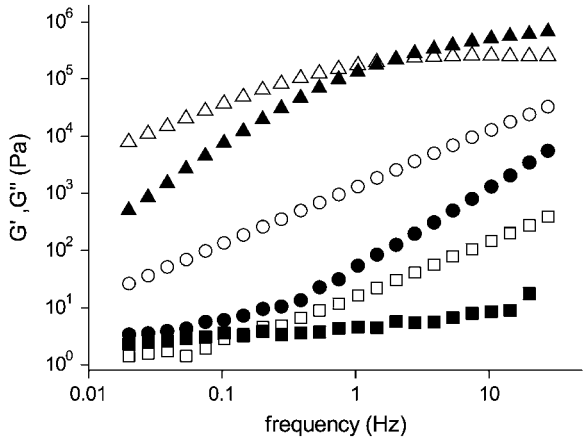

FIGURE 10 Frequency sweep of the complex shear modulus of concentrated BLG solutions at pH 5.1 with 1.0 M NaCl for mass fractions: 45% w/w (■,□); 52% w/w (●,○); 54% w/w (▲,△). The storage modulus, G', and loss modulus, G'', are the solid and open symbols, respectively.

a dynamic transition which can be compared to the colloidal glass transition (5,70). For particles such as BLG in 1.0 M NaCl where the dominant interaction is repulsive, the glasslike transition is primarily influenced by particle crowding (5,70). In this case the particle motions become constrained in cages and the particles can no longer diffuse freely. The dominant elasticity results from distortions in the average particle configurations and is thought to be entropic in nature (70). In addition to the divergence of viscosity (Fig. 9), the change in viscoelasticity is a further indication of the onset of a glass transition with increasing BLG concentration.

Recent studies have indicated that there is a qualitatively different glass transition at high volume fractions for particles which have a weak attraction (1). With increasing particle attraction, solidlike behavior may be obtained through the formation of particle networks within which the solvent is dispersed. We did not observe either of these phenomena in our experiments. At pH 5.1 the osmotic pressure measurements indicate there are short-ranged attractive interactions at low ionic strength, but these result in liquid-liquid phase separation which is apparently unhindered by any kinetic arrest. In the range in which we were able to measure these systems, the dynamic shear moduli show the system to be predominantly liquidlike. Theoretically the occurrence of particle gel formation is linked with percolation although this is a necessary rather than a sufficient condition for gelation to occur (21). For AHS both approximate analytic (71) and recent machine calculations (20) indicate that to a very large extent the metastable liquid-liquid coexistence curve lies below the percolation line, and so particle gel formation rather than liquid-liquid separation is predicted. Calculations (21) show that if a longer ranged attraction is added on to the AHS model, although the percolation line does not move, the effective stickiness varies such that the liquid-liquid coexistence line is no longer below the percolation line, a potential explanation for the absence of particle gelation.

GENERAL DISCUSSION

The compositions at which the relative viscosity (Fig. 9) diverges provide an indication of the position of the liquid-glass transition. For the sample with no added NaCl, the divergence occurs at a mass fraction of ~52% w/w, increasing to 56% w/w at 1M NaCl. These points and the liquid-glass transition boundary have been added to the nonequilibrium phase diagram (Fig. 6). The liquid-liquid coexistence region and glass transition are well separated, and so the two processes will not affect one another. As we discussed previously (13), the behavior in this study is relevant to globular proteins subjected to osmotic stress in biological situations. Cytoplasmic concentrations relevant to macromolecular crowding are typically up to 40% v/v (72). If the cytoplasm is dehydrated as, for example, in the desiccation of a seed, the results indicate that when the concentration of globular proteins exceeds 60% w/w this component will vitrify. This will arrest diffusion at the protein globule length scale. However, flexible polymers and lower molecular weight components typically vitrify at much lower water contents (<20% w/w). Conversely, in a germinating seed the hydration of vitrifed storage proteins will be a necessary step to mobilize them and make them available for use.

We thank Dr. Fred Mellon for performing the mass spectrometry and Professor Lindsay Sawyer for advice on the literature.

This work was supported through the core strategic grant of the United Kingdom Biotechnology and Biological Sciences Research Council. K.L. acknowledges support from a European Community Marie Curie fellowship (contract No. QLK-1999-50512).

REFERENCES

1. Pham, K. N., A. M. Puertas, J. Bergenholtz, S. U. Egelhaaf, A. Moussaid, P. N. Pusey, A. B. Schofield, M. E. Cates, M. Fuchs, and W. C. K. Poon. 2002. Multiple glassy states in a simple model system. *Science*. 296:104–106.
2. Stradner, A., H. Sedgwick, F. Cardinaux, W. C. K. Poon, S. U. Egelhaaf, and P. Schurtenberger. 2004. Equilibrium cluster formation in concentrated protein solutions and colloids. *Nature*. 432:492–495.
3. Krieger, I. M. 1972. Rheology of monodisperse latices. *Adv. Colloid Interface Sci*. 3:111–136.
4. Phan, S. E., W. B. Russel, Z. D. Cheng, J. X. Zhu, P. M. Chaikin, J. H. Dunsmuir, and R. H. Ottewill. 1996. Phase transition, equation of state, and limiting shear viscosities of hard sphere dispersions. *Phys. Rev. E*. 54:6633–6645.
5. Mason, T. G., and D. A. Weitz. 1995. Linear viscoelasticity of colloidal hard-sphere suspensions near the glass-transition. *Phys. Rev. Lett*. 75:2770–2773.
6. Mason, T. G., M. D. Lacasse, G. S. Grest, D. Levine, J. Bibette, and D. A. Weitz. 1997. Osmotic pressure and viscoelastic shear moduli of concentrated emulsions. *Phys. Rev. E*. 56:3150–3166.
7. Rintoul, M. D., and S. Torquato. 1998. Hard-sphere statistics along the metastable amorphous branch. *Phys. Rev. E*. 58:532–537.
8. Torquato, S., T. M. Truskett, and P. G. Debenedetti. 2000. Is random close packing of spheres well defined? *Phys. Rev. Lett*. 84:2064–2067.
9. Trappe, V., V. Prasad, L. Cipelletti, P. N. Segre, and D. A. Weitz. 2001. Jamming phase diagram for attractive particles. *Nature*. 411: 772–775.
10. Segre, P. N., V. Prasad, A. B. Schofield, and D. A. Weitz. 2001. Glasslike kinetic arrest at the colloidal-gelation transition. *Phys. Rev. Lett*. 86:6042–6045.
11. Muschol, M., and F. Rosenberger. 1997. Liquid-liquid phase separation in supersaturated lysozyme solutions and associated precipitate formation. *J. Chem. Phys*. 107:1953–1962.
12. Rosenbaum, D. F., and C. F. Zukoski. 1996. Protein interactions and crystallization. *J. Cryst. Growth*. 169:752–758.
13. Brownsey, G. J., T. R. Noel, R. Parker, and S. G. Ring. 2003. The glass transition behavior of the globular protein bovine serum albumin. *Biophys. J*. 85:3943–3950.
14. Moreno, F. J., J. A. Jenkins, F. A. Mellon, N. M. Rigby, J. A. Robertson, N. Wellner, and E. N. C. Mills. 2004. Mass spectrometry and structural characterization of 2S albumin isoforms from Brazil nuts (*Bertholletia excelsa*). *Biochim. Biophys. Acta*. 1698:175–186.
15. Parsegian, V. A., R. P. Rand, N. L. Fuller, and D. C. Rau. 1986. Osmotic stress for the direct measurement of intermolecular forces. *Methods Enzymol*. 127:400–416.

16. Ryden, P., A. J. Macdougall, C. W. Tibbits, and S. G. Ring. 2000. Hydration of pectic polysaccharides. *Biopolymers.* 54:398–405.

17. Baxter, R. J. 1968. Percus-Yevick equation for hard spheres with surface adhesion. *J. Chem. Phys.* 49:2770–2774.

18. Watts, R. O., D. Henderson, and R. J. Baxter. 1971. Hard spheres with surface adhesion: the Percus-Yevick approximation and the energy equation. *Adv. Chem. Phys.* 21:421–430.

19. Farrer, D., and A. Lips. 1999. On the self-assembly of sodium caseinate. *Int. Dairy J.* 9:281–286.

20. Miller, M. A., and D. Frenkel. 2003. Competition of percolation and phase separation in a fluid of adhesive hard spheres. *Phys. Rev. Lett.* 90:art-135702.

21. Noro, M. G., N. Kern, and D. Frenkel. 1999. The role of long-range forces in the phase behavior of colloids and proteins. *Europhys. Lett.* 48:332–338.

22. Brown, W. 1993. Dynamic light scattering. *In* Monographs on the Physics and Chemistry of Materials. Oxford Science Publications, Oxford.

23. Sawyer, L., G. Kontopidis, and S. Y. Wu. 1999. beta-Lactoglobulin—a three-dimensional perspective. *Int. J. Food Sci. Technol.* 34:409–418.

24. Verheul, M., J. S. Pedersen, S. P. F. M. Roefs, and K. G. de Kruif. 1999. Association behavior of native beta-lactoglobulin. *Biopolymers.* 49:11–20.

25. Aymard, P., D. Durand, and T. Nicolai. 1996. The effect of temperature and ionic strength on the dimerisation of beta-lactoglobulin. *Int. J. Biol. Macromol.* 19:213–221.

26. Sakurai, K., M. Oobatake, and Y. Goto. 2001. Salt-dependent monomer-dimer equilibrium of bovine beta-lactoglobulin at pH 3. *Protein Sci.* 10:2325–2335.

27. Gottschalk, M., H. Nilsson, H. Roos, and B. Halle. 2003. Protein self-association in solution: the bovine beta-lactoglobulin dimer and octamer. *Protein Sci.* 12:2404–2411.

28. Townend, R., R. J. Winterbottom, and S. N. Timasheff. 1960. Molecular interactions in β-lactoglobulin. II. Ultracentrifugal and electrophoretic studies of the association of β-lactoglobulin below its isoelectric point. *J. Am. Chem. Soc.* 82:3161–3168.

29. Tanford, C., L. G. Bunville, and Y. Nozaki. 1959. The reversible transformation of β-lactoglobulin at pH 7.5. *J. Am. Chem. Soc.* 81: 4032–4036.

30. Qin, B. Y., M. C. Bewley, L. K. Creamer, H. M. Baker, E. N. Baker, and G. B. Jameson. 1998. Structural basis of the Tanford transition of bovine beta-lactoglobulin. *Biochemistry.* 37:14014–14023.

31. Baldini, G., S. Beretta, G. Chirico, H. Franz, E. Maccioni, P. Mariani, and F. Spinozzi. 1999. Salt-induced association of beta-lactoglobulin by light and x-ray scattering. *Macromolecules.* 32:6128–6138.

32. Beretta, S., G. Chirico, and G. Baldini. 2000. Short-range interactions of globular proteins at high ionic strengths. *Macromolecules.* 33:8663–8670.

33. Le Bon, C., T. Nicolai, M. E. Kuil, and J. G. Hollander. 1999. Self-diffusion and cooperative diffusion of globular proteins in solution. *J. Phys. Chem. B.* 103:10294–10299.

34. Takata, S., T. Norisuye, N. Tanaka, and M. Shibayama. 2000. Heat-induced gelation of beta-lactoglobulin. 1. Time-resolved dynamic light scattering. *Macromolecules.* 33:5470–5475.

35. Tanford, C. 1961. Physical Chemistry of Macromolecules. John Wiley and Sons, New York.

36. Cannan, R. K., A. H. Palmer, and A. C. Kibrick. 1942. The hydrogen ion dissociation curve of β-lactoglobulin. *J. Biol. Chem.* 142:803–822.

37. Scatchard, G. 1946. Physical chemistry of protein solutions. I. Derivation of the equations for the osmotic pressure. *J. Am. Chem. Soc.* 68:2315–2319.

38. Scatchard, G., A. C. Batchelder, and A. Brown. 1946. Preparation and properties of serum and plasma proteins. VI. Osmotic equilibria in solutions of serum albumin and sodium chloride. *J. Am. Chem. Soc.* 68:2320–2329.

39. Piazza, R., and S. Iacopini. 2002. Transient clustering in a protein solution. *Eur. Phys. J. E.* 7:45–48.

40. Schaink, H. M., and J. A. M. Smit. 2000. Determination of the osmotic second virial coefficient and the dimerization of beta-lactoglobulin in aqueous solutions with added salt at the isoelectric point. *Phys. Chem. Chem. Phys.* 2:1537–1541.

41. Grönwall, A. 1942. Studies on the solubility of lactoglobulin. I. The solubility of lactoglobulin in dilute solutions of sodium chloride at varying ionic strength and hydrogen ion activity. *C R Trans. Labs. Carls.* 24:185–200.

42. Ferry, J. D., and J. L. Oncley. 1941. Studies of the dielectric properties of protein solutions. III. Lactoglobulin. *J. Am. Chem. Soc.* 63:272–278.

43. Tavares, F. W., D. Bratko, A. Striolo, H. W. Blanch, and J. M. Prausnitz. 2004. Phase behavior of aqueous solutions containing dipolar proteins from second-order perturbation theory. *J. Chem. Phys.* 120:9859–9869.

44. Cheng, Z. D., J. X. Zhu, P. M. Chaikin, S. E. Phan, and W. B. Russel. 2002. Nature of the divergence in low shear viscosity of colloidal hard-sphere dispersions. *Phys. Rev. E.* 65:art-041405.

45. Senff, H., and W. Richtering. 1999. Temperature sensitive microgel suspensions: colloidal phase behavior and rheology of soft spheres. *J. Chem. Phys.* 111:1705–1711.

46. Senff, H., W. Richtering, C. Norhausen, A. Weiss, and M. Ballauff. 1999. Rheology of a temperature sensitive core-shell latex. *Langmuir.* 15:102–106.

47. Weiss, A., N. Dingenouts, M. Ballauff, H. Senff, and W. Richtering. 1998. Comparison of the effective radius of sterically stabilized latex particles determined by small-angle x-ray scattering and by zero shear viscosity. *Langmuir.* 14:5083–5087.

48. Macosko, C. W. 1994. Rheology—Principles, Measurements and Applications. Wiley-VCH, New York.

49. Ikeda, S., and K. Nishinari. 2000. Intermolecular forces in bovine serum albumin solutions exhibiting solidlike mechanical behaviors. *Biomacromolecules.* 1:757–763.

50. Ikeda, S., and K. Nishinari. 2001. On solid-like rheological behaviors of globular protein solutions. *Food Hydrocoll.* 15:401–406.

51. Inoue, H., and T. Matsumoto. 1994. Viscoelastic and SAXS studies of the structural transition in concentrated aqueous colloids of ovalbumin and serum albumins. *J. Rheol.* 38:973–984.

52. Gosal, W. S., A. H. Clark, P. D. A. Pudney, and S. B. Ross-Murphy. 2002. Novel amyloid fibrillar networks derived from a globular protein: beta-lactoglobulin. *Langmuir.* 18:7174–7181.

53. Tobitani, A., and S. B. Ross-Murphy. 1997. Heat-induced gelation of globular proteins. 1. Model for the effects of time and temperature on the gelation time of BSA gels. *Macromolecules.* 30:4845–4854.

54. Bantchev, G. B., and D. K. Schwartz. 2003. Surface shear rheology of beta-casein layers at the air/solution interface: formation of a two-dimensional physical gel. *Langmuir.* 19:2673–2682.

55. Martin, A., M. Bos, M. C. Stuart, and T. van Vliet. 2002. Stress-strain curves of adsorbed protein layers at the air/water interface measured with surface shear rheology. *Langmuir.* 18:1238–1243.

56. Murray, B. S. 2002. Interfacial rheology of food emulsifiers and proteins. *Curr. Opin. Colloid Interface Sci.* 7:426–431.

57. Renault, A., S. Pezennec, F. Gauthier, W. Vie, and B. Desbat. 2002. Surface rheological properties of native and S-ovalbumin are correlated with the development of an intermolecular beta-sheet network at the air-water interface. *Langmuir.* 18:6887–6895.

58. Cicuta, P., E. J. Stancik, and G. G. Fuller. 2003. Shearing or compressing a soft glass in 2D: time-concentration superposition. *Phys. Rev. Lett.* 90:art-236101.

59. Freer, E. M., K. S. Yim, G. G. Fuller, and C. J. Radke. 2004. Interfacial rheology of globular and flexible proteins at the hexadecane/water interface: comparison of shear and dilatation deformation. *J. Phys. Chem. B.* 108:3835–3844.

60. Petkov, J. T., T. D. Gurkov, B. E. Campbell, and R. P. Borwankar. 2000. Dilatational and shear elasticity of gel-like protein layers on air/water interface. *Langmuir*. 16:3703–3711.

61. Berli, C. L. A., and D. Quemada. 2000. Rheological modeling of microgel suspensions involving solid-liquid transition. *Langmuir*. 16: 7968–7974.

62. Meeker, S. P., W. C. K. Poon, and P. N. Pusey. 1997. Concentration dependence of the low-shear viscosity of suspensions of hard-sphere colloids. *Phys. Rev. E*. 55:5718–5722.

63. Wierenga, A. M., and A. P. Philipse. 1998. Low-shear viscosity of isotropic dispersions of (Brownian) rods and fibres; a review of theory and experiments. *Colloids Surf. A*. 137:355–372.

64. Donev, A., I. Cisse, D. Sachs, E. Variano, F. H. Stillinger, R. Connelly, S. Torquato, and P. M. Chaikin. 2004. Improving the density of jammed disordered packings using ellipsoids. *Science*. 303:990–993.

65. de la Torre, J. G., M. L. Huertas, and B. Carrasco. 2000. Calculation of hydrodynamic properties of globular proteins from their atomic-level structure. *Biophys. J*. 78:719–730.

66. Halle, B., and M. Davidovic. 2003. Biomolecular hydration: from water dynamics to hydrodynamics. *Proc. Natl. Acad. Sci. USA*. 100: 12135–12140.

67. Modig, K., E. Liepinsh, G. Otting, and B. Halle. 2004. Dynamics of protein and peptide hydration. *J. Am. Chem. Soc*. 126:102–114.

68. Dawson, K. A. 2002. The glass paradigm for colloidal glasses, gels, and other arrested states driven by attractive interactions. *Curr. Opin. Colloid Interface Sci*. 7:218–227.

69. Dawson, K. A., A. Lawlor, P. DeGregorio, G. D. McCullagh, E. Zaccarelli, G. Foffi, and P. Tartaglia. 2003. The nature of the colloidal 'glass' transition. *Faraday Discuss*. 123:13–26.

70. Prasad, V., V. Trappe, A. D. Dinsmore, P. N. Segre, L. Cipelletti, and D. A. Weitz. 2003. Universal features of the fluid to solid transition for attractive colloidal particles. *Faraday Discuss*. 123:1–12.

71. Chiew, Y. C., and E. D. Glandt. 1983. Percolation behavior of permeable and of adhesive spheres. *J. Phys. A*. 16:2599–2608.

72. Hall, D., and A. P. Minton. 2003. Macromolecular crowding: qualitative and semiquantitative successes, quantitative challenges. *Biochim. Biophys. Acta*. 1649:127–139.

APPENDIX 1

ARTICLE II

Laos, K., Ring, S.G. 2005. Characterisation of furcellaran samples from Estonian *Furcellaria lumbricalis*. – Journal of Applied Phycology, vol. 17, 461-464

Journal of Applied Phycology (2005) 17: 461–464
DOI: 10.1007/s10811-005-1635-2

Note

Characterisation of furcellaran samples from Estonian *Furcellaria lumbricalis* (Rhodophyta)

Katrin Laos[1,2,*] & Stephen G. Ring[1]
[1]*Division of Food Materials Science, Institute of Food Research, Norwich Research Park, Colney, Norwich NR4 7UA, UK;* [2]*Present address: Department of Food Processing, Tallinn University of Technology, Ehitajate tee 5, 19086 Tallinn, Estonia*

*Author for correspondence: e-mail: katrin.laos@mail.ee; phone +372-6202956; fax +372-6202950

Received 4 April 2005; accepted 23 June 2005

Key words: furcellaran, gelation, monosaccharide composition, structure

Abstract

The structure of furcellarans obtained from red algae *Furcellaria lumbricalis* collected in Estonia was determined. Native and alkali-modified furcellarans were examined by gas chromatography/mass spectrometry (GC/MS), and ^{13}C-nuclear magnetic resonance spectroscopy (NMR) and were compared with commercial furcellaran (FMC Food Ingredients). The polysaccharide preparation consisted mainly of (1→3) linked β-D-galactopyranose, (1→4) linked 3,6-anhydro-α-D-galactopyranose and (1→3) linked β-D-galactopyranose 4-sulphate. Alkaline treatment removed the sulphate precursor sequences with formation of 3,6-anhydrogalactose that improved the furcellaran gelling ability.

Furcellaran is an anionic sulphated polysaccharide extracted from the red alga *Furcellaria lumbricalis*. Estonia is a large potential source of this marine alga. In Kattegat (Denmark) it is declining and no longer present in Puck Bay (Poland). The current abundance of these seaweeds in Estonia is the greatest in Europe and probably in the world (Truus et al., 1997). Furcellaran has a repeating backbone of alternating 3-linked β-D-galactose and 4-linked α-D-galactose residues (Knutsen et al., 1990) and is currently considered to be a type of κ-carrageenan (Glicksman, 1983). The formation of 3,6-anhydro-α-D-galactose units from α-D-galactose 6-sulphate residues by alkaline treatment is an important and well known reaction of the carrageenans. It is used commercially to enhance gelation behaviour and, in the laboratory, for the quantitative determination of α-galactose 6-sulphate residues (Ciancia et al., 1993). Although a particular carrageenan has the same basic structure (Glicksman, 1983), there is potential for structural and functional variation with geographical origin. In this note, we characterise the composition and structural features of the furcellarans from Estonian *F. lumbricalis* (water extracted and alkali modified) and compare them with a commercial furcellaran.

Fronds of *F. lumbricalis* were collected in Kassari Bay (the Baltic Sea, Estonia) and cleaned of epiphytes. The alga was washed thoroughly with tap water and galactans were extracted according to Amimi et al. (2001). The alga was extracted with deionised water (1.5 L) under agitation for 3 h at 95 °C. The aqueous phase was clarified by passing through a nylon cloth, and then precipitated in 2.5 volumes of isopropanol, filtered and dried at room temperature (yield 38%). The crude furcellaran preparation (3 g) was dissolved in 2 L milliQ water at ~100 °C. The solution was passed through diatomaceous earth (Sigma-Aldrich Co. Ltd., UK) and dialysed (yield 80%). The soluble form of Na^+ furcellaran was obtained by elution through an ion-exchange (Amberlite IR-120) column in the Na^+ form at 4 °C. The molecular size of furcellaran samples prepared (as indicated by intrinsic viscosity measurements q.v.) was relatively high indicating only limited

Table 1. Characteristics of the furcellarans.

Sample	Neutral sugar* composition (% w/w carbohydrate)						Sulphate (%, w/w)	η (mL g^{-1})	Yield (%)
	Gal	3,6-AGal	6-*O*-MeGal	Glu	Xyl	Man			
Native	64–65	25–26	3.9–4.4	2.7–2.8	1.8–1.9	1.1–1.7	17.5–18.3	507	37.8
Alkali modified	59–60	31–32	4.7–4.8	1.8–1.9	1.6–1.8	1.1–1.2	16.2–17	1304	24.3
Commercial	55–57	36–37	4.7–4.8	1.8–1.9	0.52–0.53	0.52–0.53	17.6–18.3	482	

* Gal: galactose; 3,6-AGal: 3,6-anhydrogalactose; 6-*O*-MeGal: 6-*O*-methylgalactose; Glu: glucose; Xyl: xylose; Man: mannose.

degradation during the extraction process. The eluant was freeze-dried. The commercial furcellaran was a gift from FMC BioPolymer.

For alkaline treatment 150 mL of aqueous KOH solution (2%, w/w) was added to 30 g of the dry alga and stored for 7 days at room temperature. The alga was washed thoroughly with tap water until the wash water was neutral. The furcellaran was extracted as described above to obtain a yield of 24%.

For the determination of monosaccharide composition, the furcellaran was hydrolysed by a double-hydrolysis-reduction method as described by Stevenson and Furneaux (1991). The alditols were converted to their acetates and analysed by GC/MS as described by Harris et al. (1998). The sulphate content was measured colorimetrically as described by Silvestri et al. (1982).

Measurements of specific viscosity as a function of concentration of furcellaran (0.025–0.2%, w/w) in 0.1 M NaCl were carried out using an Ubbelohde viscometer at 20 °C. The efflux time for 0.1 M NaCl was 143.7 s and no shear rate corrections were made. The intrinsic viscosity (η) was calculated from the extrapolation of specific viscosity to zero concentration.

For ^{13}C-nuclear magnetic resonance (NMR) spectroscopy, the polysaccharide samples were dissolved in D_2O (5%, w/v) and spectra were recorded in JEOL EX spectrometer at 85 °C. Chemical shifts were calculated with reference to the C-6 signal from the galactose residue at 61.3 ppm.

For characterisation of gelation behaviour of furcellarans the samples were dissolved in deionised-water and dialysed against 100 mM KCl solution at 4 °C overnight. The stiffness of the gels at 25 °C was determined as the shear modulus (G′) at 200 Hz calculated from the measured velocity of a shear-wave passing through the gel using a Rank pulse shearometer. In experiments on elastic gels (such as gelatin and carrageenan) which behaved as Hookean solids, it was found that the shear modulus measured in this way was comparable to that measured using small static deformations (Ring and Stainsby, 1985).

The differences in yields between water extracted (38%) and alkali extracted (24%) furcellarans can be explained in that alkali treatment is known to degrade polysaccharides. In the present case, although a reduced yield was obtained, the sample had the highest intrinsic viscosity.

The monosaccharide composition, sulphate content and intrinsic viscosity of the furcellaran preparations is shown in Table 1. The neutral sugars present were predominantly galactose and 3,6-anhydrogalactose, with smaller amounts of 6-*O*-methylgalactose, xylose, glucose and mannose. The xylose is most likely to occur as single branches on the 3-linked galactosyl units in carrageenans and the glucose is likely to be derived from floridean starch present in these samples (Falshaw et al., 2001). The composition is similar to that obtained in a previous study (Truus et al., 1997) and indicates that the polysaccharide structure may be somewhat more complex than that represented by a simple repeating unit. The monosaccharide composition of the alkali-modified preparation was similar to that of the native preparation, except that the proportion of galactose and glucose was lower (5 and 0.9%, respectively) and the proportion of 3,6-anhydrogalactose and 6-*O*-methylgalactose was higher (6 and 0.6%, respectively). The alkali modification of native furcellaran decreased also the sulphate content of these preparations. These observations indicated that alkali treatment resulted the conversion of precursor 4-linked galactose 6-sulphate into 3,6-anhydrogalactose units. The commercial furcellaran has more 3,6-anhydrogalactose and less galactose, xylose and mannose content compared with Estonian furcellaran.

The sulphate contents of 17–18% for native Estonian furcellaran and commercial furcellaran, and 16–17% (w/w) for alkali-treated Estonian furcellaran indicate that there is an average approximately one charge for every three monomer residues. This is

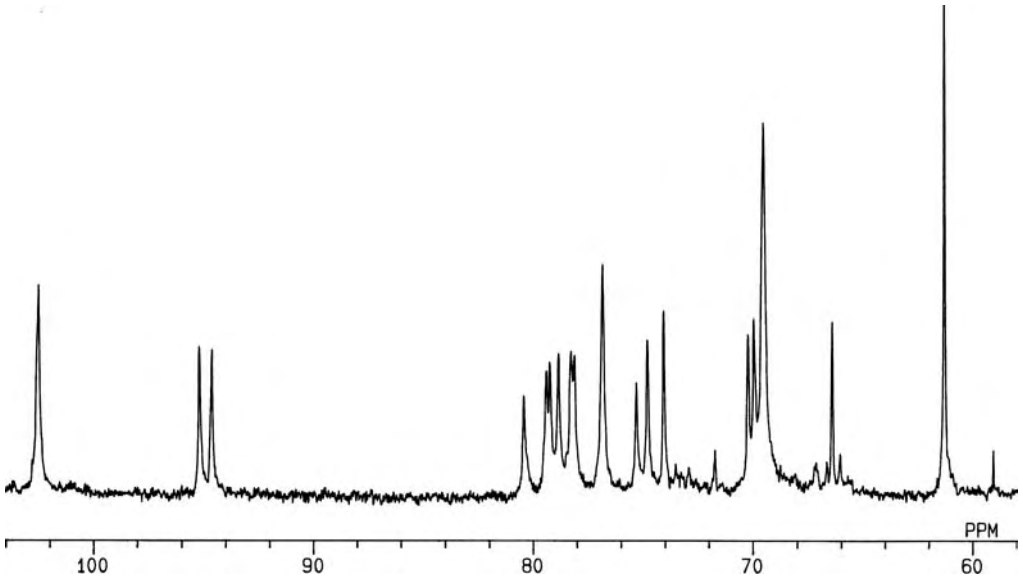

Figure 1. NMR spectrum of Estonian furcellaran.

comparable with previous study, and indicates that furcellaran has on average half the ester sulphate content of κ-carrageenan (Glicksman, 1983; Nussinovich, 1997).

The intrinsic viscosity results indicate that the polysaccharides have a relatively expanded conformation in 0.1 M NaCl. The high intrinsic viscosity for alkali modified furcellaran of 1304 mL g^{-1}, is almost 2.5× that of the native furcellaran.

^{13}C-NMR spectrum of sulphated polysaccharide from *F. lumbricalis* is shown in Figure 1. The signal assignments (Table 2) were made on the basis of comparison with chemical shifts of basic agar and carrageenan structures (Van de Velde, 2002). The main signals are due to (1→3) linked β-D-galactopyranose; (1→4) linked 3,6-anhydro-α-D-galactopyranose; and (1→3) linked β-D-galactopyranose 4-sulphate. The different furcellarans had similar spectra; the observed differences in intensity were in agreement with the results obtained by GC/MS. The native Estonian furcellaran had more intense peaks corresponding to (1→3) linked β-D-galactopyranose residues and alkali-modified Estonian furcellaran and commercial furcellaran had more intense peaks corresponding to (1→4) linked 3,6-anhydro-α-D-galactopyranose.

The dependence of shear modulus G' on the furcellaran concentration is shown in Figure 2. The shear modulus increased with increasing concentration of furcelleran for all three furcellaran preparations, showing most stiff gels of commercial furcellaran. The native Estonian furcellaran showed the lowest gel

Table 2. Chemical shift assignments for ^{13}C-NMR spectra of furcellaran (G: (1→3) linked β-D-galactopyranose; AG: (1→4) linked 3,6-anhydro-α-D-galactopyranose; G4S: (1→3) linked β-D-galactopyranose 4-sulphate.

	Chemical shifts (ppm)					
Unit	C-1	C-2	C-3	C-4	C-5	C-6
G	102.5	69.5	80.4	66.4	75.3	61.3
AG	94.6	70.2	79.4	78.1	76.8	69.5
G4S	102.5	69.5	78.8	74.1	74.8	61.3

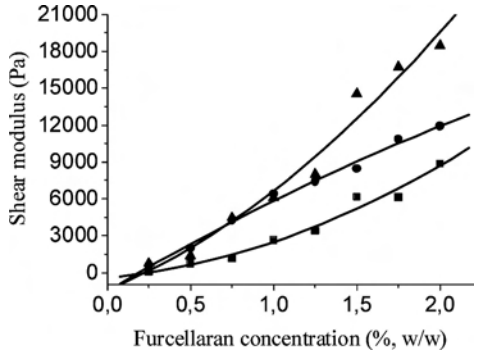

Figure 2. Dependence of shear modulus on furcellaran concentration. Native furcellaran (■), alkali treated furcellaran (●), commercial furcellaran (▲).

stiffness that was improved with alkali treatment. There is positive correlation between 3,6-anhydrogalactose content and gel stiffness, with the alkali treatment increasing gel stiffness.

In conclusion, it can be said that comparing the Estonian furcellaran with the commercially available furcellaran, there is no difference in structure as assessed by NMR but there is some difference in monosaccharide composition: the Estonian furcellaran has less 3,6-anhydrogalactose and more galactose, xylose and mannose content compared with commercial furcellaran. Differences were observed in the rheological properties of the furcellarans. The Estonian furcellaran had a higher intrinsic viscosity in aqueous solution and the gels gave a smaller shear modulus than the commercial furcellaran.

Acknowledgments

The authors thank the BBSRC core strategic grant for financial support; the EC Commission for the award of a Marie Curie fellowship to K.L. (Contract Number QLK-1999-50512).

References

Amimi A, Mouradi A, Givernaud T, Chiadmi N, Lahaye M (2001) Structural analysis of *Gigartina pistillata* carrageenans (Gigartinaceae, Rhodophyta). Carbohydr. Res. 333: 271–279.

Ciancia M, Noseda MD, Matulewicz MC, Cerezo AS (1993) Alkali-modification of carrageenans: Mechanism and kinetics in the kappa/iota-, mu/nu- and lambda-series. Carbohydr. Polym. 20: 95–98.

Falshaw R, Bixler HJ, Johndro K (2001) Structure and performance of commercial kappa-2 carrageenan extracts: I. Structure analysis. Food Hydrocolloids 15: 441–452.

Glicksman M (1983) Red seaweed extracts (agar, carrageenan, furcellaran). In Glicksman M (ed), Food Hydrocolloids, CRC Press, Baton Raton, Florida, pp. 73–113.

Harris PJ, Blakeney AB, Henry RJ, Stone BA (1998) Gas chromatographic determination of the monosaccharide composition of plant cell wall preparations. J. Assoc. Off. Anal. Chem. 71: 272–275.

Knutsen SH, Myslabodsky DE, Grasdalen H (1990) Characterization of carrageenan fractions from Norwegian *Furcellaria lumbricalis* (Huds.) Lamour. by ^{1}H-N.M.R. spectroscopy. Carbohydr. Res. 206: 367–372.

Nussinovitch A (1997) Carrageenans. In Nussinovitch A (ed), Hydrocolloid Applications. Blackie Academic & Professional, London, pp. 40–62.

Ring SG, Stainsby G (1985) A simple method for determining the shear modulus of food dispersions and gels. J. Sci. Food Agric. 36: 607–613.

Silvestri LJ, Hurst RE, Simpson L, Settine JM (1982) Analysis of sulfate in complex carbohydrates. Anal. Biochem. 123: 303–309.

Stevenson TT, Furneaux RH (1991) Chemical methods for the analysis of sulphated galactans from red algae. Carbohydr. Res. 210: 277–298.

Truus K, Vaher M, Usov AI, Pehk T, Kollist A (1997) Gelling galactans from the algal community of *Furcellaria lumbricalis* and *Coccotylus truncatus* (the Baltic Sea, Estonia): A structure-property study. Int. J. Biol. Macromol. 21: 89–96.

Van de Velde F, Knutsen SH, Usov AI, Rollema HS, Cerezo AS (2002) ^{1}H and ^{13}C high resolution NMR spectroscopy of carrageenans: Applications in research and industry. Trends Food Sci. Technol. 13: 73–92.

APPENDIX 1

ARTICLE III

Laos, K., Brownsey, G.J., Friedenthal, M., Ring, S.G. 2005. Rheological properties of gels formed with furcellaran and globular proteins bovine serum albumin and β-lactoglobulin. – ***Annual Transactions of Nordic Rheology Society, Vol. 13, 269-275***

Rheological properties of gels formed with furcellaran and globular proteins bovine serum albumin and β-lactoglobulin

Katrin Laos[1], Geoffrey J. Brownsey[2], Margus Friedenthal[1] and Stephen G. Ring[2]

[1] Department of Food Processing, Tallinn University of Technology, Ehitajate tee 5, Tallinn 19086, Estonia
[2] Division of Food Materials Science, Institute of Food Research, Norwich Research Park, Colney, Norwich NR4 7UA, UK

ABSTRACT

The effect of the addition of the globular proteins, bovine serum albumin and β-lactoglobulin, on the properties of furcellaran gels was studied. The gels were found to be physically cross-linked networked gels. Proteins strongly influence the shear modulus. At low pH the phase-separation occurred with the change in loss tangent.

INTRODUCTION

Both proteins and polysaccharides contribute to the structural properties of foods through their aggregation and gelation behaviour. The development of novel gelled products from proteins and polysaccharides and their control needs a better understanding of gelation mechanisms and physical properties of mixed gels[1].

When gelation occurs between two different polymers, three basic types of gel structure can be observed, namely interpenetrating, associative, and phase-separated networks. Interpenetrating networks form when the two components gel separately and form independent networks. Both networks are continuous throughout the sample but any interaction between them is only topological[2]. Associative networks are formed when there are direct associations between polymers prior to network formation. Phase-separation can be segregative (also called thermodynamic incompatibility) and associative (also called complex coacervation). In associative phase separation one of the separating phases is enriched in both polymers, whilst, in a segregative phase separation each phase is enriched in one of the polymers[3]. When phase separation takes place, a competition between the phase separation and gelation process generally takes place, resulting in an increase in the complexity of the system[4].

The understanding of the mechanisms of interaction and the effect of changing conformation on these interactions is of great interest for predicting the structure and the properties of mixed systems[5].

Furcellaran is an anionic sulphated polysaccharide extracted from the red alga *Furcellaria lumbricalis*. It is currently considered to be a copolymer of β- and κ-carrageenan and usually represented structurally as a repeating unit of alternating 3-linked β-D-galactopyranose and 4-linked α-D-galactopyranose residues, with part of the latter existing as a 3,6-anhydro derivate[6] (Figure 1). Hydroxyl groups in the polysaccharide chain may be substituted (sulphated, methylated, etc.) and other monomer residues such as xylose and glucose may be found[7]. Furcellaran is a

polyelectrolyte that carries sulphate groups and it is negatively charged over a wide range of pH. The charge density is usually one sulphate per three or four monomer units[8].

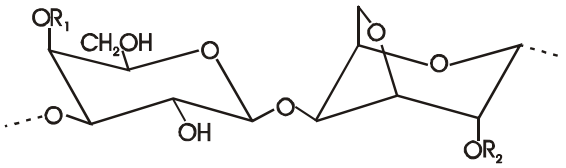

Figure 1. Primary structure formulae of the repeating disaccharide unit of β-(R_1=R_2=H) and κ-(R_1=OSO_3^-, R_2=H)

A characteristic of furcellaran is its ability to form gels in the presence of specific ions which is associated with a conformational change from coil to helix. Gelation of furcellaran is believed to proceed like κ-carrageenan via a two-step mechanism, as shown in Figure 2. Carrageenan chains associate themselves by the formation of intermolecular double helices, but these do not in themselves produce a gel network. Gelation occurs with the subsequent aggregation of these helices mediated by specific binding of gel promoting cations (particularly K^+ and Ca^{2+})[9].

Bovine serum albumin (BSA) is one of the most widely studied and applied proteins in biochemistry. It is an important, globular blood protein with molecular mass of 66,000. Serum albumins comprise about 580 amino acid residues and are characterized by a low content of tryptophan and a high content of cystine and charged amino acids, such as aspartic and glutamic acids, lysine and arginine[10].

β-lactoglobulin (BLG) is a major protein of the whey fraction of milk in many mammals. At physiological conditions, bovine β-lactoglobulin forms dimer, with each monomer consisting of 162 amino acid residues and characterized by a molecular mass 18,300. The conformation of BLG is pH dependent. At pH 3.5 the protein

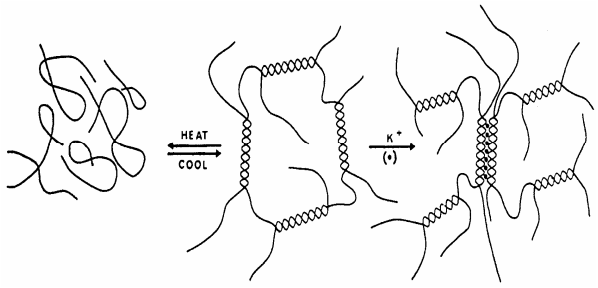

Figure 2. The two-step "domain" model for gelation of κ-carrageenan[9].

dimerizes, at pH 4.6 the dimers may further aggregate to form an octamer and at pH 7.5 the protein conformation undergoes a reversible transition which leads to a swelling of the monomeric unit[11].

The aim of this study is to investigate the rheological behaviour of mixed gels formed with furcellaran and globular proteins, BSA and BLG.

EXPERIMENTAL

Materials

The furcellaran was a gift from FMC Food Ingredients.

BSA and BLG were supplied by Sigma-Aldrich. They were used without further purification. The potassium acetate and potassium phosphate buffer solutions were prepared with analytical grade reagents.

Purification of furcellaran

The furcellaran preparation (3g) was dissolved in 2 L milliQ water at ~100°C. The solution was passed through diatomaceous earth (Sigma-Aldrich Co, Ltd., UK) and dialyzed (yield 80%). The Na^+ furcellaran was obtained by elution through an ion-exchange (Amberlite IR-120) column in the Na^+ form at 4 °C. The eluant was freeze-dried.

Preparation of gels

Protein and furcellaran samples were dispersed separately in water or buffer solutions and then mixed. The gels were

prepared by dialysing the solutions against 1M KCl solution in water or buffer solution at 4°C for overnight.

Rheometry

The stiffness of the gels at 25°C was determined as the shear modulus at 200 Hz calculated from the measured velocity of a shear-wave passing through the gel using a Rank pulse shearometer[12].

The rheological properties of the gels were analysed by dynamic oscillatory controlled strain measurements using the Advanced Rheometric Expansion System (ARES-LS2). The viscoelastic properties of the gels were analysed by recording the storage modulus (*G'*), loss modulus (*G''*), and loss tangent (tanδ) during strain and frequency sweeps at 25°C. A parallel plate measuring geometry was used with gel diameter 4mm. The gel pieces were carefully placed on the lower plate of the rheometer, and a compression of not more than 0.5% was applied to the gel by the upper plate. Strain sweep measurements were performed at a constant frequency of 1 Hz whilst frequency measurements were performed using 0.1% strain, which was within the linear viscoelastic region for furcellaran and mixed gels.

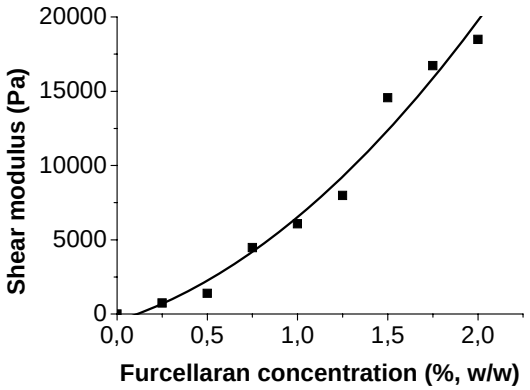

Fig.3. Dependence of shear modulus on furcellaran concentration.

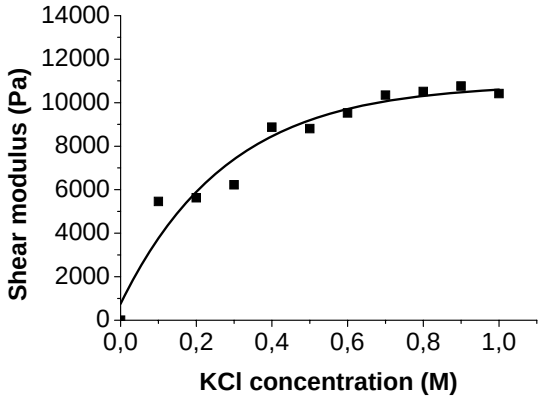

Fig.4. Dependence of shear modulus on KCl concentration

RESULTS AND DISCUSSION

The dependence of shear modulus on the furcellaran concentration is shown in Figure 3. The shear modulus increased with increasing concentration of furcellaran. In Figure 4 is shown dependence of shear modulus on the KCl concentration (0.1-1M) for the 1.5% furcellaran gel. The shear modulus increased with KCl concentration, and was more marked in the concentration range 0 to 0.4 M KCl.

Dynamic oscillatory rheology was used to monitor more detailed gel characteristics. To ensure that the gel properties were measured within the linear viscoelastic region, strain sweep measurement were first carried out (Figure 5). It can be seen that of 1% (1.5% furcellaran gel) and 0.8% (mixed gel) the gel characteristics start to change. This is caused by gel slipping between the plates of the rheometer and can be explained by syneresis. The same behaviour had been observed before also with κ-carrageenan gels[9,13,14] and is said to be a limiting factor in the measurements of the mechanical properties of carrageenan gels. In our case the syneresis was more marked gels with low pH. For all samples the linear viscoelastic region was below a strain of 0.5%. Thus for frequency sweep measurements a strain value 0.1% was chosen.

The furcellaran and mixed gels in the studied pH range, showed a frequency

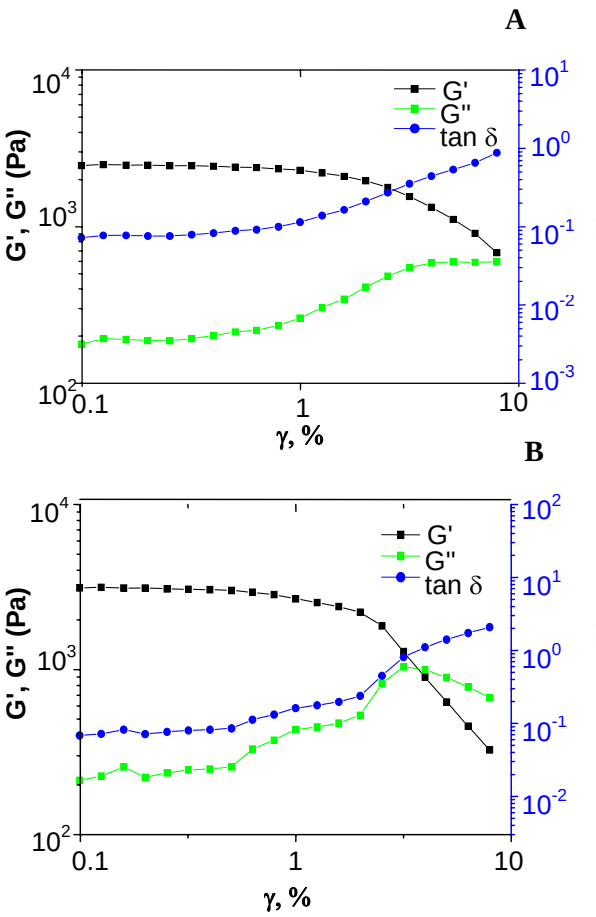

Figure 5. Shear modulus (G'), loss modulus (G'') and loss tangent (tan δ) as a function of strain for furcellaran (1.5% w/w) (A) and furcellaran (1.5% w/w) -BSA (0.5% w/w) mixture (B).

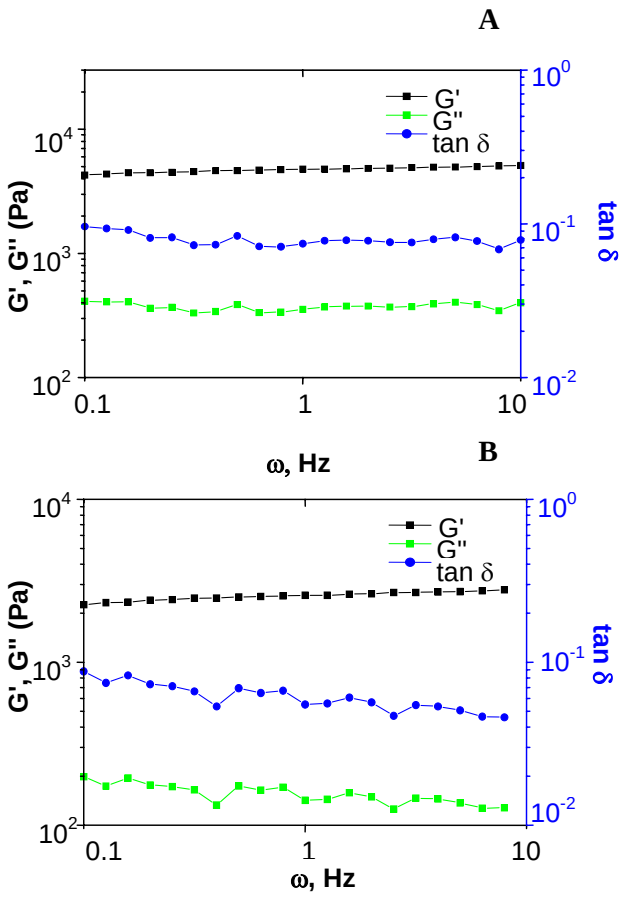

Figure 6. Shear modulus (G') and loss modulus (G'') as a function of frequency for furcellaran (1.5% w/w) (A) and furcellaran (1.5% w/w) -BSA (0.5% w/w) mixture (B).

dependence of *G'* but no *G'-G''* crossover and can be categorised as a typical physically cross-linked network gel (Figure 6). A physical gel is a polymer network in which junctions can break and recombine due to thermal fluctuation. The variation of storage modulus and loss modulus was small with added protein (Figure 6B) or changing pH.

For the shear modulus in mixed furcellaran/protein gels, complex behaviour was observed. The initial addition of 0.1% w/w protein to the 1.5% furcellaran solution increased shear modulus, further increase in protein content lead to a decrease in gel stiffness (Figure 7). In the range 0.5% to 2.5% (w/w) BSA and 0.75 to 2.5% (w/w) BLG, increase in modulus was observed. From a protein content of 2.5% (w/w) the gel stiffness decreased again. Similar behaviour in G' was recently reported by Oakenfull et al.[9] with gels made with κ-carrageenan and sodium caseinate. Considering their work, the behaviour between furcellaran and protein can be explained as follows:

1. When small amounts of protein are added, the dry matter content is increased and the *G'* increases.

2. When more protein is added, some of the furcellaran is bound to the protein. Bound furcellaran is no longer available to contribute to the furcellaran network. Thus *G'* decreases.
3. As the concentration of protein increases, protein aggregates with bound furcellaran become sufficiently abundant to form a continuous network, *G'* then increases.

In figure 7 (dotted curves) is shown the separate contributions to *G'* from the complex and furcellaran. The contribution of furcellaran decreases, as with increasing concentration of protein the furcellaran forms the complex with protein; the contribution from the complex increases, once it has passed the gel threshold.

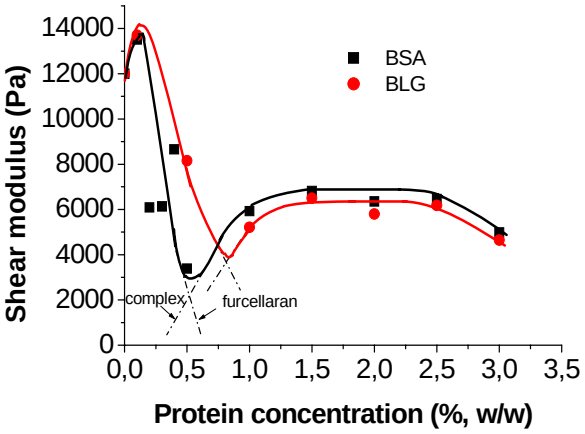

Figure 7. Dependence of shear modulus, *G'* 1 Hz, on BSA or BLG concentration in 1.5% w/w furcellaran gels.

Studying the dependence of pH on the gels, we observed that the structure of the mixed furcellaran/protein gels was pH dependent. At pH 7 the gels were translucent but became turbid with decreasing pH (Figure 8). This change indicates a phase separation between furcellaran and the protein. Looking the furcellaran/BSA mixed gel at pH=3.4 under the microscope we can see a coarse, phase separated structure (Figure 9).

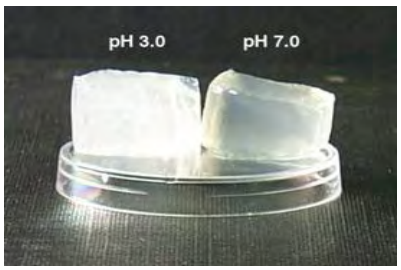

Figure 8. 1.5% w/w furcellaran gels with 1.5% w/w BSA at different pH's.

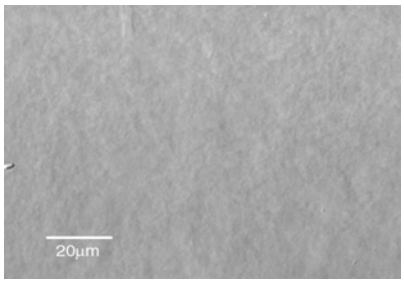

Figure 9. Optical micrograph of a 1.5% w/w furcellaran gel containing 1.5% w/w BSA at pH 3.

The dependence of shear modulus on the pH of furcellarans gels is shown in Figure 10. The shear modulus is increasing with increasing pH of medium, goes through maximum at pH 4.3 and begins to decrease. The gel stiffness starts to increase again from pH 6.2. The mixed systems behave in a similar way but the shear modulus values are higher. This behaviour indicates that low pH increases the stiffness of the gel but from pH 4.3 it starts to decrease again.

As in these measurements there wasn't a marked behaviour difference between furcellaran and furcellaran/protein gels, dynamic oscillatory rheology was applied. In Figure 11 it can be seen that for furcellaran gels the loss tangent increased linearly with increasing pH. But for mixed systems there was decrease in loss tangent between pH 3.4 and 4. From pH 4 the loss tangent increased linearly with increasing pH.

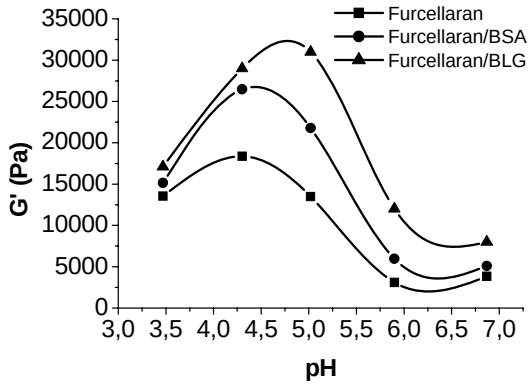

Fig.10. Dependence of shear modulus *G'* at 0.1 Hz on the pH of gels formed from 1.5% (w/w) furcellarans and 1.5% furcellaran and 1.5% protein (w/w) mixed gels.

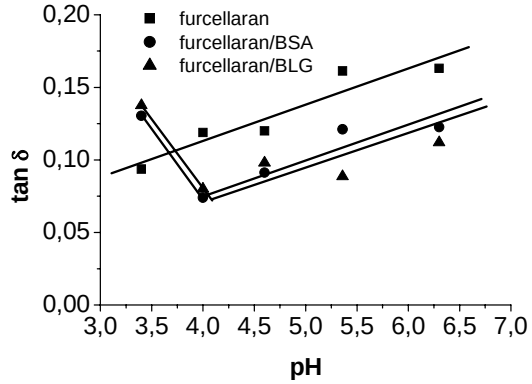

Fig.11. Dependence of loss tangent tan δ at 0.1 Hz on the pH of gels formed 1.5% w/w furcellarans and 1.5% furcellaran and 1.5% protein (w/w) mixed gels.

The results obtained show that when gelation occurs in furcellaran globular protein systems, at pH's in the vicinity of neutrality, an associative network forms. On decreasing the pH of the medium to pH 3.4 a phase separated structure forms.

CONCLUSIONS

This study shows that furcellaran and globular proteins form physically cross-linked network gels. The initial addition of protein to furcellaran solution increased shear modulus, further increase in BSA content leads to a decrease in gel shear modulus. Studying the dependence of pH on the gels we observed that the structure of the mixed furcellaran/protein gels was pH dependent. At low pH the associated phase separation occurred and loss tangent changed.

ACKNOWLEDGEMENTS

The authors thank the BBSRC core strategic grant for financial support; the EC Commission for the award of a Marie Curie fellowship to K.L. (Contract Number QLK-1999-50512)

REFERENCES

1. Baeza, R., Gugliotta, L.M., Pilosof, A.M.R. (2003), "Gelation of β-lactoglobulin in the presence of propylene glycol alginate: kinetics and gel properties", *Colloids and Surfaces B: Biointerfaces*, **31**, 81-93.
2. Morris, V. J. (1986). „Multicomponent gels." In Philips G.O., Wedlock, D.J., Williams, P.A. (Eds.) *Gums and stabilisers for the food industry*, 3. Elsevier, London, pp. 87-99
3. Piculell, L., Bergfeld, K., Nilsson, S. (1995). „Factors determing phase behaviour of multi-component polymer systems". In Harding, S., Hill, S.E., Mitchell, J.R. (Eds.) *Biopolymer mixtures*, Nottingham University Press, Nottingham, pp. 13-35.
4. Ould Eleya, M.M., Turgeon, S.L. (2000), "Rheology of κ-carrageenan and β-lactoglobulin mixed gels", *Food Hydrocolloids*, **14**, 29-40
5. Michon, C., Konatè, K., Cuvelier, G., Launay, B. (2002), "Gelatin/carrageenan interactions in coil and ordered conformations followed by a methylene blue spectrophotometric method", *Food Hydrocolloids*, **16**, 613-618.
6. Hugerth, A., Sundelöf, L.-O. (2001), "The effect of polyelectrolyte counterion specificity, charge density, and conformation on polyelectrolyte-amphiphile interaction: the carrageenan/ furcellaran -

amitriptyline system", *Biopolymers*, **58**, 186-159.
7. Van de Velde, F., Knutsen, S.H., Usov, A.I., Rollema, H.S., Cerezo, A.S. (2002), "^{1}H and ^{13}C high resolution NMR spectroscopy of carrageenans: Application in research and industry", *Trends in Food Science & Technology*, **13**, 73-92.
8. Glicksman, M. (1983), "Food Hydrocolloids", CRC Press, New York, pp 83-107.
9. Oakenfull, D., Miyoshi, E., Nishinari, K., Scott, A. (1999), "Rheological and thermal properties of milk gels formed with κ-carrageenan. I. Sodium caseinate", *Food Hydrocolloids*, **13**, 525-533
10. Peters, T. (1985), „Advances in Protein Chemistry", vol. **37**, Academic Press, New York, pp. 161–245.
11. Verheul, M., Pedersen, J.S., Roefs, S.P.F.M., de Kruif, K.G. (1999), "Association behaviour of native β-lactoglobulin", *Biopolymers*, **49**, 11-20.
12. Ring, S.G., Stainsby, G. (1985), "A simple method for determining the shear modulus of food dispersions and gels", *J. Sci. Food Agric.*, **36**, 607-613
13. Lai, V.M.F., Wong, P.A.-L., Lii, C.-Y. (2000), "Effects of Cation Properties on Sol-gel Transition and Gel Properties of κ-carrageenan", *Journal of Food Science*, **65**, 1332-1337.
14. MacArtain, P., Jacquier, J.C., Dawson, K.A. (2003), "Physical Characteristics of Calcium Induced Kappa- Carrageenan Networks", *Carbohydrate Polymers*, **53**, 395-400

APPENDIX 1

ARTICLE IV

Laos, K., Mironova, M., Friedenthal, M. Physical and mechanical properties of furcellaran and furcellaran/bovine serum albumin films. – INTRADFOOD 2005 – Innovations in Traditional Foods, Vol. 2, pp. 1343-1346

APPENDIX 1

ARTICLE V

Laos, K., Brownsey, G.J., Ring, S.G. Interactions between furcellaran and the globular proteins bovine serum albumin and β-lactoglobulin. – Carbohydrate Polymers. Accepted.

Interactions between furcellaran and the globular proteins bovine serum albumin and β-lactoglobulin.

Katrin Laos, Geoffrey J. Brownsey and Stephen G. Ring.

Division of Food Materials Science, Institute of Food Research, Norwich Research Park, Colney, Norwich NR4 7UA, UK

Abstract

The interaction between the algal polysaccharide furcellaran and the globular proteins, bovine serum albumin and β-lactoglobulin was examined as a function of pH using potentiometric and turbidimetric titration and photon correlation spectroscopy. On decreasing pH, the furcellaran first formed a soluble complex with the globular proteins at a pH_c, which showed a maximum in its dependence on ionic strength. On further decrease in pH, the onset of a more substantial aggregation, as indicated by a marked increase in turbidity occurred in the vicinity of the isoelectric point of the protein. Between these pH's the protein/furcellaran complex had a characteristic average size which was larger than the isolated furcellaran chain in solution. Complexation occurred when the protein carried an average net charge of the same sign as the furcellaran.

Keywords: Furcellaran; Lactoglobulin; Serum Albumin; Complexation.

1. Introduction

Protein/polysaccharide mixtures are widely encountered in nature and in industrial products, including manufactured foods. The resulting microstructures which form from these mixtures is influenced by the intermolecular interactions

between biopolymers. Many such systems are far from equilibrium, with kinetic arrest having a major impact on microstructure.

Attractive interactions between positively charged peptides/proteins and anionic polysaccharides can lead to gelation (MacDougall, Brett, Morris, Rigby, Ridout, & Ring 2001), where the cationic fragment acts as a crosslink; coacervation (Turgeon, Beaulieu, Schmitt & Sanchez 2003) where the attraction of opposite charges on the biopolymers leads to phase separation/precipitation of a protein/polysaccharide mixture (Weinbreck, de Vries, Schrooyen, & de Kruif 2003), and multilayer formation where sequential deposition of oppositely charged polymers leads to surface crosslinking and successive charge reversal at the surface and the build up of a multilayer (Decher 1997). Proteins and polysaccharides carrying charge of the same sign, can phase separate from concentrated solution with the formation of a protein-rich and a polysaccharide-rich phase (Dickinson 2003). It is has been found that under some conditions the polyampholyte protein can form complexes with polycations and polyanions under conditions where the average charge on the protein has the same sign as the polycation or polyanion (Park, Muhoberac, Dubin, & Xia 1992). This interaction has mainly been examined in mixtures of a protein with a synthetic polyelectrolyte (Hallberg & Dubin 1998; Wen & Dubin 1997). During the titration of a polyanion/protein mixture from a high pH, as the charge on the protein is reduced there is a transition, at pH_c, where complexation of the protein and polysaccharide occurs, with the formation of a soluble complex. This transition can be probed experimentally by a range of techniques including turbidimetry (Hattori, Kimura, Seyrek, & Dubin 2001), dynamic light scattering (Li, Mattison, Dubin, Havel, & Edwards 1996), and potentiometry (Wen & Dubin 1997). In this region, complexation behaviour is reversible. As the charge on the protein is further reduced

and becomes opposite in sign, another transition is observed which signifies the onset of complex coacervation. Charge is not evenly distributed over the protein surface. While the net charge on the protein may be of the same sign as that of the polyelectrolyte, oppositely charged ‘patches’ on the protein surface may help stabilise complex formation. The ionic strength dependence of complexation also points to the involvement of electrostatic interactions in complex formation. At low ionic strength, long range repulsive interactions between the polyampholyte and polyelectrolyte dominate. As the ionic strength increases, these interactions become progressively screened and the attractive interaction between charge patches on the polyampholyte and the polyelectrolyte become significant (Seyrek, Dubin, Tribet, & Gamble 2003). An important entropic driving force for complex formation is the release of counterions ‘associated’ with the charged regions on polyampholyte and polyelectrolyte on complexation (Mascotti & Lohman 1990; Record, Lohman, & deHaseth 1976). Further increase in ionic strength reduces the strength of the attractive interaction (Skepo & Linse 2002) and the entropic effect favouring complexation. A combination of these effects produces the observed maximum in the extent of complexation as a function of ionic strength. The complex may be further stabilised through other intermolecular forces. For example, in the case of the complexation of proteins and synthetic polyelectrolytes it is suggested that hydrophobic effects could also play a role (Hallberg & Dubin 1998).

Much of the earlier research on these interactions focused on the behaviour of synthetic polyelectrolytes. One advantage in their study is that polyelectrolyte characteristics such as charge, charge density and its distribution, can be relatively well defined and controlled. These effects also play an important role in the behaviour of biopolymer systems, such as synovial fluid (Moss, VanDamme, Murphy, &

Preston 1997); the DNA histone complex (Luger, Mader, Richmond, Sargent, & Richmond 1997); the interaction between prion proteins and sulphated polysaccharides (Brimacombe, Bennett, Wusteman, Gill, Dann, & Bostock 1999); and the behaviour of proteins at the interface in the bulk and at the surface in fabricated biopolymeric materials. Many complex foods consist of protein/polysaccharide mixtures. Food polysaccharides include both weak (pectin, alginate) and strong polyelectrolytes (carrageenan), having carboxylate and sulphate groups respectively. Recent studies have examined the complexation of whey proteins with carrageenan (Weinbreck, Nieuwenhuijse, Robijn & de Kruif 2004). As part of our continuing research on the behaviour of polysaccharides in complex foods we examine the interaction between a strong polyelectrolyte of the carrageenan family (furcellaran) and the globular proteins bovine serum albumin (BSA) and β-lactoglobulin (BLG).

Furcellaran is a sulphated galactan which can be extracted from the seaweed *Furcellaria lumbricalis* (Lahaye 2001; Truus, Vaher, Usov, Pehk, & Kollist 1997). Sugar and methylation analysis have shown that it consists of residues of 3-linked β-D-galactopyranose and its 4-sulphate and 4-linked α-D-galactopyranose. The latter residues may exist as a 3,6-anhydro residue which may be partially sulphated at position 2. Furcellaran preparations may also contain small amounts of other sugar residues (Truus, Vaher, Usov, Pehk, & Kollist 1997). Structurally, furcellaran is related to the algal polysaccharide kappa carrageenan, with a major structural difference being that furcellaran has a smaller degree of sulphation (Lahaye 2001). A characteristic of these polysaccharides is their ability to form gels in the presence of specific ions, associated with a molecular conformational change from coil to helix (Lahaye 2001). They also have the potential to interact with oppositely charged

macroions, including globular proteins. It is this latter aspect which is the focus of the current study.

2. Materials and methods

2.1. Source of materials

Furcellaria lumbricalis was collected in Kassari Bay (the Baltic Sea, Estonia) and cleaned of epiphytes. The algae were washed thoroughly with tap water and the galactans were extracted according to the method of Amimi, Mouradi, Givernaud, Chiadmi, & Lahaye (2001), using deionized-water (1.5 L) under agitation for 3 hours at 95 °C. The aqueous phase was clarified by passing through a nylon cloth and then precipitated in 2.5 volumes of isopropanol, filtered and dried at room temperature. The yield of furcellaran was 37.8% w/w. 3 g of furcellaran were dissolved in 2 L milliQ water at ~100 °C. The solution was passed through diatomaceous earth (Sigma-Aldrich Co, Ltd., UK) and dialyzed. The Na^+ furcellaran was obtained by elution through an ion-exchange (Amberlite IR-120) column in the Na^+ form at 4 °C. The eluant was freeze-dried. The behaviour of this laboratory-prepared furcellaran was similar to that of a commercial sample obtained from FMC Food Ingredients. Bovine serum albumin and β-lactoglobulin, were obtained from Sigma-Aldrich Co, Ltd., UK, and used without further purification.

2.2. Characterization of furcellarans

For the determination of monosaccharide composition, the furcellaran was hydrolysed by a double-hydrolysis-reduction method as described by Stevenson and Furneaux.(1991) The alditols were converted to their acetates and analysed by GC/MS as described.(Harris, Blakeney, Henry, & Stone 1988) The sulphate content was measured colorimetrically as described by Silvestri, Hurst, Simpson, & Settine

(1982). For ^{13}C-NMR spectroscopy, the polysaccharide samples were dissolved in D_2O (5% w/v) and spectra were recorded in a JEOL EX spectrometer at 85 °C. Chemical shifts were calculated with reference to the C-6 signal from the galactose residue at 61.3 ppm. Measurements of specific viscosity as a function of concentration of furcellaran (0.025-0.2% w/w) in 0.1 M NaCl were carried out using an Ubbelohde viscometer at 20 °C. The efflux time for 0.1 M NaCl was 143.7 s and no shear rate corrections were made. The instrinsic viscosity [η] was calculated from the extrapolation of specific viscosity to zero concentration.

2.3. Potentiometric and turbidimetric titration

pH titrations were carried out with a Jenway pH meter equipped with a combination electrode, under N_2, at room temperature. A microburette was used to add 0.1 M HCl to 15 mL of a 3 g/L protein solution in 0.03 M NaCl with or without 0.6 g/L furcellaran. Prior to titration the pH was adjusted to 9.0 with dilute NaOH, the alkali was added slowly, through narrow bore capillary tubing, with a microburette to the stirred protein-containing solution. pH values were recorded when the change in pH with time was < 0.01 pH units per minute. For turbidimetric titration, solutions of 3.0 g/L of protein and 0.6 g/L of furcellaran were prepared in 0.03 M NaCl. The initial pH was adjusted to 10.0 for BSA and 9.0 for BLG. The solution was titrated with 0.1 M HCl as described above. Changes in turbidity were monitored at 600 nm (Perkin-Elmer Lambda 15 UV/VIS Spectrophotometer, Beaconsfield, Bucks) and reported as 100 - %T. The net charge of protein was determined by titrating a 15 mL of a protein solution (3 g/L) in 0.03 M NaCl from the reported pI, either with 0.1 M HCl or with 0.1 M NaOH. A solvent blank was used to determine the direct contribution of HCl or NaOH to the solution pH. The protein titration data were in

good agreement with published research (Cannan, Palmer, & Kibrick 1942; Tanford, Swanson, & Shore 1955). All experiments were performed in triplicate

2.4. Photon correlation spectroscopy.

The apparatus employed was an ALV/SP-86 spectrogoniometer (ALV, Langen, Germany) equipped with a Coherent Radiation Innova 100-10 vis Argon Ion laser operating at 0.5 W and wavelength of 514 nm. Furcellaran (1.2 g/L) and protein solution (6g/L), at pH 9.0, were filtered through a 0.2 μm Millipore filter. The biopolymer solutions were weighed into a washed cuvette, mixed (to give concentrations of furcelleran and protein of 0.6 and 3 g/L respectively), and the pH of the mixture adjusted through the addition of dilute HCl. After the experiment the pH was measured.

The scattered light intensity was monitored using an ALV/PM-15 ODSIII detection system at a fixed scattering angle of 90 °. After amplification and discrimination, signals were directed to an ALV/5000E digital multiple-tau correlator and time-intensity correlation functions recorded, typically for 600 s duration. Size distribution functions were computed using the appropriate Windows-based ALV software which incorporated regularised inverse Laplace transform and ALV-CONTIN packages. Additional analysis was undertaken using Origin V6 (Microcal) proprietory software. All experiments were performed in triplicate

3. Results and Discussion

3.1.Furcellaran characterisation.

The monosaccharide composition of the furcellaran preparation is shown in Table 1, and includes galactose; 3,6 anhydro galactose; and smaller amounts of 6-O-methyl galactose. The composition is similar to that obtained in a previous study and

indicates that the polysaccharide structure may be somewhat more complex than that represented by a simple repeating unit (Truus, Vaher, Usov, Pehk, & Kollist 1997). The sulphate content of 14.9% w/w indicates that there is on average one charge for every 2.8 monomer residues, which is in broad agreement with commonly accepted value of one charge for every three residues (Lahaye 2001). The intrinsic viscosity of 507 mL g^{-1} indicates a relatively large molecular size in 0.1 M NaCl. The ^{13}C NMR spectra of the polysaccharide is shown in Fig. 1. The chemical shift assignments (Truus, Vaher, Usov, Pehk, & Kollist 1997) indicate the presence of (1→3) linked β-D-galactopyranose; (1→4) linked 3,6 anhydro-α-D-galactopyranose; and (1→3) linked β-D-galactopyranose 4-sulphate.

3.2. Turbidimetric titration

The interaction between furcellaran and the globular proteins bovine serum albumin (BSA) and β-lactoglobulin (BLG) was examined by turbidimetric titration. The change in turbidity with decreasing pH for a furcellaran solution (0.6 g/L) containing either 3 g/L of BSA or BLG is shown in Figs. 2a and b respectively. At high pH's the turbidity is essentially independent of pH. As pH is decreased the turbidity starts to show a weak dependence on pH which occurs at a pH_c. As pH is further decreased there is a marked increase in turbidity over a narrow pH range. In previous research on polyelectrolyte/protein complexes (Hattori, Kimura, Seyrek, & Dubin 2001; Seyrek, Dubin, Tribet, & Gamble 2003) it was shown that pH_c is associated with the formation of a soluble polyelectrolyte/protein complex, and the more marked change in turbidity is associated with precipitation and complex coacervation of the polyelectrolyte with the protein. For the mixtures shown, in 0.03 M NaCl, pH_c occurs in the region of 7.5 for both BLG and BSA. At this pH, the average net charge on the protein molecule is ~ -13 (Cannan, Palmer, & Kibrick 1942;

Fogolari, Ragona, Licciardi, Romagnoli, Michelutti, Ugolini, & Molinari 2000; Tanford, Swanson, & Shore 1955). The onset of a more marked change in turbidity, associated with the formation of larger aggregates, occurs in the region of pH 5.0 and 5.3 for BSA and BLG respectively. As the isoionic point of the isolated proteins is ~ 5.3 for defatted BSA (Tanford, Swanson, & Shore 1955) and ~ 5.1 for BLG (Cannan, Palmer, & Kibrick 1942) this change in behaviour is occurring in the region of the isoelectric point. The more substantial aggregation and turbidity increase at lower pH's is occurring when the protein is expected to have a net positive charge (Cannan, Palmer, & Kibrick 1942; Tanford, Swanson, & Shore 1955).

At pH > 6.0 the turbidity is stable over minutes and the turbidity increase can be reversed by raising the pH. If the pH is lowered to pH 4.0, and then raised again, then for both BSA and BLG the turbidity increase is substantially reversible (>95%) indicating that the more substantial aggregation observed at pH's below the isoelectric point also involves a limited kinetic arrest. The values of pH_c showed a dependence on ionic strength as shown in Fig. 3. In dilute salt solutions in the range 0.01 to 0.075 M, the pH_c transition is shifted to higher pH's as the ionic strength increases and then decreases on further increase in ionic strength for both BLG and BSA. This ionic strength dependence is a generally observed feature for the complexation of polyelectrolytes and proteins (Seyrek, Dubin, Tribet, & Gamble 2003). Over the range of ionic strength examined the net charge on the protein at pH_c ranges from ~-9 to ~-15 (Cannan, Palmer, & Kibrick 1942; Fogolari, Ragona, Licciardi, Romagnoli, Michelutti, Ugolini, & Molinari 2000; Tanford, Swanson, & Shore 1955). At each ionic strength, the charge on the proteins, BSA and BLG, at pH_c is comparable. Based on previous research on polyelectrolyte/protein complexation, the dependence of turbidity on pH in these mixtures indicates that there is complexation between

furcellaran and the globular proteins at pH's between pH_c and the isoelectric point of the protein. Below the isoelectric point of the protein there is a more marked aggregation as indicated by the substantial increase in turbidity of the mixtures.

The development of turbidity as a function of furcellaran concentration was probed at pH 4.0 and pH 7.0 for both BSA (Fig. 4a) and BLG (Fig. 4b) in 0.03M NaCl at a fixed protein concentration of 1 g/L. At pH 7.0 for both BSA and BLG there is a slow increase in turbidity with increasing furcellaran concentration consistent with complex formation. At pH 4.0 there is a more marked increase with increasing furcellaran concentration. At pH 4.0 the BSA molecule carries a net positive charge of 26, and the BLG monomer a charge of 15. From the known molecular masses of BSA and the BLG monomer (66 kD and 18.3 kD respectively), and the measured sulphate content of furcellaran, charge balance would occur at furcellaran concentrations of ~0.22 and ~0.48 g/L for BSA and BLG respectively. The observed maximum in turbidity as a function of furcellaran concentration, which is observed for BSA, occurs in the region of charge balance. For BLG there is a broad plateau in the expected region of charge balance. For the interaction of synthetic polyelectrolytes with globular proteins, similar behaviour is observed (Wen & Dubin 1997). At pH's where the polyelectrolyte and protein carry a net charge opposite in sign, the observed maximum in turbidity as a function of polyelectrolyte concentration can be much sharper (Wen & Dubin 1997). Indeed at higher concentrations of polyelectrolyte the turbidity falls markedly as the aggregates redisperse. One origin of these differences in behaviour with furcellaran is that the synthetic polyelectrolytes have a relatively high charge density per mass of polymer compared to furcellaran.

The extent of aggregation of polymers in the pH range below pH_c was further investigated by photon correlation spectroscopy.

3.3. Photon correlation spectroscopy.

Photon correlation spectroscopy was used to further characterise the interaction between furcellaran and the globular proteins, BSA and BLG, through the determination of an effective particle size from measurements of a translational diffusion coefficient D_t. For a particle in solution subject to Brownian motion, the translational diffusion coefficient is related to the measured scattered light intensity correlation function $g^{(2)}\tau$ by the expression

$$g^{(2)}\tau = 1 + \exp(-2 D_t k_s^2 \tau) \quad (1)$$

where k_s, the scattering vector, is given by

$$k_s = \frac{4\pi n}{\lambda} \sin\frac{\theta}{2} \quad (2)$$

where n is the refractive index of the solution, θ, the scattering angle and λ the wavelength of light. For the diffusion of particles in dilute solution, the hydrodynamic radius of the particle, R_h, may be obtained from

$$D_t = kT / 6\pi\eta R_h \quad (3)$$

where, η, is the solvent viscosity and k and T have their usual meanings.

The published X-ray crystal structure of serum albumin indicates a heart-shaped molecule which can be approximated to an equilateral triangular prism with sides of 8 nm and a depth of 3 nm (Carter & Ho 1994). Under conditions of neutral pH BSA has an axial ratio of approximately 2.66. The conformation of BSA shows a pH dependence (Carter & Ho 1994), with the native form being found between pH's 4 and 8. Size exclusion chromatography of BSA solution showed that it was largely unaggregated (> 93%). For a 0.6% w/w solution of BSA in 30 mM sodium chloride at

pH 5.4 and 20 °C, the measured diffusion coefficient was 5.7 x 10^{-11} m^2s^{-1}. The measured value of D_t is in good agreement with published research (Gaigalas, Hubbard, McCurley, & Woo 1992; Meechai, Jamieson, & Blackwell 1999), with a calculated hydrodynamic radius of 4.2 nm.

The conformation of BLG is pH dependent (Sawyer, Kontopidis, & Wu 1999; Verheul, Pedersen, Roefs, & de Kruif 1999). The monomeric unit has a molecular mass of 18.3 kDa. At pH 3.5 the protein dimerizes. This dimerization is dependent on ionic strength and protein concentration with higher ionic strength and concentrations stabilising the dimer to repulsive interactions at lower pH's (Aymard, Durand, & Nicolai 1996; Sakurai, Oobatake, & Goto 2001). At pH 4.6 the dimers may further aggregate to form an octamer. At pH 7.5 the protein conformation undergoes a reversible transition which leads to a swelling of the monomeric unit (Qin, Bewley, Creamer, Baker, Baker, & Jameson 1998; Tanford, Bunville, & Nozaki 1959). There are also some reports that above pH 7.5 the dimers may dissociate into monomeric units (Witz, Timasheff, & Luzzati 1964). At higher pH's there is the potential for a time-dependent irreversible aggregation. At pH 7.9 the measured value of D_t for a 0.6% w/w BLG solution in 0.03 M NaCl was 7.5 x 10^{-11} m^2s^{-1}, in agreement with previous measurements carried out under similar conditions (Beretta, Chirico, & Baldini 2000; Le Bon, Nicolai, Kuil, & Hollander 1999; Phillies, Benedek, & Mazer 1976), with a calculated hydrodynamic radius of 3.2 nm. As the pH was reduced the presence of a slower diffusive process in the autocorrelation function was observed, which was attributed to a limited aggregation, in agreement with published research (Takata, Norisuye, Tanaka, & Shibayama 2000). At pH's of 5.5 and 4.2 a more substantial aggregation was noted, related to the phase separation/precipitation of BLG from aqueous solution.

In dilute NaCl solution, algal galactans of the κ-carrageenan family exist as expanded flexible coils. In the presence of NaI a coil to helix transition is observed, and the presence of K^+ ions can additionally lead to the aggregation of helices. The D_t of furcellaran in 0.03 M NaCl solution (0.6% w/w) at pH 7.4 was 5.2 x 10^{-12} m^2s^{-1}, and similar to (6.9 x 10^{-12} m^2s^{-1}) a κ-carrageenan preparation in 0.1 M NaCl, with a weight average molecular weight of 421 kDa (Meunier, Nicolai, & Durand 2001).

Photon correlation spectroscopy of mixtures of furcellaran and BSA or BLG, at pH's above pH_c showed the presence of two diffusive processes corresponding to the translational diffusion of the furcellaran macromolecule and the globular protein. As the pH was lowered below pH_c there was a marked reduction in the slower process. The faster process had diffusion coefficients comparable to that of the globular protein in solution, although determination of D_t was complicated due to the polydisperse nature of the system. For both BSA and BLG mixtures with furcellaran, the hydrodynamic radius, R_h, of the components was calculated from D_t. The dependence of R_h on pH is shown in Figs. 5a, b for BSA/furcellaran and BLG/furcellaran mixtures respectively. Above the pH_c determined by turbidimetric titration, the hydrodynamic radius of the polymers in the mixture is comparable to that of the pure polymer in solution under the same conditions. Below pH_c there is a marked stepped increase in the hydrodynamic radius of the furcellaran component. Although the total intensity of the scattered light continues to increase with decreasing pH, at pH's between pH_c and the pH at which the onset of coacervation/precipitation is observed, the hydrodynamic radius of the furcellaran component does not show a strong pH dependence. Above pH_c the furcellaran in solution can be approximated to an equivalent sphere with an R_h, ~32 nm. In the region below pH_c, where it is proposed that the furcellaran forms a complex with the globular protein, this size had

increased to ~135 nm for the furcellaran/BLG mixture, and ~115 nm for the furcellaran/BSA mixture. Various models could be considered for the structure of the complex. If the globular protein could bind to more than one furcellaran chain it is possible that it could act as a crosslink. This crosslinking process would lead to the formation of large aggregates. The relatively well defined size of the BLG and BSA furcellaran complexes over a range of pH's argues against this proposal. An alternative view is that the globular proteins 'decorate' the furcellaran chain. Polysaccharides in general are fairly stiff molecules with a relatively long persistence length, it is therefore unlikely that the furcellaran chain can completely wrap around the globular protein but rather that part of the globular protein surface can interact with the polysaccharide chain and that the polysaccharide chain becomes decorated with globular protein. This interaction then results in an effective increase in size of the equivalent sphere which represents the behaviour of the complex in solution. The related increase in size could result from a more expanded/extended conformation, or a denser, less free-draining, conformation of the complex compared to the furcellaran chain in solution. The maintenance of particle size below pH_c while the intensity of scattered light is increasing, suggests competition between different processes and a progressive complexation with decreasing pH in this region. For polyelectrolyte/protein complexation both an increase (Ball, Winterhalter, Schwinte, Lavalle, Voegel, & Schaaf 2002; Grymonpre, Staggemeier, Dubin, & Mattison 2001) and a decrease (Weinbreck, de Vries, Schrooyen, & de Kruif 2003) in particle size of the complex relative to that of the polyelectrolyte have been observed. The origins of these differences in behaviour are not clear.

3.4. Potentiometric titration

The interaction between the globular protein and the furcellaran was also probed by potentiometric titration. In Fig. 6 is shown the measured pH as a function of added HCl over the pH range 9 to 4 for BSA (a) and BLG (b) in 0.03 M NaCl. The titration curves for the globular proteins are in agreement with published research (Cannan, Palmer, & Kibrick 1942; Tanford, Swanson, & Shore 1955). For the furcellaran/BSA mixture there is a gradual divergence in the titration curve at a pH in the region of ~7.5-8.0. For BLG there is a more marked divergence at pH ~7.5. For both proteins there is another change in the titration behaviour in the region of pH 5.0 – 6.0, associated with a marked increase in turbidity on precipitation. In previous research (Wen & Dubin 1997), the transition at the higher pH was associated with complex formation at pH_c. It was proposed that the binding of charged groups of the polyelectrolyte to proteins results in changes in local environment of the charged residues on the protein and in the pK_a of the titrable groups of the protein (Mattison, Brittain, & Dubin 1995). This is consistent with ligand binding studies on proteins. For example, the binding of the phosphate ion to Ribonuclease A increases the basicity of some of the histidine residues (Antosiewicz, Mccammon, & Gilson 1996). The values of pH_c obtained by turbidimetric and potentiometric titration differ somewhat, perhaps as a result of their different physicochemical origins.

4. Conclusions

It has been shown that the algal polysaccharide furcellaran can form soluble complexes with the globular proteins, bovine serum albumin and β-lactoglobulin. The complexation occurs at a pH where the protein carries a net negative charge. With increasing ionic strength, as the charge on the polymers becomes screened, the attractive interaction between the negatively charged furcellaran and positively charged patches on the protein becomes more favoured. Further increase in ionic

strength then reduces the strength of this interaction. The observed ionic strength dependence is consistent with observation and indicates that the release of counterions associated with the protein on complexation, is an important driving force for complex formation. The onset of complex coacervation/precipitation occurs in the region of the isoelectric point of the protein and becomes increasingly favoured as the protein acquires a net positive charge, opposite in sign to that of the furcellaran.

Acknowledgements

The authors thank the BBSRC core strategic grant for financial support; the EC Commission for the award of a Marie Curie fellowship to K.L. (Contract Number QLK-1999-50512).

References

Amimi, A., Mouradi, A., Givernaud, T., Chiadmi, N., & Lahaye, M. (2001) Structural analysis of Gigartina pistillata carrageenans (Gigartinaceae, Rhodophyta). *Carbohydrate Research, 333,* 271-279.

Antosiewicz, J., Mccammon, J. A., & Gilson, M. K. (1996) The determinants of pK(a)s in proteins. *Biochemistry, 35,* 7819-7833.

Aymard, P., Durand, D., & Nicolai, T. (1996) The effect of temperature and ionic strength on the dimerisation of beta-lactoglobulin. *International Journal of Biological Macromolecules, 19,* 213-221.

Ball, V., Winterhalter, M., Schwinte, P., Lavalle, P., Voegel, J. C., & Schaaf, P. (2002) Complexation mechanism of bovine serum albumin and poly(allylamine hydrochloride). *Journal of Physical Chemistry B, 106,* 2357-2364.

Beretta, S., Chirico, G., & Baldini, G. (2000) Short-range interactions of globular proteins at high ionic strengths. *Macromolecules, 33,* 8663-8670.

Brimacombe, D. B., Bennett, A. D., Wusteman, F. S., Gill, A. C., Dann, J. C., & Bostock, C. J. (1999) Characterization and polyanion-binding properties ef purified recombinant recombinant protein. *Biochemical Journal, 342,* 605-613.

Cannan, R. K., Palmer, A. H., & Kibrick, A. C. (1942) The hydrogen ion dissociation curve of beta-lactoglobulin. *Journal of Biological Chemistry, 142,* 803-822.

Carter, D. C. & Ho, J. X. (1994) Structure of serum albumin. *Advances in Protein Chemistry, 45,* 153-203.

Decher, G. (1997) Fuzzy nanoassemblies: Toward layered polymeric multicomposites. *Science, 277,* 1232-1237.

Dickinson, E. (2003) Hydrocolloids at interfaces and the influence on the properties of dispersed systems. *Food Hydrocolloids, 17,* 25-39.

Fogolari, F., Ragona, L., Licciardi, S., Romagnoli, S., Michelutti, R., Ugolini, R., & Molinari, H. (2000) Electrostatic properties of bovine beta-lactoglobulin. *Proteins-Structure Function and Genetics, 39,* 317-330.

Gaigalas, A. K., Hubbard, J. B., McCurley, M., & Woo, S. (1992) Diffusion of bovine serum albumin in aqueous solutions. *Journal of Physical Chemistry, 96,* 2355-2359.

Grymonpre, K. R., Staggemeier, B. A., Dubin, P. L., & Mattison, K. W. (2001) Identification by integrated computer modeling and light scattering studies of an electrostatic serum albumin-hyaluronic acid binding site. *Biomacromolecules, 2,* 422-429.

Hallberg, R. K. & Dubin, P. L. (1998) Effect of pH on the binding of beta-lactoglobulin to sodium polystyrenesulfonate. *Journal of Physical Chemistry B, 102,* 8629-8633.

Harris, P. J., Blakeney, A. B., Henry, R. J., & Stone, B. A. (1988) Gas-chromatographic determination of the monosaccharide composition of plant cell wall preparations. *Journal of the Association of Official Analytical Chemists, 71,* 272-275.

Hattori, T., Kimura, K., Seyrek, E., & Dubin, P. L. (2001) Binding of bovine serum albumin to heparin determined by turbidimetric titration and frontal analysis continuous capillary electrophoresis. *Analytical Biochemistry, 295*, 158-167.

Lahaye, M. (2001) Developments on gelling algal galactans, their structure and physico-chemistry. *Journal of Applied Phycology, 13*, 173-184.

Le Bon, C., Nicolai, T., Kuil, M. E., & Hollander, J. G. (1999) Self-diffusion and cooperative diffusion of globular proteins in solution. *Journal of Physical Chemistry B, 103*, 10294-10299.

Li, Y. J., Mattison, K. W., Dubin, P. L., Havel, H. A., & Edwards, S. L. (1996) Light scattering studies of the binding of bovine serum albumin to a cationic polyelectrolyte. *Biopolymers, 38*, 527-533.

Luger, K., Mader, A. W., Richmond, R. K., Sargent, D. F., & Richmond, T. J. (1997) Crystal structure of the nucleosome core particle at 2.8 angstrom resolution. *Nature, 389*, 251-260.

MacDougall, A. J., Brett, G. M., Morris, V. J., Rigby, N. M., Ridout, M. J., & Ring, S. G. (2001) The effect of peptide behaviour-pectin interactions on the gelation of a plant cell wall pectin. *Carbohydrate Research, 335*, 115-126.

Mascotti, D. P. & Lohman, T. M. (1990) Thermodynamic extent of counterion release upon binding oligolysines to single-stranded nucleic acids. *Proceedings of the National Academy of Sciences of the United States of America, 87*, 3142-3146.

Mattison, K. W., Brittain, I. J., & Dubin, P. L. (1995) Protein-polyelectrolyte phase boundaries. *Biotechnology Progress, 11*, 632-637.

Meechai, N., Jamieson, A. M., & Blackwell, J. (1999) Translational diffusion coefficients of bovine serum albumin in aqueous solution at high ionic strength. *Journal of Colloid and Interface Science, 218*, 167-175.

Meunier, V., Nicolai, T., & Durand, D. (2001) Structure of aggregating kappa-carrageenan fractions studied by light scattering. *International Journal of Biological Macromolecules, 28*, 157-165.

Moss, J. M., VanDamme, M. P. I., Murphy, W. H., & Preston, B. N. (1997) Dependence of salt concentration on glycosaminoglycan-lysozyme interactions in cartilage. *Archives of Biochemistry and Biophysics, 348*, 49-55.

Park, J. M., Muhoberac, B. B., Dubin, P. L., & Xia, J. L. (1992) Effects of protein charge heterogeneity in protein-polyelectrolyte complexation. *Macromolecules, 25*, 290-295.

Phillies, G. D. J., Benedek, G., & Mazer, N. A. (1976) Diffusion in protein solutions at high concentrations: a study by quasielastic light scattering. *Journal of Chemical Physics, 65*, 1883-1892.

Qin, B. Y., Bewley, M. C., Creamer, L. K., Baker, H. M., Baker, E. N., & Jameson, G. B. (1998) Structural basis of the tanford transition of bovine beta- lactoglobulin. *Biochemistry, 37*, 14014-14023.

Record, M. T., Lohman, T. M., & deHaseth, P. L. (1976) *Journal of Molecular Biology, 107*, 145-158.

Sakurai, K., Oobatake, M., & Goto, Y. (2001) Salt-dependent monomer-dimer equilibrium of bovine beta- lactoglobulin at pH 3. *Protein Science, 10*, 2325-2335.

Sawyer, L., Kontopidis, G., & Wu, S. Y. (1999) beta-Lactoglobulin - a three-dimensional perspective. *International Journal of Food Science and Technology, 34*, 409-418.

Seyrek, E., Dubin, P. L., Tribet, C., & Gamble, E. A. (2003) Ionic strength dependence of protein-polyelectrolyte interactions. *Biomacromolecules, 4*, 273-282.

Silvestri, L. J., Hurst, R. E., Simpson, L., & Settine, J. M. (1982) Analysis of sulfate in complex carbohydrates. *Analytical Biochemistry, 123*, 303-309.

Skepo, M. & Linse, P. (2002) Dissolution of a polyelectrolyte-macroion complex by addition of salt. *Physical Review e, 66*, art-051807.

Stevenson, T. T. & Furneaux, R. H. (1991) Chemical methods for the analysis of sulfated galactans from red algae. *Carbohydrate Research, 210*, 277-298.

Takata, S., Norisuye, T., Tanaka, N., & Shibayama, M. (2000) Heat-induced gelation of beta-lactoglobulin. 1. Time-resolved dynamic light scattering. *Macromolecules, 33*, 5470-5475.

Tanford, C., Bunville, L. G., & Nozaki, Y. (1959) The reversible transformation of β-lactoglobulin at pH 7.5. *Journal of the American Chemical Society, 81*, 4032-4036.

Tanford, C., Swanson, S. A., & Shore, W. S. (1955) Hydrogen ion equilibria of bovine serum albumin. *Journal of the American Chemical Society, 77*, 6414-6421.

Truus, K., Vaher, M., Usov, A. I., Pehk, T., & Kollist, A. (1997) Gelling galactans from the algal community of Furcellaria lumbricalis and Coccotylus truncatus (the Baltic Sea, Estonia): a structure-property study. *International Journal of Biological Macromolecules, 21*, 89-96.

Turgeon, S.L., Beaulieu, M., Schmitt, C. & Sancez, C. (2003) Protein-polysaccharide interactions: phase ordering kinetics thermodynamic and structural aspects. *Current Opinion in Colloid and Interface Science, 8*, 401-14.

Verheul, M., Pedersen, J. S., Roefs, S. P. F. M., & de Kruif, K. G. (1999) Association behavior of native beta-lactoglobulin. *Biopolymers, 49*, 11-20.

Weinbreck, F., de Vries, R., Schrooyen, P., & de Kruif, C. G. (2003) Complex coacervation of whey proteins and gum arabic. *Biomacromolecules, 4*, 293-303.

Weinbreck, F., Nieuwenhuijse, H., Robijn, G.W., & de Kruif, C.G. (2004) Complexation of whey proteins with carrageenan. Journal of Agricultural and Food Chemistry, *52*, 3550-3555.

Wen, Y. P. & Dubin, P. L. (1997) Potentiometric studies of the interaction of bovine serum albumin and poly(dimethyldiallylammonium chloride). *Macromolecules, 30*, 7856-7861.

Witz, J., Timasheff, S. N., & Luzzati, V. (1964) Molecular interactions of beta-lactoglobulin VIII Small-angle light scattering investigation of the geometry of beta-lactoglobulin A tetramerization. *Journal of the American Chemical Society, 86*, 168-173.

Table 1 Characteristics of the furcellaran.

Monosaccharide composition (% w/w carbohydrate) (Mole ratio)						SO_3^- (% w/w)	[η] ml/g
Gal	3,6-AGal	6-O-MeGal	Gluc	Xyl	Man		
59 (0.56)	32 (0.34)	5 (0.044)	2 (0.019)	2 (0.023)	1 (0.009)	14.9	507

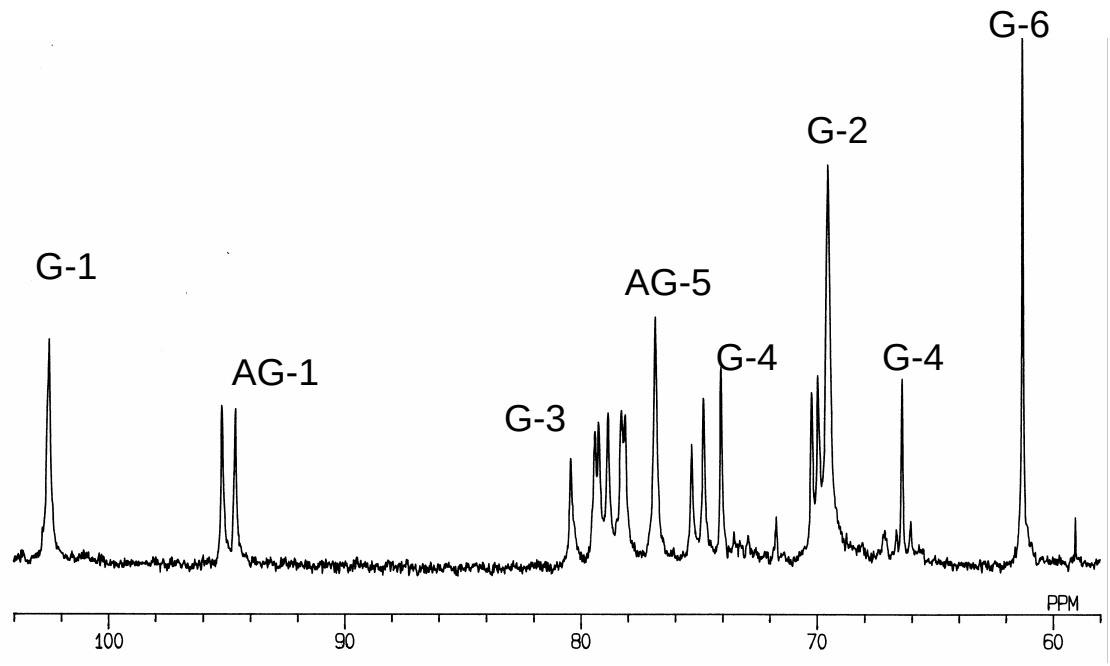

Fig. 1. ^{13}C NMR of 5% (w/v) furcellaran in D_2O at 85 °C, where AG is anydrogalactose and G galactose.

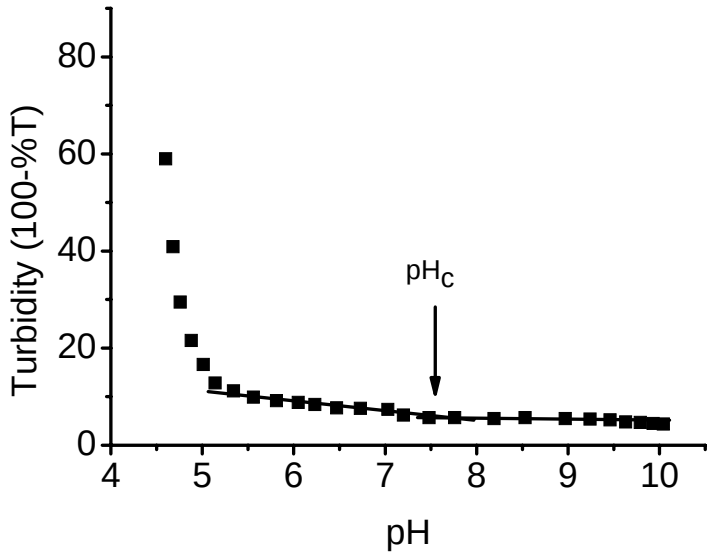

Fig. 2a. Turbidimetric titration of furcellaran (0.6g/L) BSA (3g/L) mixture in 0.03 M NaCl at 20 °C.

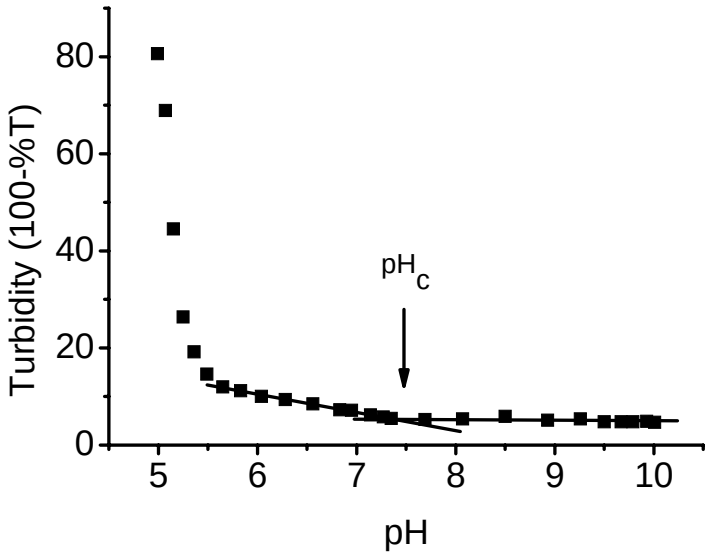

Fig. 2b. Turbidimetric titration of furcellaran (0.6g/L) BLG (3g/L) mixture in 0.03 M NaCl at 20 °C.

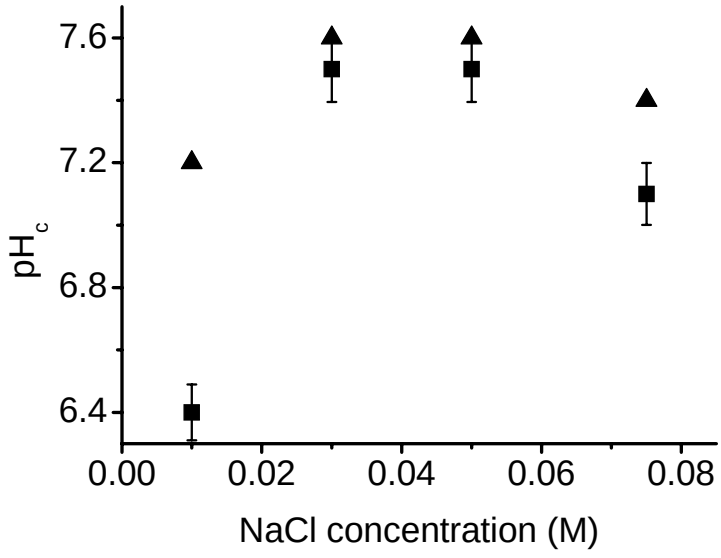

Fig. 3. Variation of pH_c with salt concentration for furcellaran/BSA (▲) and furcellaran/BLG (■) mixtures at 20 °C.

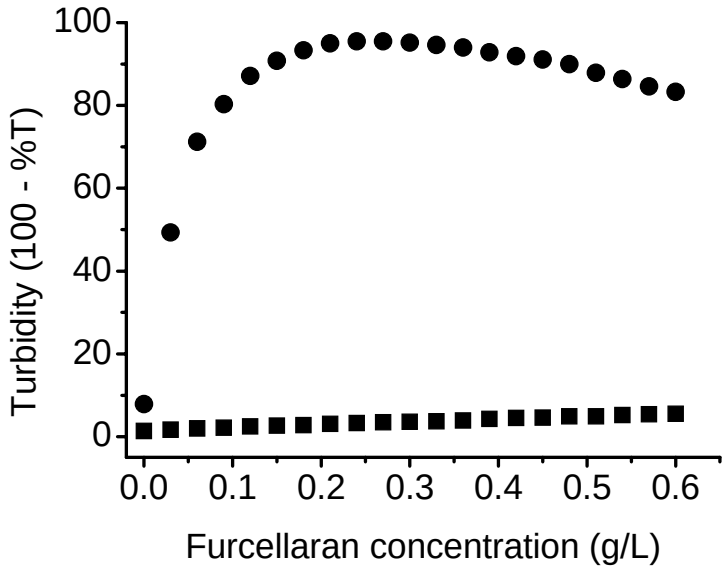

Fig. 4a. Development of turbidity as a function of furcellaran concentration for a furcellaran/BSA mixture at a BSA concentration of 1 g/L at pH 4 (●), and pH 7(■) at 20 °C in 0.03M NaCl.

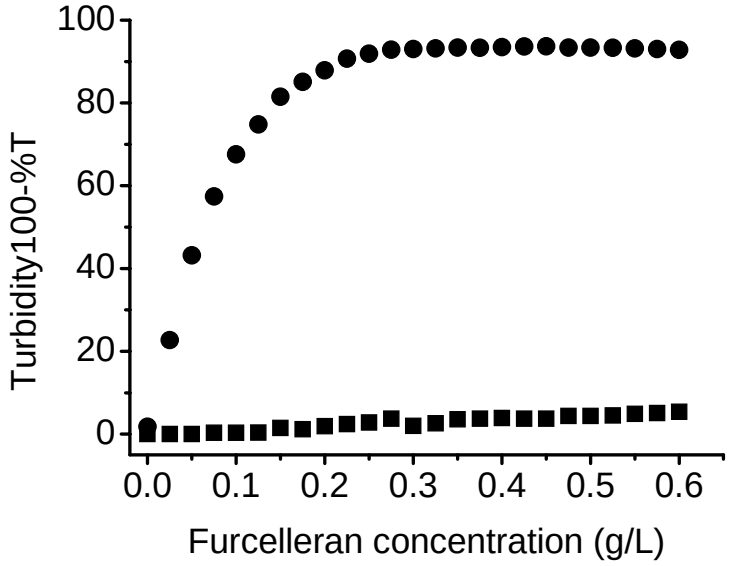

Fig. 4b. Development of turbidity as a function of furcellaran concentration for a furcellaran/BLG mixture at a BLG concentration of 1 g/L at pH 4 (●), and pH 7 (■) at 20 °C in 0.03M NaCl.

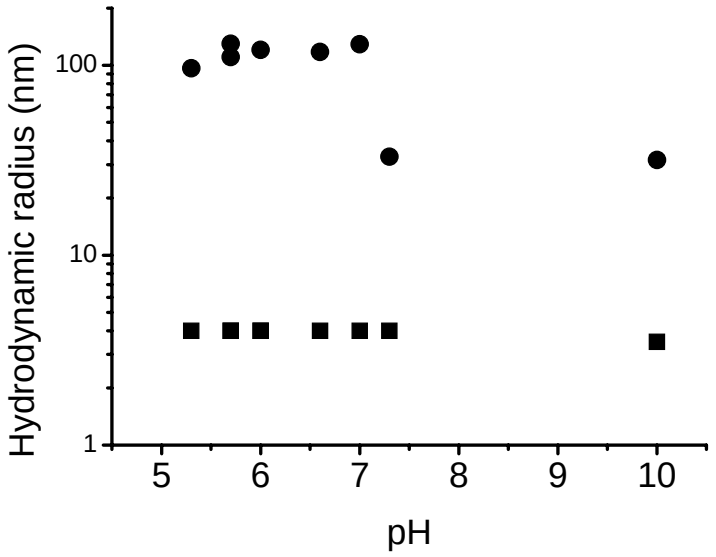

Fig. 5a. Plot of hydrodynamic radius (R_h) versus pH for a mixture of BSA (3g/L) and furcelleran (0.6g/L) where (■) is the R_h of the faster component and (●) the R_h of the slower component.

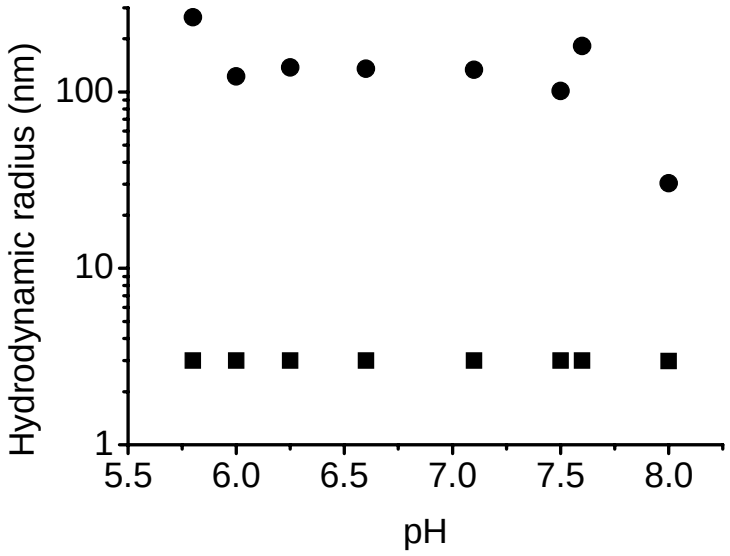

Fig. 5b. Plot of hydrodynamic radius versus pH for a mixture of BLG (3g/L) and furcellaran (6g/L) where (■) is the R_h of the faster component and (●) the R_h of the slower component (●).

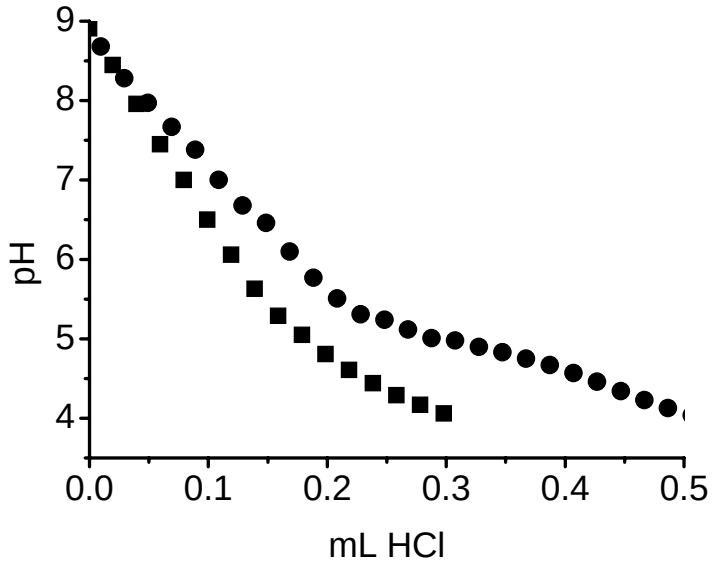

Fig. 6a. Potentiometric titration of 15 mL of BSA (3g/L) (■); and 15mL of a BSA/furcellaran mixture (3g/L and 0.6 g/L) (●) in 0.03 M NaCl at 20 °C.

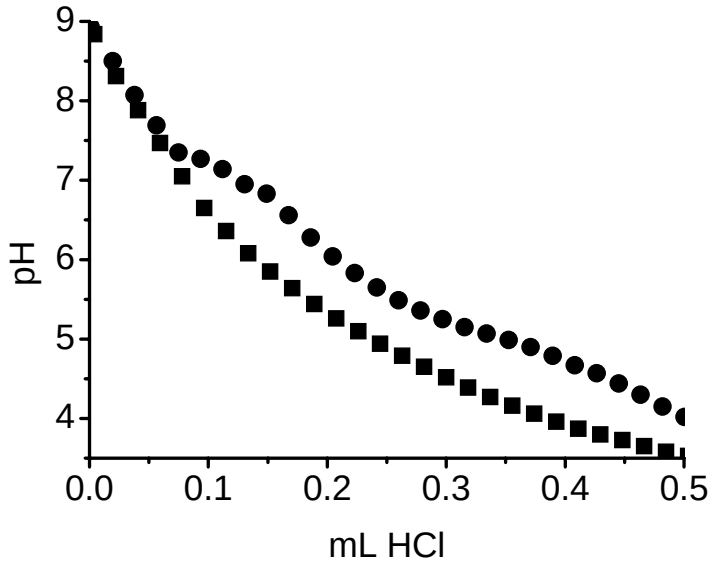

Fig. 6b. Potentiometric titration of 15 mL of BLG (3g/L) (■); and 15mL of a BLG/furcellaran mixture (3g/L and 0.6 g/L) (●) in 0.03 M NaCl at 20 °C.

APPENDIX 1

ARTICLE VI

K. Laos, R. Parker, J. Moffat, N. Wellner and S. G. Ring. 2005. The adsorption of globular proteins, bovine serum albumin and β-lactoglobulin, on poly-L-lysine – furcellaran multilayers. – Manuscript.

The adsorption of globular proteins, bovine serum albumin and β-lactoglobulin, on poly-L-lysine – furcellaran multilayers.

K. Laos[†], R. Parker, J. Moffat, N. Wellner and S. G. Ring

Institute of Food Research, Norwich Research Park, Colney, Norwich NR4 7UA, UK.

[†] Department of Food Processing, Tallinn University of Technology, Ehitajate tee 5, 19086 Tallinn, Estonia

Abstract

The formation of multilayer films of poly-L-lysine (PLL) and furcellaran was investigated surface plasmon resonance (SPR), quartz crystal microbalance with dissipation monitoring (QCM-D) and Fourier transform infrared spectroscopy with attenuated total reflection (FTIR-ATR). The progressive form of the growth of mass of polymer deposited for the multilayer was consistent with the ability of the PLL to diffuse within the furcellaran layer. Using the same experimental approaches the pH-dependent adsorption of the globular proteins bovine serum albumin (BSA) and β-lactoglobulin (BLG) to the PLL/furcellaran multilayers was also examined. Substantial adsorption was observed even at pH's where the net charge on the protein was of the same sign as that of the furcellaran.

1. Introduction

Polyelectrolyte multilayers may be formed by the sequential dipping of a charged surface into solutions of a polyanion and polycation (Decher 1997). A requirement for multilayer formation is that the binding of polyelectrolyte to the growing multilayer surface results in charge reversal, permitting the subsequent deposition of oppositely charged polyelectrolyte. Polyelectrolyte multilayers are non-equilibrium structures whose properties

are strongly influenced by the conditions of their preparation, including molecular size (Picart, Mutterer, Richert, Luo, Prestwich, Schaaf, Voegel, & Lavalle 2002; Sui, Salloum, & Schlenoff 2003); ionic strength; (Dubas & Schlenoff 2001; Schlenoff, Ly & Li 1998), and for weak polyelectrolytes, pH (Burke & Barrett 2003; Shiratori & Rubner 2000).

The interaction between opposite charges may also be used to incorporate other species/structures into the growing multilayer such as protein polyampholytes (Caruso, Furlong, Ariga, Ichinose, & Kunitake 1998; Gergely, Bahi, Szalontai, Flores, Schaaf, Voegel, & Cuisinier 2004; Ladam, Gergely, Senger, Decher, Voegel, Schaaf, & Cuisinier 2000; Salloum & Schlenoff 2004); unilamellar vesicles (Michel, Vautier, Voegel, Schaaf, & Ball 2004) ; and wax droplets (Glinel, Prevot, Krustev, Sukhorukov, Jonas, & Mohwald 2004). This versatility means that these structures have a potential wide range of application as barriers and coatings (Quinn & Caruso 2004; Shi & Caruso 2001). Most studies have been performed with synthetic polyelectrolytes. For some applications, including those in the food and pharmaceutical sectors, it is important to consider the fabrication of biopolymer multilayers. Recent examples include alginate/poly-L-lysine (Elbert, Herbert, & Hubbell 1999); hyaluronan/poly-L-lysine (Burke & Barrett 2003); and hyaluronan/chitosan (Richert, Lavalle, Payan, Shu, Prestwich, Stoltz, Schaaf, Voegel, & Picart 2004) and pectin/chitosan (Marudova, Lang, Brownsey, & Ring 2005).

In this article we examine the fabrication of a furcellaran/poly-L-lysine multilayer using surface plasmon resonance (SPR), FTIR-ATR and a quartz crystal microbalance with dissipation monitoring (QCMD). Furcellaran is a sulphated galactan, and therefore a strong polyelectrolyte, which can be extracted from the seaweed *Furcellaria lumbricalis* (Lahaye 2001; Truus, Vaher, Usov, Pehk, & Kollist 1997). It consists of residues of (1→3) β-D-galactopyranose and its 4-sulphate and (1→4) linked α-D-galactopyranose. The latter may exist as a 3,6-anhydro residue which may be partially sulphated at position 2. Structurally,

furcellaran is related to the algal polysaccharide κ-carrageenan, with a major structural difference being that furcellaran has a smaller degree of sulphation (Truus, Vaher, Usov, Pehk, & Kollist 1997). We also investigate the capacity of the multilayer to adsorb globular proteins, including bovine serum albumin and β-lactoglobulin.

2. Materials and methods

2.1. Materials

Furcellaran was obtained from FMC Food Ingredients. The Na^+ furcellaran was obtained by elution through an ion-exchange (Amberlite IR-120) column in the Na^+ form at 4 °C. The intrinsic viscosity of 482 mL g^{-1} indicates a relatively large molecular size in 0.1 M NaCl. Poly-L-lysine hydrobromide (PLL) with a mean degree of polymerisation of 70, bovine serum albumin (BSA) and β-lactoglobulin (BLG), were obtained from Sigma-Aldrich UK. For multilayer fabrication, aqueous biopolymer solutions (0.6 mg/mL) were prepared in 0.1M acetate buffer pH 5.6 containing 0.03M NaCl. For the protein binding studies aqueous protein solutions (0.6 mg mL^{-1}) in 0.01M acetate or phosphate buffer with pH's in the range 5,0 to 8,0 containing 0.03M NaCl, were used.

2.2. Surface Plasmon Resonance (SPR)

Measurements were carried out using a Biacore X instrument. The sensing element was a thin film of gold (~50 nm), deposited on a glass substrate mounted in a sensor chip cartridge (Biacore AB, Uppsala, Sweden). The instrument monitors changes in refractive index adjacent to the surface of the gold film by measuring the intensity of polarised light reflected from the reverse side of the glass-gold interface. The plasmon resonance causes a minimum in intensity to occur at a certain angle of incidence, θ_m. The value of θ_m varies with changes in refractive index of the region adjacent the gold surface. The size of this region depends on the penetration of an evanescent wave into the flow channel which typically

extends 25-50% of the wavelength of the incident light from the surface (Jung, Campbell, Chinowsky, Mar, & Yee 1998). The Biacore instrument reports θ_m in resonance units (RU) where 10,000 RU represents a shift in θ_m of 1°. The instrument was calibrated at 20 °C with methanol/water and sucrose/water systems of known refractive indices. The response to changes in refractive index was found to be linear with a shift in θ_m of 86.6° per unit change in refractive index. The change in θ_m, $\Delta\theta$, due to the adsorption of a uniform adsorbed layer is related to refractive index through the relationship (Jung, Campbell, Chinowsky, Mar, & Yee 1998):

$$\Delta\theta = m(n_{adl} - n_s)\left[1 - \exp\left(-2h / d_{spr}\right)\right] \quad (1)$$

where n_{adl} and n_s are the refractive indices of the adsorbed layer and bulk solution, respectively. The thickness of the layer is h and d_{spr} is the characteristic decay length of the evanescent electromagnetic field, and can be estimated as 37% ± 13% of the wavelength of incident light (760 nm) (Jung, Campbell, Chinowsky, Mar, & Yee 1998). If it is assumed that the refractive index of the layer is proportional to the adsorbate concentration, the exponential in equation 1 can be expanded to yield an explicit expression for the mass of adsorbed polymer per unit area (c_{spr})

$$c_{spr} = \frac{d_{spr}\, c_{\max}\, \Delta\theta}{2m\left(n_{ads} - n_S\right)} \quad (2)$$

where c_{max} and n_{ads} are the density and refractive index of the pure adsorbate. Expanding the exponential is accurate to within 10% when $h < 0.1\, d_{spr}$.

Multilayers were built up by the layer-by-layer technique at a flow rate of 25 μL min^{-1}. A buffer baseline was established, then a PLL base layer was laid down by injecting 50 μL of PLL solution, followed by ~75 μL of buffer, 50 μL of furcellaran solution, and a buffer rinse as before. The sequence was repeated to form the multilayer which was then ready for globular protein adsorption studies. Between each experiment the gold surface was

regenerated by flowing 0.1 M NaOH through the measurement cell. All measurements were made at 20 °C.

2.3. FTIR-ATR spectroscopy

FTIR has been extensively used to probe polyelectrolyte adsorption at surfaces(Sukhishvili, Dhinojwala, & Granick 1999; Sukhishvili & Granick 1999). Infrared spectra were collected on the 860 Nicolet FTIR spectrometer fitted with a micro CIRCLE liquid ATR cell (Spectra-Tech, Warrington, UK). The ATR crystal was a cylindrical ZnSe prism, with 11 internal reflections, mounted in a thermostatted steel jacket set at a temperature of 20 °C. Biopolymer solutions were prepared as described above using D_2O instead of H_2O. 1 mL of biopolymer solution was injected and left for 16 min. After each deposition step the cell was rinsed with 2 ml volumes of deuterated buffer. Spectra were accumulated by averaging 1024 scans at a resolution of 2 cm^{-1} and subtracted from a background of the buffer alone.

In the ATR mode, a light beam strikes the interface between a medium of high refractive index (n_1) and a medium of low refractive index (n_2). The beam is totally reflected if the angle of incidence θ_i is larger than the critical angle θ_c, where $\theta_c = \sin^{-1}(n_2/n_1)$. At the point of reflection an evanescent wave of exponentially decreasing intensity penetrates the medium of lower refractive index. The depth of penetration (d_{ir}) of the evanescent wave - defined as the distance normal to the interface at which the intensity falls to 1/e of the intensity at the surface - is given by:

$$d_{ir} = \frac{\lambda}{2\pi n_1 (\sin^2 \theta_i - n_{12}^{\ 2})^{1/2}} \qquad (3)$$

where λ is the wavelength of the light in vacuum and $n_{12} = n_2/n_1$. The refractive index of the crystal is 2.41 and that of the dilute polymer in solution is 1.33. The angle of incidence is 45°. As the penetration depth is large (~631 nm at 1645 cm^{-1}) compared to the layer thickness, the

FTIR signal potentially contains contributions from the polymer in bulk solution as well as from the polymer adsorbed onto the surface of the crystal. However, at the concentrations used in the present experiment, the polymer in solution does not make a significant contribution to the observed spectra.

2.4. Quartz Crystal Microbalance

Measurements were carried out using a D300 quartz crystal microbalance with dissipation monitoring (QCMD) from Q-Sense AB (Västra Frölunda, Sweden) with a QAFC 302 axial flow measurement chamber. The sensing element is a disc-shaped, AT-cut piezoelectric quartz crystal sandwiched between two gold electrodes. The crystal is excited to oscillation at its fundamental resonant frequency (~5 MHz). A small mass deposited (Δm) on the gold sensing surface will cause a decrease in resonant frequency (Δf). If the mass is deposited evenly and is sufficiently rigid then the mass adsorbed is directly proportional to the change in frequency according to the Sauerbrey equation (Sauerbrey 1959):

$$\Delta m = -C\Delta f / n \qquad (4)$$

where C is the mass sensitivity constant (C = 17.7 ng cm^{-2} Hz^{-1} for a 5 MHz crystal (Hook, 2001) and n is the overtone number (n = 1, 3, 5…). For elastic, cross-linked gel networks, the mass of solvent trapped within the gel contributes to the overall mass adsorbed and the observed frequency change. For viscoelastic materials the adsorbed mass does not fully couple to the oscillation of the crystal and hence dampens the oscillation. The QCMD measures this dissipation from the response of the crystal at its resonant frequency (5 MHz) and at three of its overtones (15, 25 or 35 MHz) following the excitation of the crystal to resonance. The decrease in the amplitude of the oscillation with time provides a single-exponential decay constant which characterises the dissipation.

The QCMD response to dissipative viscoelastic films has been modelled using a Voigt model (Voinova, Rodahl, Jonson, & Kasemo 1999). The full expression for the resonance

frequency and dissipation shifts with a thick adsorbed layers can be concisely expressed using complex variables. Some physical insight into how the material properties of the bulk liquid and adsorbed layer affect the QCMD response can be obtained for single thin viscoelastic adsorbed layers for which the equations simplify as follows (retaining Voinova *et al.*'s notation):

$$\Delta f \approx -\frac{1}{2\pi\rho_0 h_0}\left\{\frac{\eta_3}{\delta_3} + h_1\rho_1\omega - 2h_1\left(\frac{\eta_3}{\delta_3}\right)^2 \frac{\eta_1\omega^2}{\mu_1^{\,2} + \omega^2\eta_1^{\,2}}\right\} \tag{5}$$

$$\Delta D \approx \frac{1}{\pi f\rho_0 h_0}\left\{\frac{\eta_3}{\delta_3} + 2h_1\left(\frac{\eta_3}{\delta_3}\right)^2 \frac{\mu_1\omega}{\mu_1^{\,2} + \omega^2\eta_1^{\,2}}\right\} \tag{6}$$

where ρ_0 and h_0 are the density and thickness of the crystal, respectively. The viscosity of the bulk liquid is η_3, and δ_3 $(=(2\eta_3/\rho_3\omega)^{1/2})$ is the viscous penetration depth of the shear wave in the bulk liquid and ρ_3 is the liquid's density. The thickness, density, viscosity and elastic shear modulus of the adsorbed layer is represented by h_1, ρ_1, η_1 and μ_1, respectively; ω is the angular frequency of the oscillation. The first term in the brackets in eqs. 5 and 6, η_3/δ_3, is the frequency and dissipation shift due to immersing the crystal oscillator in the bulk liquid, a factor which is effectively constant in our experiments. The second term in the brackets in eq. 5 is the Sauerbrey term, as in eq. 4, due to the hydrated mass of the adsorbed layer. As this term is proportional to frequency it is common to present the frequency shift as $\Delta f/n$ to take this into account. The final term in the brackets in eq. 5 and 6 arises due to viscoelasticity. In eq. 5 this term is negative so that viscoelasticity reduces the frequency shift and the use of the Sauerbrey equation would underestimate the mass adsorbed and hydrated layer thickness. Modelling software (QTools) supplied with the QCMD use the full thick layer expressions to model the response. The program finds a best fit using a Simplex algorithm to find the minimum in the sum of the squares of the scaled errors between the experimental and model Δf and ΔD values. By assuming the density and viscosity of the bulk liquid (ρ_3 and η_3) are

1000 kg m^{-3} and 1.0 mPa s, respectively, and a fixed density of the layer (ρ_1), the package estimates the viscosity, shear modulus and the thickness of the adsorbed layer.

The formation of multilayers was investigated at 20 °C. Starting with the system primed with buffer solution, a base layer is formed by first flowing ~2.0 mL of PLL solution into a thermostatic coil in the measurement head to flush out the previous solution and allow the solution to reach thermal equilibrium. After 5 min, ~0.5 mL of this solution was allowed to flow into the measurement cell to replace the existing solution, driven by the head of liquid in the sample reservoir which flows into the thermostatic coil. The same procedure was repeated with buffer, followed by solution, buffer solution, and so on. Between each experiment the crystal chip was cleaned by sonication in 99% ethanol solution for 5 min followed by sonication in 2% Hellmanex solution (Hellma UK Ltd.) for 5 min. The chips were rinsed in distilled water and then dried with N_2.

3. Results and discussion

3.1 Multilayer fabrication – SPR

PLL/Furcellaranmultilayers were prepared by layer-by-layer deposition at pH 5.6. Under these conditions both PLL and furcellaran are essentially fully charged. PLL was initially deposited on a gold surface followed by attachment of furcellaran. Through the sequential deposition of PLL and furcellaran a 10 layer multilayer was fabricated. The build up of the multilayer was followed by surface plasmon resonance. In Fig. 1 is shown the mass deposited as a function of layer number. The mass deposited shows a relatively smooth progressive increase with each new layer, with approximately equal amounts of PLL and furcellaran being laid down. The inset in Fig. 1 shows a detail of the surface plasmon resonance response for the deposition of the 5^{th} (PLL) and 6^{th} layers (furcellaran). The deposition of PLL results in a step change in response with a limited solubilisation following

the buffer rinse. The progressive increase with increasing layer number is characteristic of polyelectolyte multilayers in which one, lower molecular size component, has the ability to diffuse to the growing multilayer surface resulting in an increased capture of the next layer of oppositely charged polymer (Lavalle, Picart, Mutterer, Gergely, Reiss, Voegel, Senger, & Schaaf 2004; Lavalle, Vivet, Jessel, Decher, Voegel, Mesini, & Schaaf 2004; Picart, Mutterer, Richert, Luo, Prestwich, Schaaf, Voegel, & Lavalle 2002). Furcellaran carries less charge per unit mass than poly-L-lysine, because of its higher average molecular mass per repeating unit, and through one residue in every ~2.8 being charged. A consequence of the approximately equal mass deposition of furcellaran and PLL, assuming that both species are fully charged, is that the multilayer carries an excess of positive charge.

3.2 Multilayer fabrication – FTIR-ATR

FTIR-ATR was used to obtain information on the chemical characteristics of the deposited species. Fig. 2 compares solution spectra of furcellaran and PLL at concentrations of 0.3 and 0.8% w/w at pD 5.6. The PLL spectrum has strong absorbances at 1643 cm^{-1} and 1460 cm^{-1}. The latter is the amide II' band which includes contributions from CN stretching and other backbone modes. The absorbance at 1643 cm^{-1} the amide I band, the precise location of which is conformation dependent, and for poly-L-lysine in a random coil conformation (Jackson, Haris, Chapman 1989) occurs in the range 1643-1648 cm^{-1}. The furcellaran spectrum is similar to reported spectra of κ-carrageenan and includes features which have been assigned to 3,6-anhydro-D-galactose (932 cm^{-1}) and glycosidic linkages (1075 cm^{-1}) (Pereira, Sousa, Coelho, Amado, & Ribeiro-Claro 2003; Volery, Besson, & Schaffer-Lequart 2004). The spectra of assembled PLL/furcellaran multilayer films in the region 800-1800 cm^{-1} is shown in Fig. 3. The spectra shown are those obtained after the deposition of the third PLL layer (layer 5) and the third furcellaran layer (layer 6). The bands at 1456 and 1643 cm^{-1} are characteristic of the presence of PLL in the multilayer. The

subsequent addition of furcellaran causes little change in the peak absorbance of these bands but does lead to an increase in absorbance of the bands associated with furcellaran at 932 and 1075 cm^{-1}. The alternating, stepwise addition is shown by examining how the absorbance of bands characteristic of furcellaran (1075 cm^{-1}) and PLL (1643 cm^{-1}) increases with increasing number of layers (Fig.4).

3.2 Multilayer fabrication – QCMD

The assembly of the multilayer film was monitored by QCM-D starting with a PLL layer (Fig. 5a). For clarity, we report QCM-D data only for the third harmonic (15 MHz). Fig. 5a shows the frequency shift for the deposition of the first 5 layers starting with the deposition of PLL on the sensor surface. The decrease in Δf observed for the first PLL and furcellaran layers is associated with an increase in adsorbed hydrated mass. Subsequent addition of PLL to the furcellaran layer leads to little significant change in Δf (Fig. 5a, b). The trends observed for layer deposition using QCM-D are qualitatively different from those observed by SPR and FTIR-ATR, with the latter techniques probing the mass of polymer deposited and the QCM-D probing hydrated mass. The large response during the contact of the film with the polyanion solution and the very small response during contact with polycation solution (Fig 5a, b), suggests that the smaller molecular size polycationic PLL is diffusing within the furcellaran layer, and that the observed QCM-D response is a balance between the small increase in mass associated with the deposition of PLL, and its effect on deswelling the multilayer arising as a result of the replacement of monovalent cationic counterions with a polyvalent counterion (PLL). The QCM-D experiment also contains information on the viscous dissipation of the multilayer (Fig. 5c). After deposition of the first furcellaran layer, addition of PLL decreases the dissipation indicating that PLL crosslinks the furcellaran layer and, interpreting this change using the fit to the Voigt viscoelastic model, a reduction in hydrated mass and shrinkage of the adsorbed layer. This phenomenon has previously been observed in the

assembly of high DE pectin /PLL multilayers (Krzeminski, Marudoova, Moffat, Noel, Parker, Wellner, & Ring 2005).

The hydrated mass from the QCM-D modelling, combined with polymer mass from the SPR, yields a solids concentration of 7,0±1,0% w/w for the adsorbed layer, indicating that under these conditions of preparation a relatively hydrated, porous multilayer was formed.

3.4 Globular protein binding to the multilayer

Six layer PLL/furcellaran multilayers were prepared with furcellaran as the topmost layer. The binding of the globular proteins BSA and BLG to the multilayer was examined as a function of pH. Fig 6a,b show the FTIR spectra of the multilayer before and after the binding of BSA and BLG at pH 5.0. There is a substantial spectral change on binding, with a particularly marked increase in the absorbance of the amide I and amide II' bands. As the isoionic point of the isolated proteins is ~ 5.3 for defatted BSA (Tanford, Swanson, & Shore 1955) and ~ 5.1 for BLG (Cannan, Palmer, & Kibrick 1942) at pH 5.0, it is expected that the proteins will carry a small net positive charge. Solution studies on the interaction of globular proteins with polyanions show that protein/polyelectrolyte complexes may be formed at pHs where the protein carries a net charge of the same sign as the polyelectrolyte (Hallberg & Dubin 1998; Mattison, Dubin, & Brittain 1998; Seyrek, Dubin, Tribet, & Gamble 2003), with a more substantial aggregation or coacervation occurring below the isoelectric point when the protein acquires a net positive charge. In the region where both polymers carry a net charge of the same sign it is considered that the polyelectrolyte interacts with oppositely charged patches on the protein surface. The pH-dependence of the adsorption of BSA and BLG to the PLL/furcellaran multilayer is shown in Fig.7. Over the pH range 6.5 to 8 there is relatively little adsorption. As the pH is reduced to 5.0 there is a progressive increase in the amount adsorbed, and the observed behaviour is comparable to the generic complexation behaviour of polyelectrolytes and proteins which is observed in aqueous solution, and more particularly the

observed complexation of furcellaran and globular proteins (Laos, Brownsey, & Ring 2005). The pH-dependent adsorption was reversible. For both BSA and BLG the amount adsorbed at pH 5.0, calculated from the resonance response, is ~ 650 ng cm^{-2}, substantially more than the amount of PLL that would be deposited on the furcellaran layer (cf Fig 1), and partially reflecting differences in mass/charge ratio. Over the pH range 6.5 to 5 the PLL/furcellaran multilayer shows a limited change in hydration leading to a frequency response in the QCMD experiment of < -50 Hz. The sign of the frequency response indicates that deposition of the globular proteins leads to an increase in hydrated mass, and the effect of partially neutralising the charge on the furcellaran with a polyampholyte (leading to deswelling, and mass loss) is more than compensated for by the mass of protein deposited. This is in contrast too the behaviour observed on PLL deposition and reflects differences in mass/charge ratio for the different species. The observed pH-dependent response (Fig. 7), is similar to the observed pHdependent complexation of the globular proteins BSA and BLG with furcellaran (Laos, Brownsey, & Ring 2005).

Studies on the binding of globular proteins to polyelectrolyte multilayers show that the observed behaviour may be rather complex(Gergely, Bahi, Szalontai, Flores, Schaaf, Voegel, & Cuisinier 2004; Ladam, Gergely, Senger, Decher, Voegel, Schaaf, & Cuisinier 2000; Salloum & Schlenoff 2004). There is general agreement that electrostatic interactions dominate the observed behaviour. In a recent study it was found that the amount of protein adsorbed showed characteristically different behaviour depending on the charge on the terminating layer. It was proposed that the protein was drawn into the whole multilayer when the terminating layer was of opposite charge, whereas a more limited adsorption occurred when the terminating layer was of like charge (Salloum & Schlenoff 2004). In the present study, the amounts of protein adsorbed are comparable to a limited adsorption. From the molecular sizes and weights of the proteins it is possible to calculate the adsorbed amount for

monolayer coverage. Assuming that both BLG and BSA can be represented as an equivalent sphere in solution, with hydrodynamic radii of 2.93 (Baldini, Beretta, Chirico, Franz, Maccioni, Mariani, & Spinozzi 1999), and 3.7 nm (Carter & Ho 1994), and that surface coverage is 60% of the available area, then monolayer adsorption for both BLG and BSA would give an adsorbed amount of ~ 130 ng cm^{-2}. For a furcellaran terminated multilayer at pH 5, the amount adsorbed is equivalent to the deposition of ~ 5 protein layers. As pH is increased towards neutrality the amount adsorbed decreases, in a similar way to that observed for the binding of human serum albumin HSA to a polyglutamic acid terminated layer. For polyanion/protein complexes, decreases in the ability of the polyanion to complex protein are also observed in this pH range (Hallberg & Dubin 1998). It is proposed that in the current study, that the furcellaran terminated layer is relatively permeable to the globular proteins and allows their complexation.

Conclusions

The results showed that furcellaran can be used to fabricate multilayer structures with PLL by a layer-by-layer technique. These structures can bind the globular proteins, BSA and BLG, the pH dependence of the binding is comparable to the observed complexation behaviour of furcellaran with globular proteins in aqueous solution, with complexation occurring at pHs where both biopolymers carry an average net charge of the same sign.

Acknowledgements

The authors thank the BBSRC core strategic grant for financial support; and the Ministry of Education and Research of Estonia and Archimedes Foundation for the award of Kristjan Jaak fellowship to K.L. (Contract Number O.06-04/06).

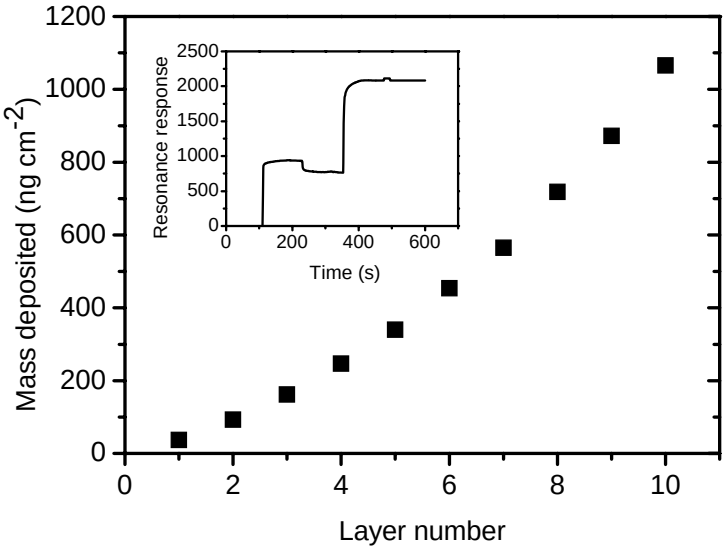

Fig. 1 Mass of polymer deposited as a function of layer number for the buildup of a PLL/furcellaran multilayer. Inset shows SPR response as a function of time for the deposition of of the 5th and 6th layers

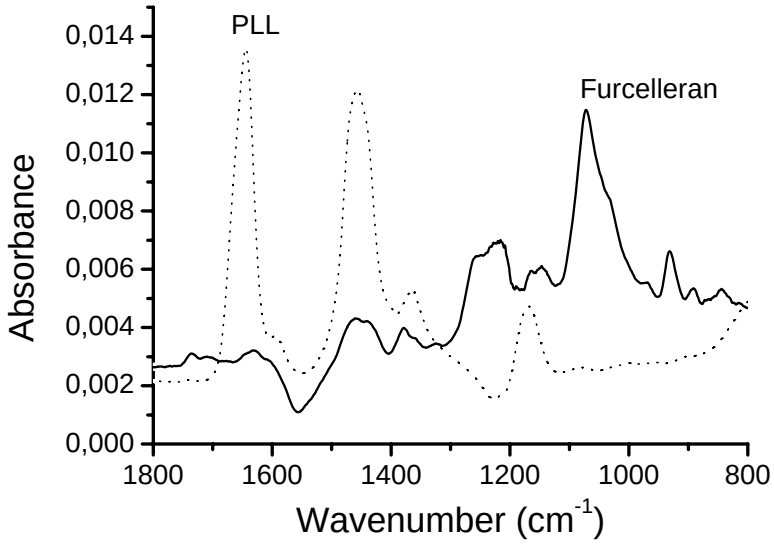

Fig. 2. Solution FTIR-ATR spectra of PLL and furcellaran in the region 1800-800 cm^{-1}

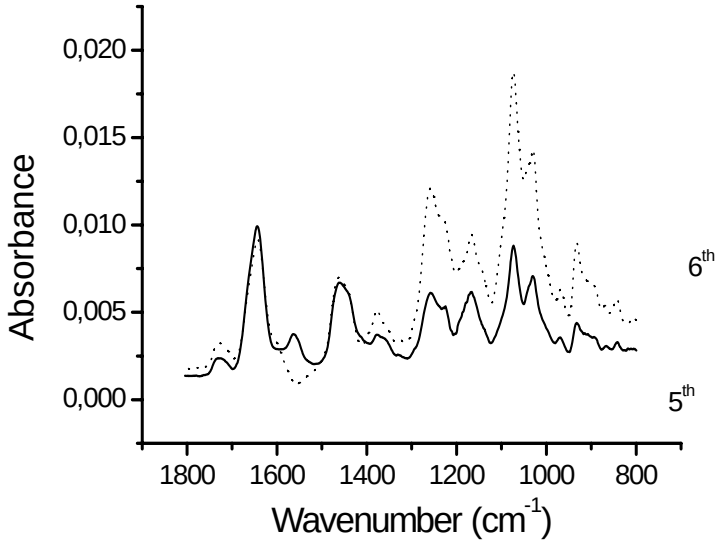

Fig. 3. FTIR spectra of PLL/furcellaran multilayer in D_2O in the region 800-1800 cm^{-1} after deposition of the 5^{th} (PLL) and 6^{th} (furcellaran) layers

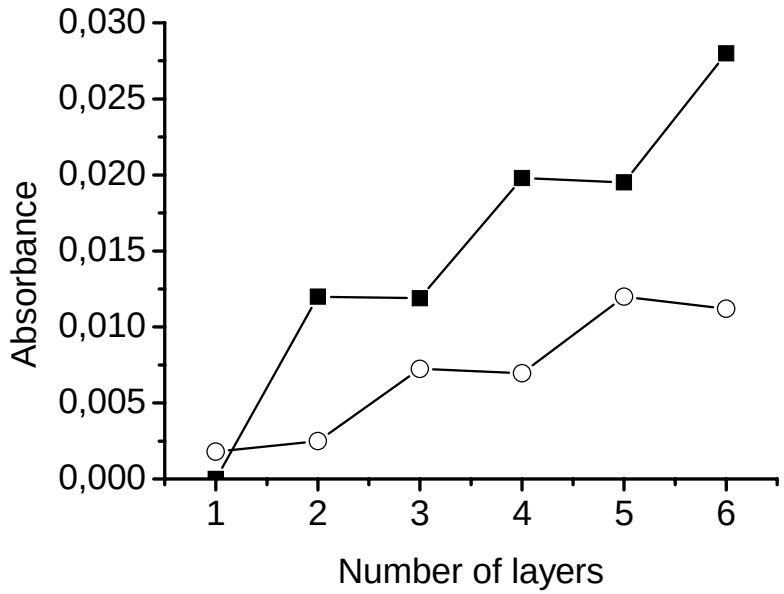

Fig. 4. The IR absorbance of PLL/furcellaran multilayer at 1075 (■) and 1643 cm^{-1} (○) as a function of number of layer

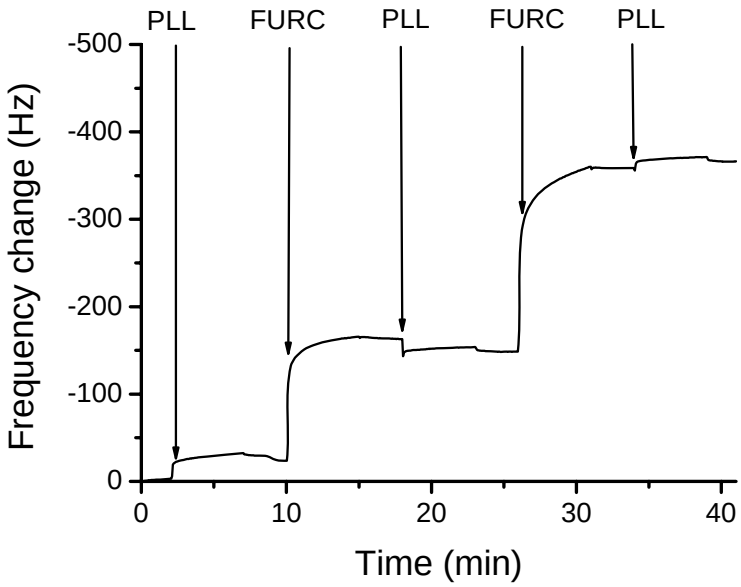

Fig. 5a.Plot of frequency change of QCM-D 15 MHz harmonic versus time for the assembly of the first 5 layers

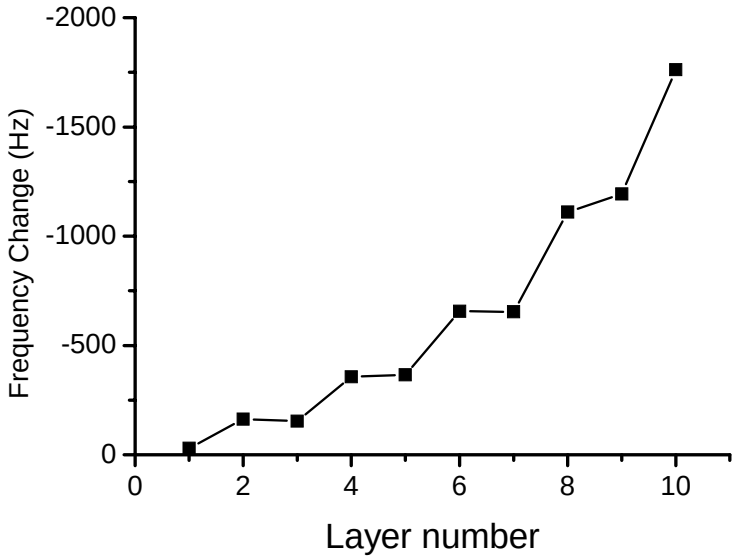

Fig. 5b. Plot of frequency change of QCM-D 15 MHz harmonic versus layer number for the assembly of a 10 layer multilayer

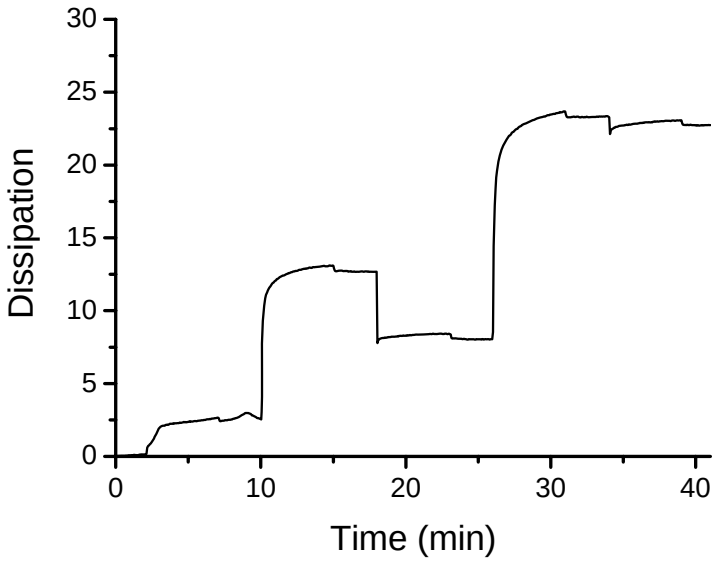

Fig. 5c. Plot of QCM-D dissipation (15 MHz harmonic) versus time for the assembly of the first 5 layers

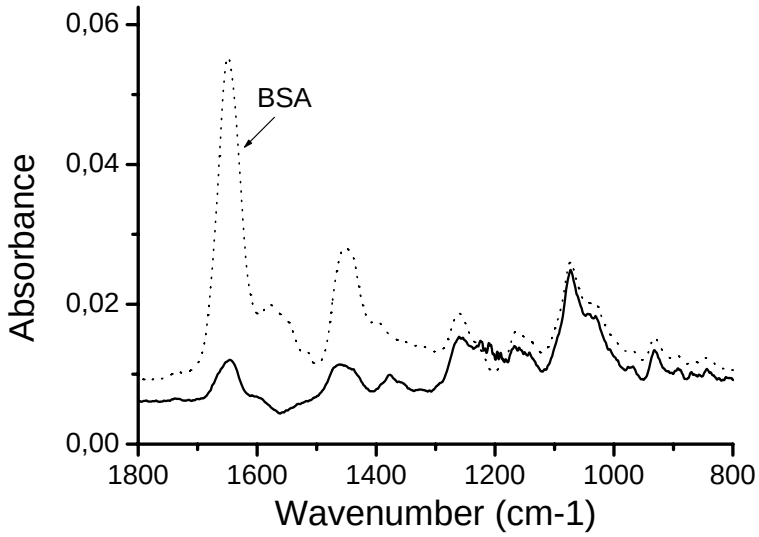

Fig. 6a. FTIR spectra of BSA deposition in D_2O at pD 5.0 to 3rd furcellaran layer (6th layer)

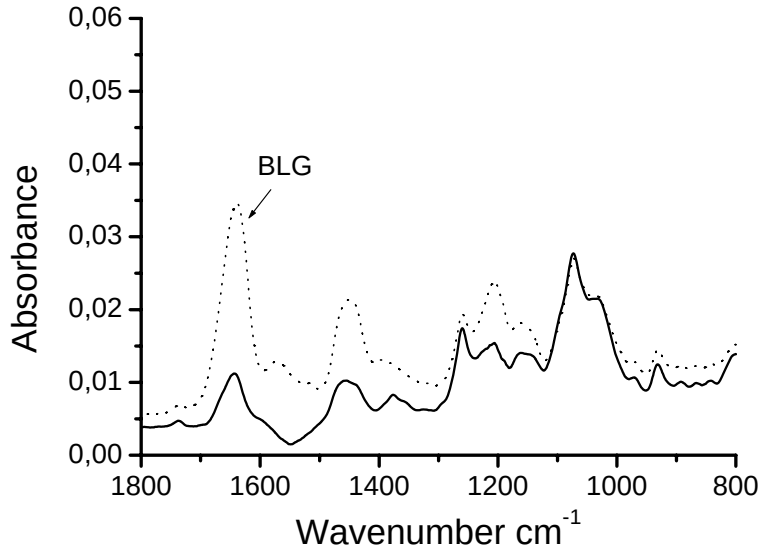

Fig. 6b. FTIR spectra of BLG deposition in D_2O at pD 5.0 to 3rd furcellaran layer (6th layer)

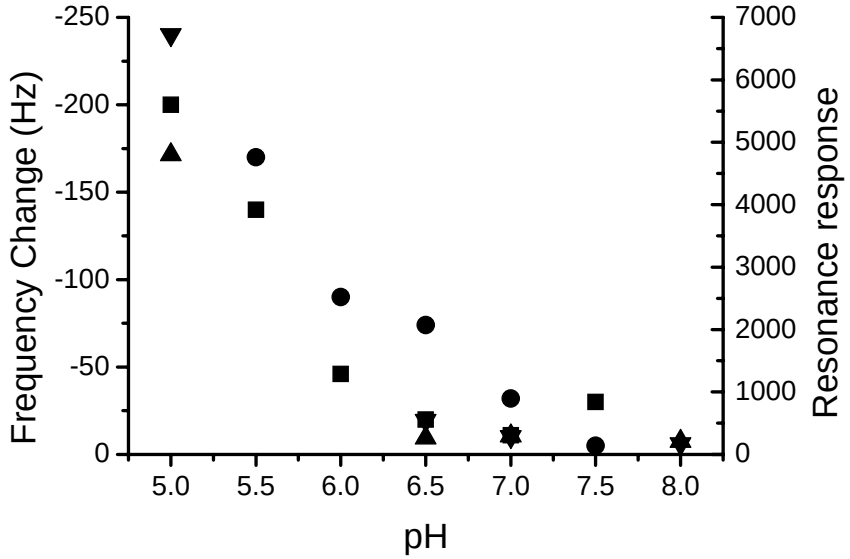

Fig. 7. Dependence of QCMD frequency change, and SPR resonance response as a function of pH for the adsorption of BSA▼(SPR); ● (QCMD); and BLG ▲(SPR) ■ (QCMD) on a 6 layer PLL/furcellaran multilayer.

References

Baldini, G., Beretta, S., Chirico, G., Franz, H., Maccioni, E., Mariani, P., & Spinozzi, F. (1999) Salt-induced association of beta-lactoglobulin by light and X- ray scattering. *Macromolecules*, 32, 6128-6138.

Burke, S. E. & Barrett, C. J. (2003) pH-responsive properties of multilayered poly(L- lysine)/hyaluronic acid surfaces. *Biomacromolecules*, 4, 1773-1783.

Cannan, R. K., Palmer, A. H., & Kibrick, A. C. (1942) The hydrogen ion dissociation curve of beta-lactoglobulin. *Journal of Biological Chemistry*, 142, 803-822.

Carter, D. C. & Ho, J. X. (1994) Structure of serum albumin. *Advances in protein chemistry*, 45, 153-203.

Caruso, F., Furlong, D. N., Ariga, K., Ichinose, I., & Kunitake, T. (1998) Characterization of polyelectrolyte-protein multilayer films by atomic force microscopy, scanning electron microscopy, and Fourier transform infrared reflection-absorption spectroscopy. *Langmuir*, 14, 4559-4565.

Decher, G. (1997) Fuzzy nanoassemblies: Toward layered polymeric multicomposites. *Science*, 277, 1232-1237.

Dubas, S. T. & Schlenoff, J. B. (2001) Swelling and smoothing of polyelectrolyte multilayers by salt. *Langmuir*, 17, 7725-7727

Elbert, D. L., Herbert, C. B., & Hubbell, J. A. (1999) Thin polymer layers formed by polyelectrolyte multilayer techniques on biological surfaces. *Langmuir*, 15, 5355-5362.

Gergely, C., Bahi, S., Szalontai, B., Flores, H., Schaaf, P., Voegel, J. C., & Cuisinier, F. J. G. (2004) Human serum albumin self-assembly on weak polyelectrolyte multilayer films structurally modified by pH changes. *Langmuir*, 20, 5575-5582.

Glinel, K., Prevot, M., Krustev, R., Sukhorukov, G. B., Jonas, A. M., & Mohwald, H. (2004) Control of the water permeability of polyelectrolyte multilayers by deposition of charged paraffin particles. *Langmuir*, 20, 4898-4902.

Hallberg, R. K. & Dubin, P. L. (1998) Effect of pH on the binding of beta-lactoglobulin to sodium polystyrenesulfonate. *Journal of Physical Chemistry B*, 102, 8629-8633.

Hook, F. (2001) Development of a novel QCM Technique for protein adsorption studies.

Jackson, M., Haris, P. I., & Chapman, D. (1989) Conformational transitions in poly(L-lysine) – studies using Fourier transform infra-red spectroscopy. *Biochimica et Biophysica Acta*, 998, 75-79.

Jung, L. S., Campbell, C. T., Chinowsky, T. M., Mar, M. N., & Yee, S. S. (1998) Quantitative interpretation of the response of surface plasmon resonance sensors to adsorbed films. *Langmuir*, 14, 5636-5648.

Krzeminski, A., Marudova, M., Moffat, J., Noel, T. R., Wellner, N., & Ring, S. G. (2005) The formation of pectin/poly-L-lysine multilayers with pectins of varying degrees of esterification. *Biomacromolecules.*

Ladam, G., Gergely, C., Senger, B., Decher, G., Voegel, J. C., Schaaf, P., & Cuisinier, F. J. G. (2000) Protein interactions with polyelectrolyte multilayers: Interactions between human serum albumin and polystyrene sulfonate/polyallylamine multilayers. *Biomacromolecules*, 1, 674-687.

Lahaye, M. (2001) Developments on gelling algal galactans, their structure and physico-chemistry. *Journal of Applied Phycology*, 13, 173-184.

Laos, K., Brownsey, G. J., & Ring, S. G. (2005) Interactions between furcellaran and the globular proteins bovine serum albumin and beta lactoglobulin. *Carbohydrate Polymers.*

Lavalle, P., Picart, C., Metterer, J., Gergely, C., Reiss, H., Voegel, J. C., Senger, B., & Schaaf, P. (2004) Modeling the builup of polyelectrolyte multilayer films having exponential growth. *Journal of Physical Chemistry B*, 108, 635-648.

Lavalle, P., Vivet, V., Jessel, N., Decher, G., Voegel, J.C., Mesini, P.J., & Schaaf, P. (2004) Direct evidence for vertical diffusion and exchange processes of polyanions and polycations in polyelectrolyte multilayer films. *Macromolecules*, 37, 1159-1162.

Marudova, M., Lang, S., Brownsey, G. J., & Ring, S. G. (2005) Pectin-chitosan multilayer formation. *Carbohydrate Research*, 340, 2144-2149.

Mattison, K. W., Dubin, P. L., & Brittain, I. J. (1998) Complex formation between bovine serum albumin and strong polyelectrolytes: Effect of polymer charge density. *Journal of Physical Chemistry B*, 102, 3830-3836.

Michel, M., Vautier, D., Voegel, J. C., Schaaf, P., & Ball, V. (2004) Layer by layer self-assembled polyelectrolyte multilayers with embedded phospholipid vesicles. *Langmuir*, 20, 4835-4839.

Pereira, L., Sousa, A., Coelho, H., Amado, A. M., & Ribeiro-Claro, P. J. A. (2003) Use of FTIR, FT-Raman and (13)GNMR spectroscopy for identification of some seaweed phycocolloids. *Biomolecular Engineering*, 20, 223-228.

Picart, C., Mutterer, J., Richert, L., Luo, Y., Prestwich, G. D., Schaaf, P., Voegel, J. C., & Lavalle, P. (2002) Molecular basis for the explanation of the exponential growth of polyelectrolyte multilayers. *Proceedings of the National Academy of Sciences of the United States of America*, 99, 12531-12535.

Quinn, J. F. & Caruso, F. (2004) Facile tailoring of film morphology and release properties using layer-by-layer assembly of thermoresponsive materials. *Langmuir*, 20, 20-22.

Richert, L., Lavalle, P., Payan, E., Shu, X. Z., Prestwich, G. D., Stoltz, J. F., Schaaf, P., Voegel, J. C., & Picart, C. (2004) Layer by layer buildup of polysaccharide films: Physical chemistry and cellular adhesion aspects. *Langmuir*, 20, 448-458.

Salloum, D. S. & Schlenoff, J. B. (2004) Protein adsorption modalities on polyelectrolyte multilayers. *Biomacromolecules*, 5, 1089-1096.

Sauerbrey, G. (1959) Use of a quartz crystal vibrator for weighing thin films on a microbalance. *Zeitschrift Fur Physik*, 155, 206-222.

Seyrek, E., Dubin, P. L., Tribet, C., & Gamble, E. A. (2003) Ionic strength dependence of protein-polyelectrolyte interactions. *Biomacromolecules*, 4, 273-282.

Shi, X. Y. & Caruso, F. (2001) Release behavior of thin-walled microcapsules composed of polyelectrolyte multilayers. *Langmuir*, 17, 2036-2042.

Shiratori, S. S. & Rubner, M. F. (2000) pH-dependent thickness behavior of sequentially adsorbed layers of weak polyelectrolytes. *Macromolecules*, 33, 4213-4219.

Sui, Z. J., Salloum, D., & Schlenoff, J. B. (2003) Effect of molecular weight on the construction of polyelectrolyte multilayers: Stripping versus sticking. *Langmuir*, 19, 2491-2495.

Sukhishvili, S. A., Dhinojwala, A., & Granick, S. (1999) How polyelectrolyte adsorption depends on history: A combined Fourier transform infrared spectroscopy in attenuated total reflection and surface forces study. *Langmuir*, 15, 8474-8482.

Sukhishvili, S. A. & Granick, S. (1999) Adsorption of human serum albumin: Dependence on molecular architecture of the oppositely charged surface. *Journal of Chemical Physics*, 110, 10153-10161.

Tanford, C., Swanson, S. A., & Shore, W. S. (1955) Hydrogen ion equilibria of bovine serum albumin. *Journal of the American Chemical Society*, 77, 6414-6421.

Truus, K., Vaher, M., Usov, A. I., Pehk, T., & Kollist, A. (1997) Gelling galactans from the algal community of Furcellaria lumbricalis and Coccotylus truncatus (the Baltic Sea, Estonia): a structure-property study. *International Journal of Biological Macromolecules*, 21, 89-96.

Voinova, M. V., Rodahl, M., Jonson, M., & Kasemo, B. (1999) Viscoelastic acoustic response of layered polymer films at fluid-solid interfaces: Continuum mechanics approach. *Physica Scripta*, 59, 391-396.

Volery, P., Besson, R., & Schaffer-Lequart, C. (2004) Characterization of commercial carrageenans by Fourier transform infrared spectroscopy using single-reflection attenuated total reflection. *Journal of Agricultural and Food Chemistry*, 52, 7457-7463.

APPENDIX 2

ELULOOKIRJELDUS

1. Isikuandmed

Ees- ja perekonnanimi	Katrin Laos
Sünniaeg ja -koht	30.03.1976, Tallinn
Kodakondsus	Eesti

1. Kontaktandmed

Aadress:	Toiduainete instituut, Tallinna Tehnikaülikool, Ehitajate tee 5, Tallinn 19086, Eesti
Telefon:	+372 6202956
E-posti aadress:	katrin.laos@mail.ee

2. Hariduskäik

Tallinna Tehnikaülikool	2001-2006	Bio- ja toiduainetehnoloogia/doktorant
Tallinna Tehnikaülikool	1999-2001	Bio- ja toiduainetehnoloogia/magister
Tallinna Tehnikaülikool	1994-1999	Toiduainete tehnoloogia/insener
Tallinna Väike-Õismäe Keskkool	1983-1994	

3. Keelteoskus

Eesti keel	emakeel
Inglise keel	väga hea
Soome keel	hea
Vene keel	rahuldav
Prantsuse keel	algteadmised

4. Täiendõpe

09.2002 – 09.2003	Institute of Food Research, Norwich, UK
11.2004 – 01.2005	Institute of Food Research, Norwich, UK

5. Teenistuskäik

Sept 2004 - …	Tallinna Tehnikaülikool, teadur
Juuni 2005 - …	Toidu- ja Fermentatsioonitehnoloogia Arenduskeskus, projektijuht
Mai 2002 – Aug 2002	Eesti Põllumajandus-Kaubanduskoda, ekspert
Nov 2001– Aug 2002	Tallinna Tehnikaülikool, teadur
Jan 1999– May 2001	Tallinna Tehnikaülikool, innovatsiooniprojekti lepinguline täitja
June 1996– Oct 1997	Eesti Buss, administraator

6. Kaitstud lõputööd

Magistritöö	"Punavetika *Furcellaria lumbricalis* erinevatest vormidest ekstraheeritud tardainete uurimine"
Diplomitöö	"Mõningate lisandite mõju estagari geelide struktuursetele omadustele

8. Teadustöö põhisuunad: toiduainete füüsikalised omadused, looduslikud polüsahhariidid, valk-polüsahhariid koostoimed

APPENDIX 2

CURRICULUM VITAE

1. Personal particulars

First name and surname	Katrin Laos
Date and Place of birth	30.03.1976, Tallinn
Citizenship	Estonian

2. Contact data

Address:	Department of Food Processing, Tallinn University of Technology, Ehitajate tee 5, Tallinn 19086, Estonia
Telephone:	+372 6202956
e-mail:	katrin.laos@mail.ee

3. Education

Tallinn University of Technology	2001-2006	Bio- and Food Technology/Ph.D.
Tallinn Technical University	1999-2001	Bio- and Food Technology/MSc.
Tallinn Technical University	1994-1999	Food Technology/graduate engineer
Tallinn Väike-Õismäe Secondary School	1983-1994	

4. Languages

Estonian	native language
English	very good
Finnish	good
Russian	satisfactory
French	basic knowledge

5. Additional studies

09.2002 – 09.2003	Institute of Food Research, Norwich, UK
11.2004 – 01.2005	Institute of Food Research, Norwich, UK

6. Professional Experience

Sept 2004 - …	Tallinn University of Technology, Research Scientist
June 2005 - …	Competence Center of Food and Fermentation Technologies, Project Manager
May 2002 – Aug 2002	Estonian Chamber of Agriculture and Commerce, Expert
Nov 2001– Aug 2002	Tallinn Technical University, Research Scientist
Jan 1999– May 2001	Tallinn Technical University, Contractural performer of innovational project
June 1996– Oct 1997	Estonian Bus, Administrator

7. Defended thesises

Master Degree thesis	"Investigation of the gelling substances extracted from different forms of red algae *Furcellaria lumbricalis*"
Diploma work	"Structural properties of estagar gels in the presence of various additives"

8. Current research program — food physics, natural polysaccharides, protein-polysaccharide interactions

APPENDIX 3

PUBLICATIONS RELATED TO THE TOPIC

1. Friedenthal, M., Vokk, R., Sirendi, M., Eha, K., **Laos, K**. (2000) "Formulating dairy and fish products with inclusion of furcellaran from the red algae stratum of Baltic Sea". // Nutritionists meet Food Scientists and Technologists. Porto, 12-14 April.
2. **Laos, K**., Sirendi, M. (2000) „Textural properties of estagar gels in the presence of potassium and calcium cations and saccharose". Food and Nutrition, VIII, Tallinn, 55-71.
3. **Laos, K.**, Sirendi, M., Eha, K., Friedenthal, M. (2001) „Piima ja tema koostisosade mõju furtsellaraani geelide tekstuursetele omadustele". Eesti XXVII Keemiapäevad. Tallinn, 15-16 November 2001.
4. Eha, K., **Laos, K**., Barndõk, T., Friedenthal, M. (2001) „The shear stress and fracture test of furcellaran at moderate concentrations". Food and Nutrition, IX, Tallinn, 41-46.
5. **Laos, K**. (2001) „The extraction and recovery of gelling galactans from the red algae stratum of Kassari bay in the Baltic Sea" Food and Nutrition, IX, Tallinn, 59-60.
6. **Laos, K**., Sirendi, M., Friedenthal, M (2002) „Rheological investigations in the Department of Food Processing" Food and Nutrition, X, Tallinn, 47-54.
7. **Laos**, **K.**, Ring, S. (2003) "Gelation of furcellaran and furcellaran/BSA mixture". // "Gums and stabilisers for the food industry", International Conference and Industry Exhibition "Designing Structure into Foods", Wrexham, UK, 23 – 27 Juuni.
8. **Laos, K.,** Brownsey, G., Ring, S. (2004) "Interactions between furcellaran and milk proteins (BSA, BLG)"// "Marine Biopolymers. Structure, Functionality and Applications", A satellite to the XVIII International Seaweed Symposium, Trondheim, Norway, 27-29 June
9. **Laos, K**., Tilk, K. (2004) „The effect of packaging on the storage of jelly" Food and Nutrition, XII, Tallinn, 55-61.
10. Lõugas, T., **Laos, K**., Vokk, R., Friedenthal, M. (2004) "Encapsulation of bioactive compounds of sea buckhorn in furcellaran beads" // "Marine Biopolymers. Structure, Functionality and Applications", A satellite to the XVIII International Seaweed Symposium, Trondheim, Norway, 27-29 June
11. **Laos, K.,** Brownsey, G.J., Ring, S.G. (2005) "Dependence of the interaction of furcellaran between the globular proteins bovine serum albumin and β-lactoglobulin on pH" // „Accessing Useful Technologies… Optimizing Food Safety and Nutrition", The 4th International Congress on Food Technology - Proceedings, Piraeus, Greece, 18-19 Feburary
12. Lõugas, T., **Laos, K**., Vokk, R., Friedenthal, M. „Rheology and encapsulation efficiency of furcellaran beads" // „Accessing Useful Technologies… Optimizing Food Safety and Nutrition", The 4th International Congress on Food Technology - Proceedings, Piraeus, Greece, 18-19 Feburary
13. **Laos, K**., Ring, S. (2005) "Characterisation of furcellaran samples from Estonian *Furcellaria lumbricalis*" Journal of Applied Phycology, 17, 461-464.
14. **Laos, K**., Brownsey, G., Friedenthal, M., Ring, S. (2005) "Rheological properties of gels formed with furcellaran and globular proteins bovine serum albumin and β-lactoglobulin" Annual Transactions of the Nordic Rheology Society, 13, 269-275
15. Parker, R., Noel, T.R., Brownsey, G.J., **Laos, K.**, Ring, S.G. (2005) "The Non-Equilibrium Phase and Glass Transition Behavior of β-Lactoglobulin" Biophysical Journal, 89, 1227-1236

16. **Laos, K**., Mironova, M., Friedenthal, M. (2005) “Development of furcellaran and furcellaran-bovine serum albumin films to improve food quality and safety”. Innovations in Traditional Foods (eds. Fito, P and Toldra, F), Elsevier, London, pp.1343-1346.
17. **Laos, K.,** Brownsey, G., Ring, S. (2005) “Interactions between furcellaran and the globular proteins bovine serum albumin and β-lactoglobulin”. (accepted for publication in “Carbohydrate Polymers”)
18. **Laos, K**., Ring, S.G. (2005) Poly-L-lysine – furcellaran multilayer formation and the adsorption of globular proteins bovine serum albumin and β-lactoglobulin on it. (manuscript)